

Applications of spherically bent crystals and Pilatus hybrid pixel array detectors (PAD) for spatially resolved Doppler x-ray spectroscopic measurements of ion temperature and plasma flow velocity in ITER and NIF: Potential applications on x-ray light sources

K. W. Hill and M. Bitter
Princeton Plasma Physics Laboratory

Presentation at Brookhaven National Laboratory
August 24, 2011

Recent Advances and Future Prospects for X-Ray Spectroscopic Imaging In Fusion Research

Kenneth W. Hill , M. L. Bitter, L. Delgado-Aparicio, D. Johnson, R. Feder, N. Pablant

Princeton Plasma Physics Laboratory, Princeton, NJ

P. Beiersdorfer, J. Dunn, K. Morris, E. Wang

Lawrence Livermore National Laboratory, Livermore, CA, USA

Y. Podpaly, M.L. Reinke, J.E. Rice

MIT Plasma Science and Fusion Center, Cambridge, MA

S. G. Lee

NFRI, Daejeon, Korea

Y. Shi, B. Wan

ASIPP, EAST, Hefei, China

S. Morita, M. Goto

NIFS, Toki, Japan

R. Barnsley

ITER International Team, Cadarache, France

M. O'Mullane

University of Strathclyde, Glasgow, UK

M. Sanchez del Rio

ESRF, Grenoble, Fr

**20th International Toki Conference (ITC-20) on
The Next Twenty Years in Plasma and Fusion Science**

December 7 - 10, 2010

Ceratopia Toki, Toki-City, Gifu, Japan

X-ray spectroscopic diagnostics are becoming increasingly important for fusion experiments

- In 1994 TFTR (US) produced 10.7 MW of fusion power for ~ 0.5 s, reaching an energy gain factor, $Q = P_{\text{fusion}}/P_{\text{heating}}$ of ~ 0.26
- In 1997 JET (UK) reached 16.1 MW of fusion power for $Q = 0.65$
- ITER (International Tokamak, Cadarache, France) and NIF (National Ignition Facility, Livermore, CA) should reach $Q > 1$ in the future
- X-ray imaging crystal spectrometry (XICS) is a primary diagnostic for measuring profiles of ion temperature and plasma flow velocity on ITER; these parameters are important for understanding and optimizing performance.
- At NIF densities ($>10^{22}$ cm $^{-3}$) only x rays with energy ≥ 8 keV escape the plasma

We would like to identify alternate applications of our x-ray optical diagnostics schemes

- X-ray imaging crystal spectrometer (XICS) using a single spherically bent crystal and a 2D imaging detector enable spatially resolved Doppler measurements of ion temperature and flow velocity in tokamaks with good spatial and temporal resolution
- The technique is also applicable to inertial confinement fusion (ICF) “point” sources
- New schemes with matched pairs of spherically bent crystals should enable 2D imaging of small x-ray sources with favorable geometry and micron resolution
- **We want to find other applications or collaborations** – x-ray lithography, x-ray imaging for biological research on light sources, x-ray beam manipulation, x-ray imaging spectroscopy on other light-source experiments

The XICS is a primary diagnostic for measurement of profiles of T_i and v on ITER

- The ITER core XICS has been assigned to the US
- A US-ITER team is doing the conceptual design toward a CDR in October, 2011
- XICS instruments have been very successful on present day machines (MIT, China, Korea, Japan, UK)
- A preliminary performance analysis for the ITER core XICS looks mostly favorable
- JET (UK) would be an ideal venue for more ITER-relevant R&D for XICS
- Our x-ray optical schemes may have applications in other areas of physics

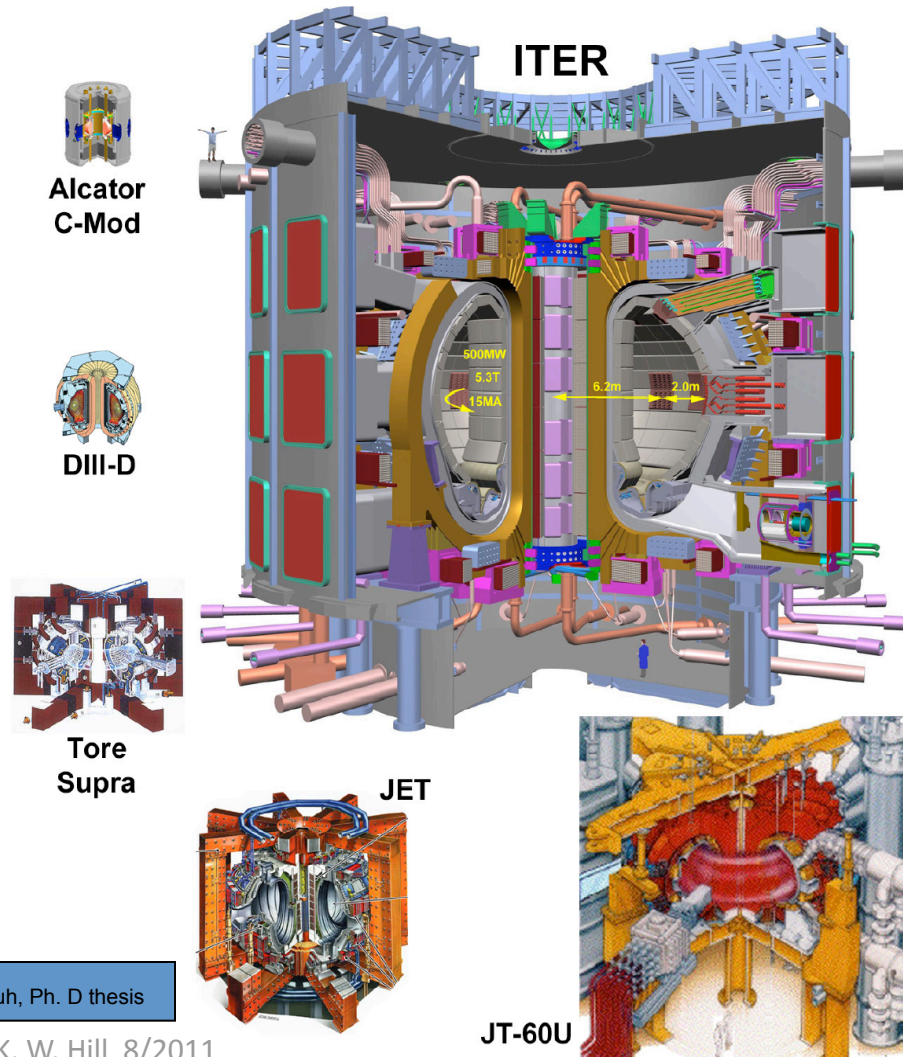
For tokamaks measurement of spatial profiles of ion temperature and plasma flow velocity are important

- Connections between rotation and plasma stability and confinement make predictive capability and active control of rotation profile a critical area of tokamak research¹
- For reactors the use of intrinsic torques will replace the torques due to neutral beam injection in present day tokamaks
- Understanding thermal transport due to turbulent fluctuations, e.g. driven by ion temperature (T_i) gradients, requires careful measurement of the T_i profile
- For large, high density tokamaks, passive spectroscopy will be required for these measurements in the plasma core

¹R.McDermott, 15th EU-US Transport Task Force Meeting, 9/2010

ITER's size requires passive spectroscopy for measuring core temperature and ion motion

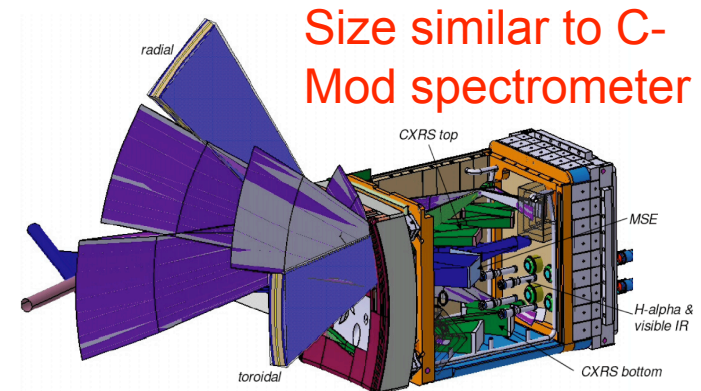
Sizes of various magnetic fusion machines



H. Yuh, Ph. D thesis

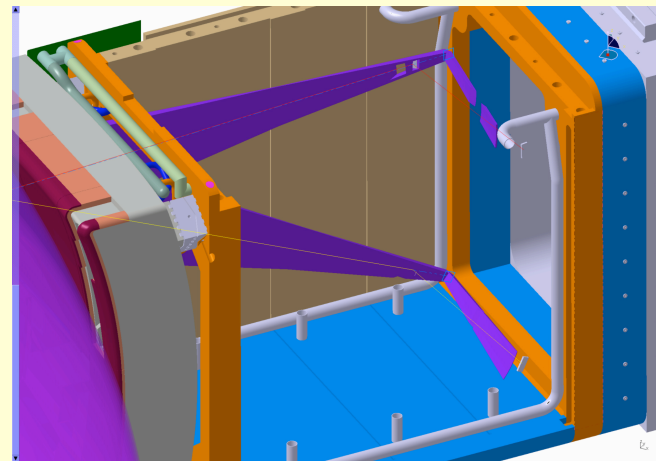
K. W. Hill 8/2011

ITER diagnostic port plug with crystal spectrometer



- Proposed system for ITER uses 6 spectrometers – 3 each looking radially and toroidally

12/04/2006 ITPA ITER Imaging X-ray Crystal Spectrometry - Interim Progress Summary

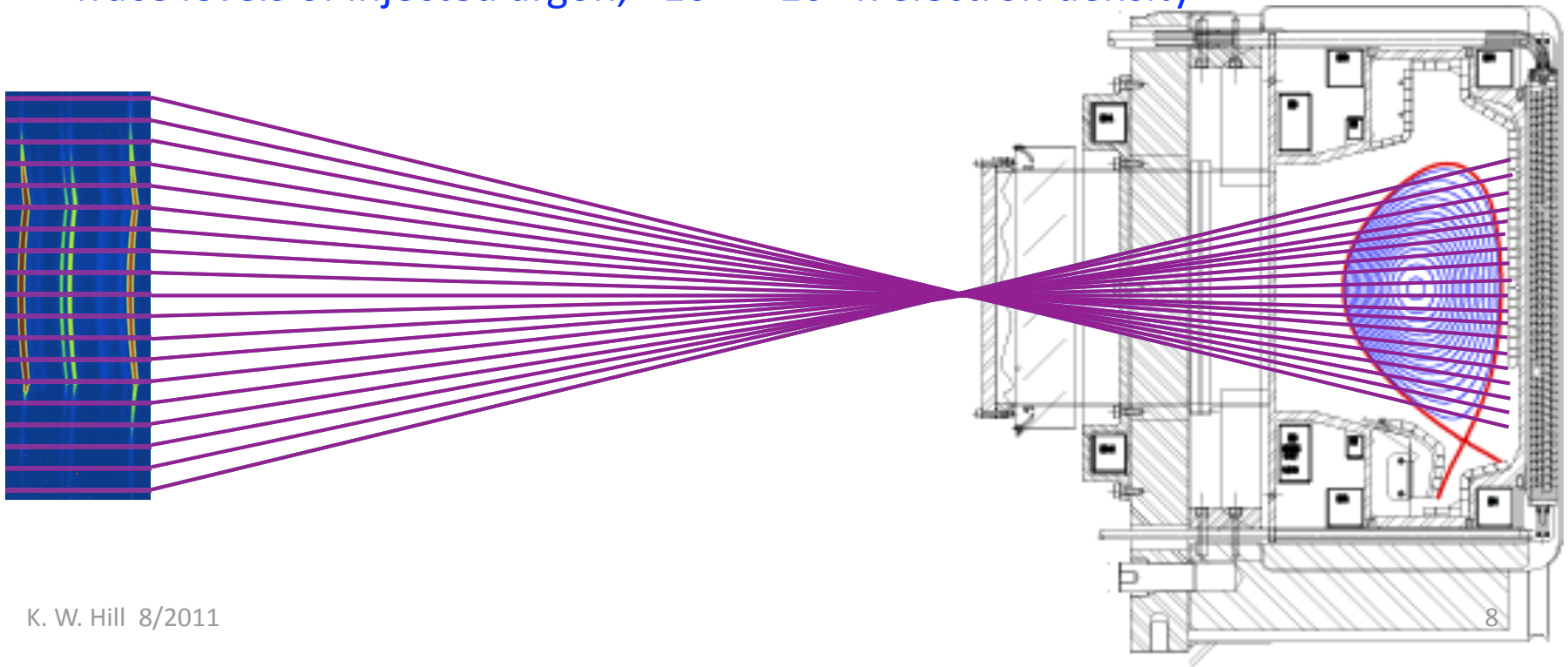


Design is being carried out at PPPL and LLNL

We need to measure x-ray spectrum across entire plasma minor cross section with good spatial and temporal resolution

- 1D x-ray imaging crystal spectroscopy (XICS)
- Single spherically bent crystal taking advantage of astigmatism
- Silicon hybrid pixel array detector (PAD) with good spatial resolution and fast readout
- He-like and H-like argon $K\alpha$ lines near 3.1 and 3.3 keV
- Trace levels of injected argon, $\sim 10^{-5} - 10^{-4}$ x electron density

Alcator C-Mod
tokamak (MIT)



Outline

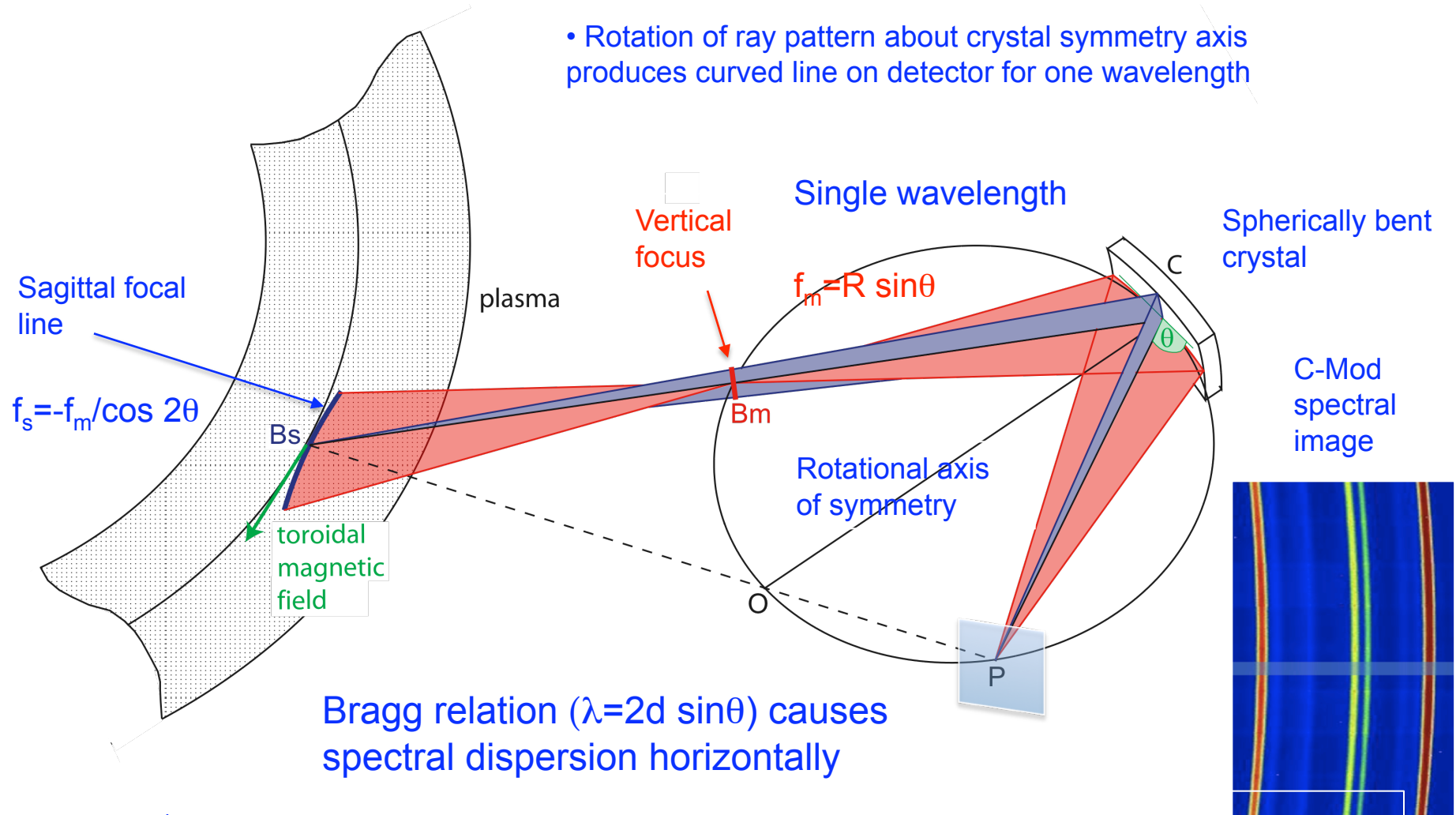
- Principle of operation of 1d imaging XCS
- Alcator C-Mod imaging XCS spectrometer at MIT and data
- Imaging XCS systems in China, Korea, Japan
- ITER imaging XCS design
- ITER XCS performance simulations
- Application of this concept to inertial confinement plasmas
- 2d imaging schemes with pairs of spherically bent crystals
- Broad-band 1d x-ray imaging pinhole camera

Imaging XCS measures profiles of **ion temperature** and plasma **flow velocity** by Doppler spectrometry

- Spherically bent Bragg crystal disperses x-ray wavelength horizontally and images emission vertically
- 2D imaging detector records spectral image
- Fast detector framing provides time resolution
- Can also measure **electron-temperature profile**, provide rigorous tests of **atomic structure theories**, and measure the target **impurity concentration profile**

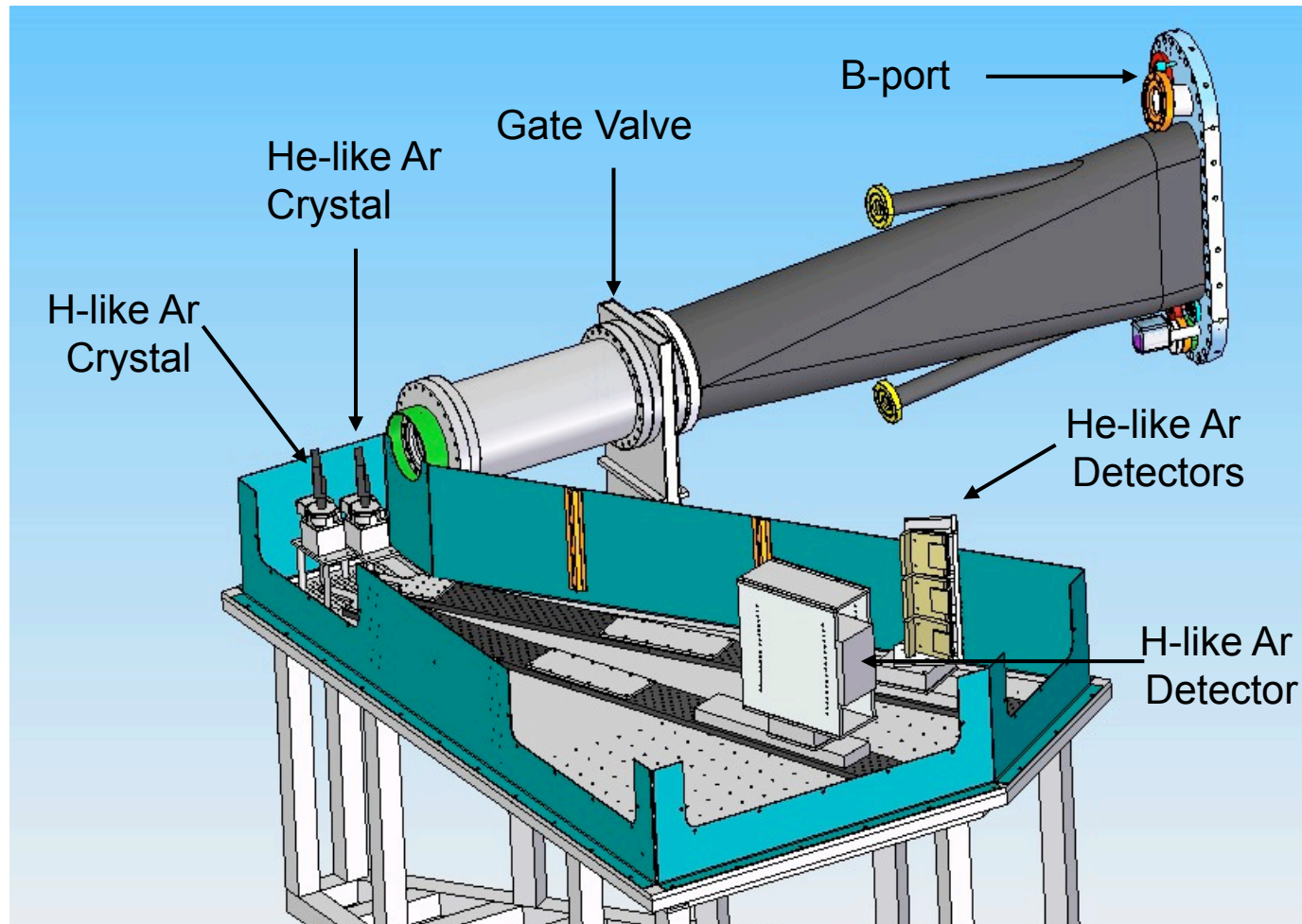
Spherically bent crystal enables vertical 1d imaging by focusing sagittal focal line from plasma to point on detector

- Tokamak spectrum is uniform in toroidal direction
- Rotation of ray pattern about crystal symmetry axis produces curved line on detector for one wavelength



The imaging x-ray crystal spectrometer (XCS) on the Alcator C-Mod tokamak at MIT

Two Imaging X-Ray Crystal Spectrometers view the full C-Mod plasma

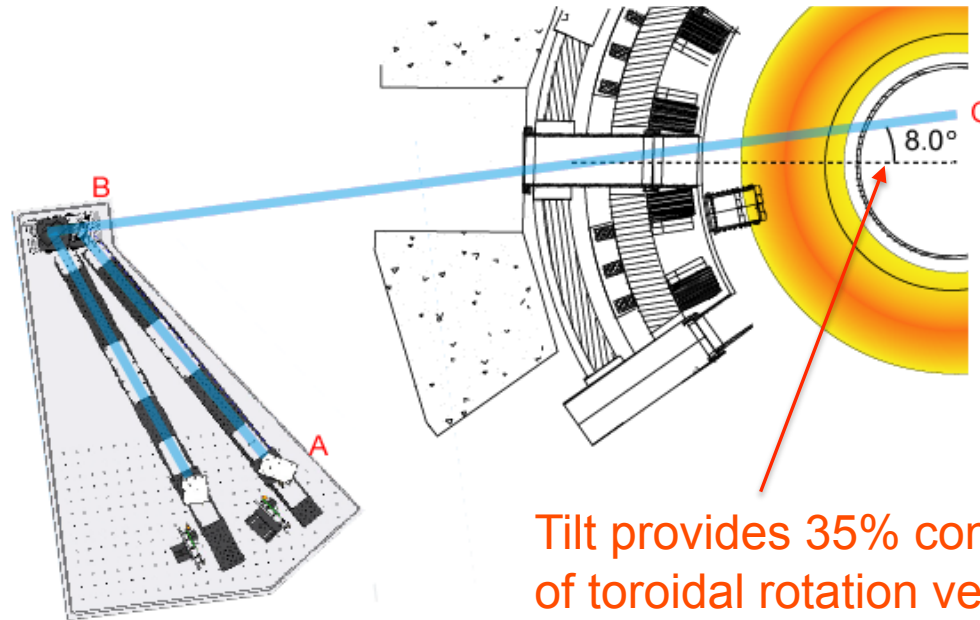


C-Mod
Tokamak
plasma

C-Mod Spectrometer Layout

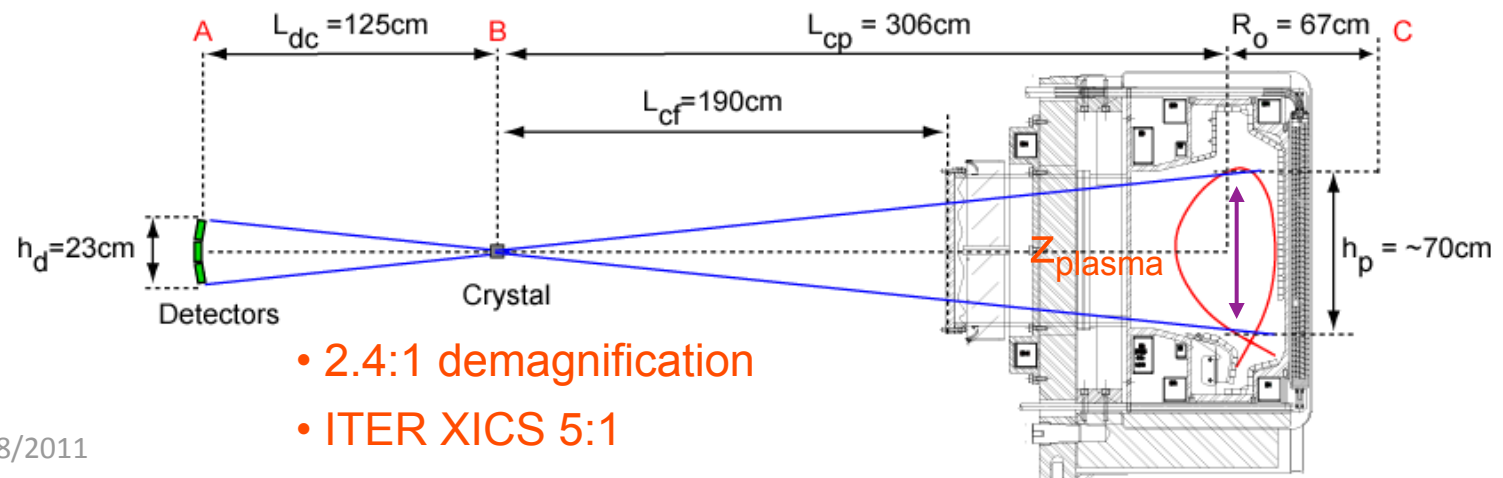
Three 2d detectors view entire plasma height for He-like Ar

Top View



Tilt provides 35% component of toroidal rotation velocity

Side View



Hybrid pixel detector arrays are the heart of the C-Mod imaging XCS

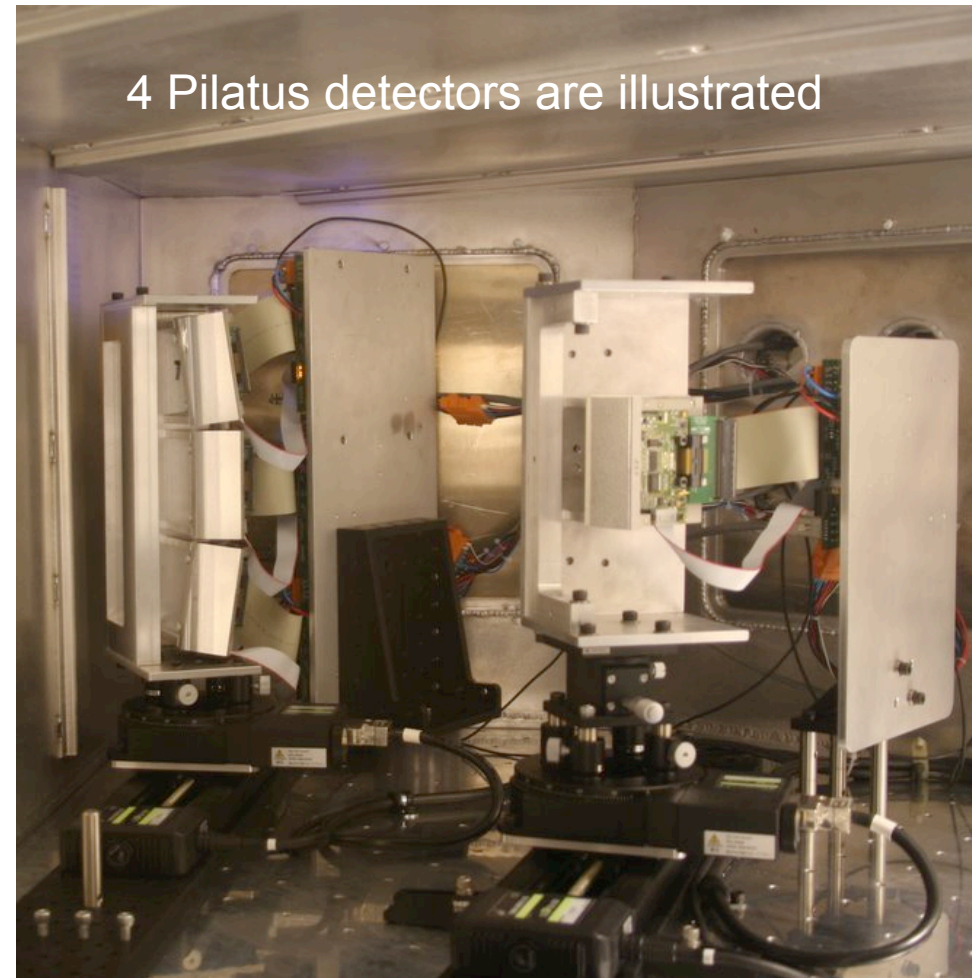
- **Pilatus:** Pixelated Large Area detectors for The Synchrotron - Paul Scherrer Institute
- Protein x-ray crystallography
- Dectris - Pilatus 100k Module (**95000 pixels**)
 - Each pixel does single photon counting via
 - Amplifier with remotely selectable gain
 - Remotely selectable shaping time
 - Remotely selectable lower level discriminator or threshold
 - Counter
 - 20-bit memory
 - Area: 8.35 x 3.35 cm²
 - Pixel size: 172x172 μm² (487x195)
 - Count Rate/pixel: 10⁶ x rays/s
 - Min. Readout Time: 2.2 ms

www.dectris.com

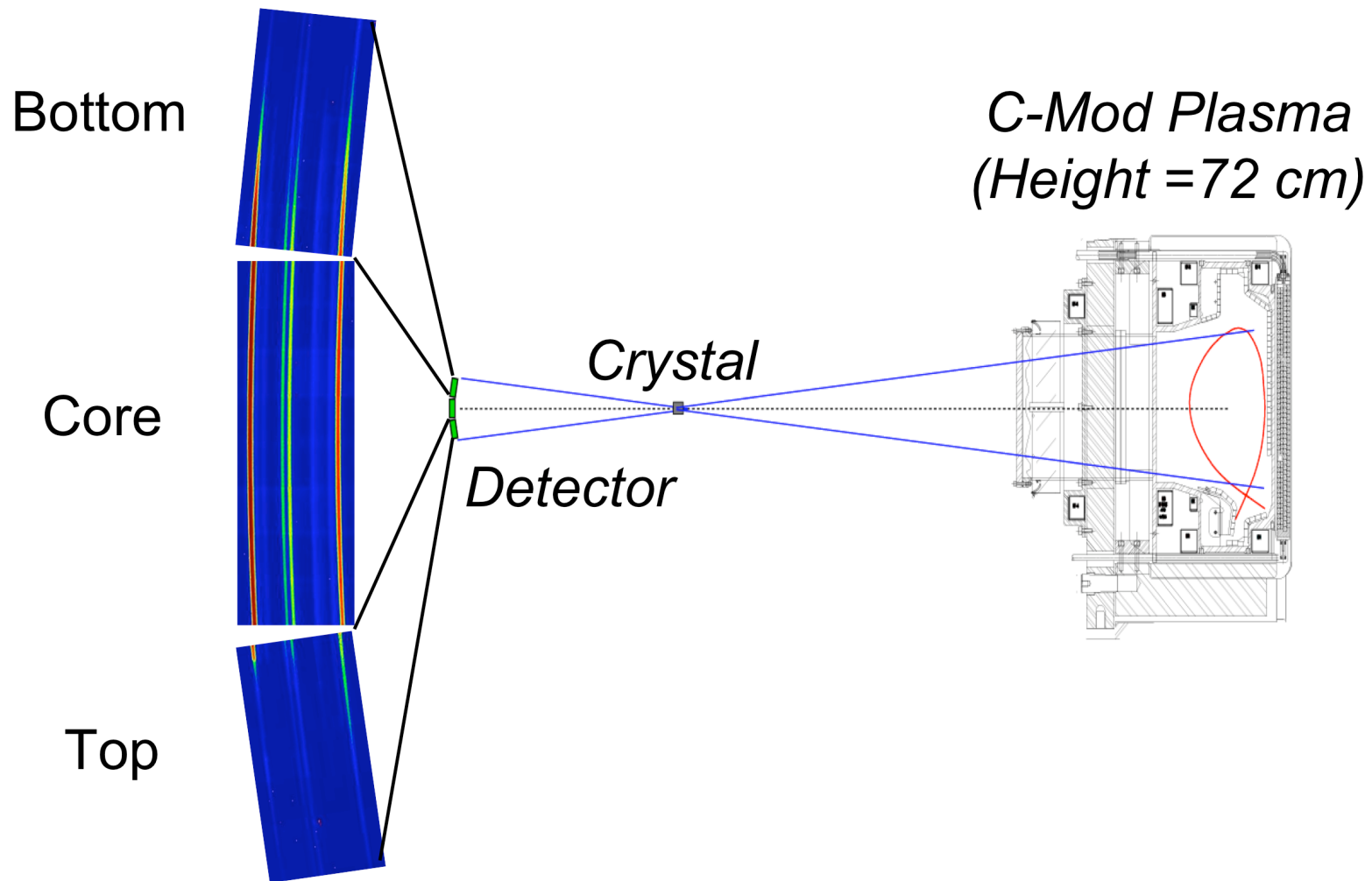
K. W. Hill 8/2011



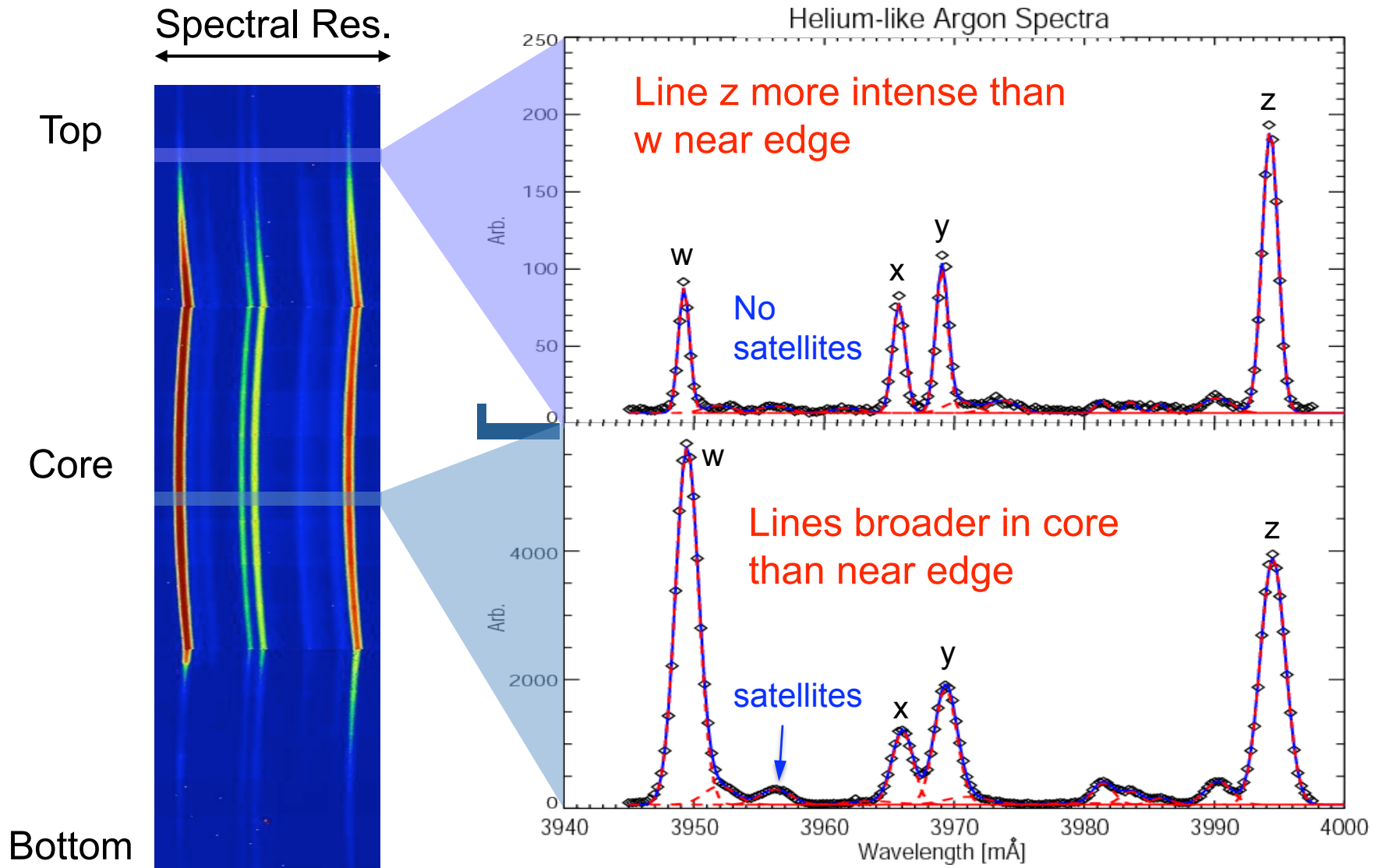
The C-Mod spectrometer worked on the first shot



3 Pilatus detector modules provide spectra from the full C-Mod plasma

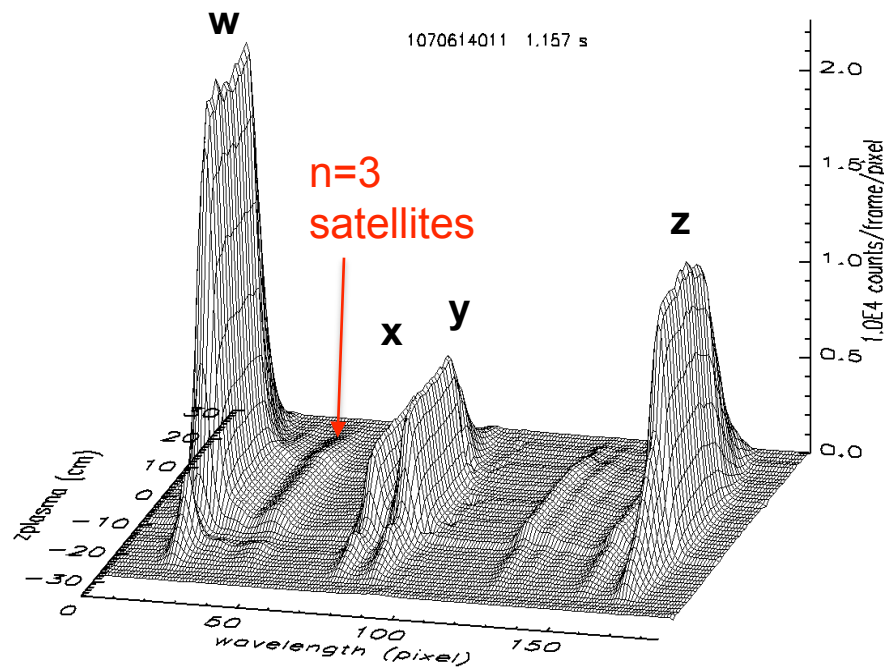


Line-outs of images on 3 detectors yield He-like Ar $K\alpha$ x-ray spectral lines



High resolution He-like Ar $K\alpha$ spectra measured across entire plasma profile with good spatial and temporal resolution

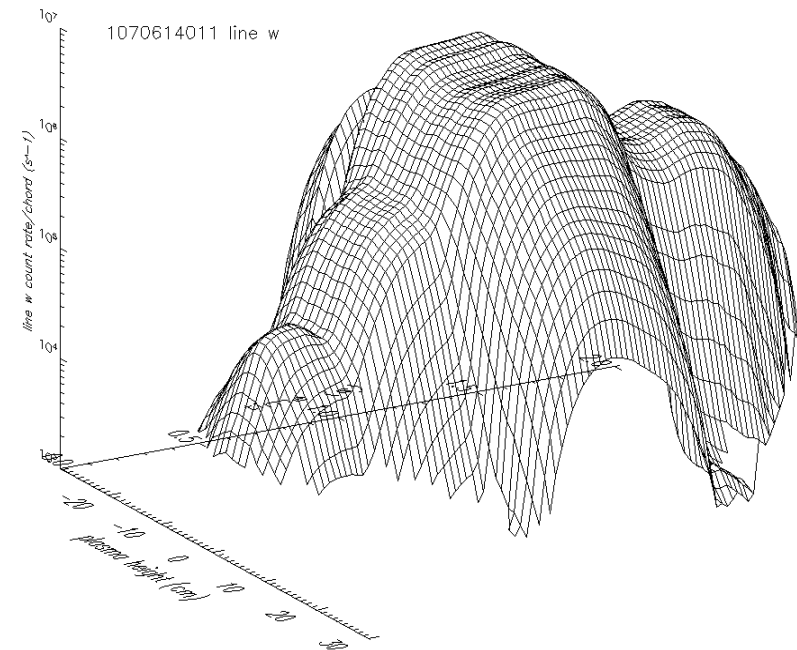
- Profile of He-like Ar $K\alpha$ spectra from C-Mod



- T_i from Doppler widths
- v_{tor} from Doppler shifts
- T_e from satellite/w line ratios

K. W. Hill 8/2011

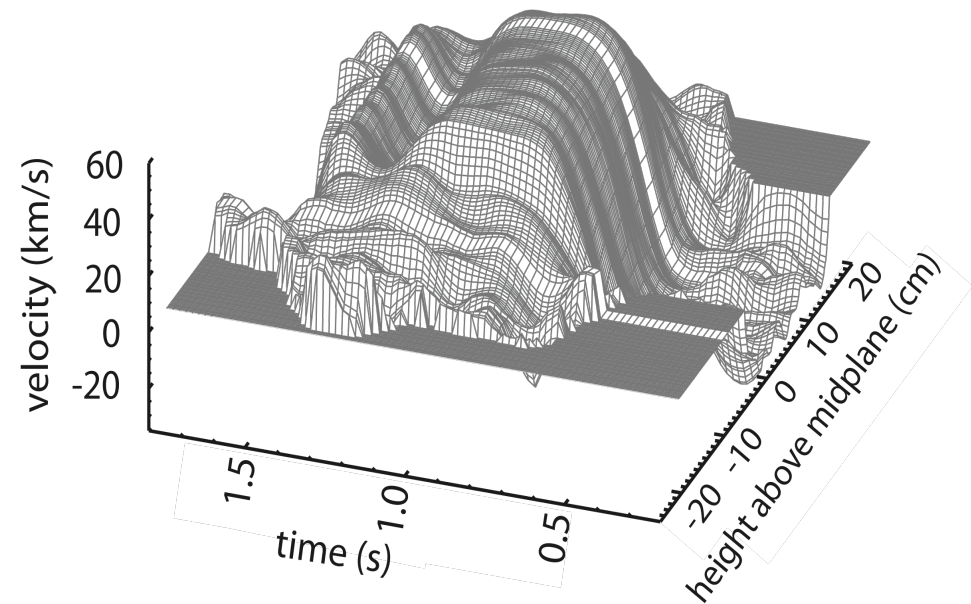
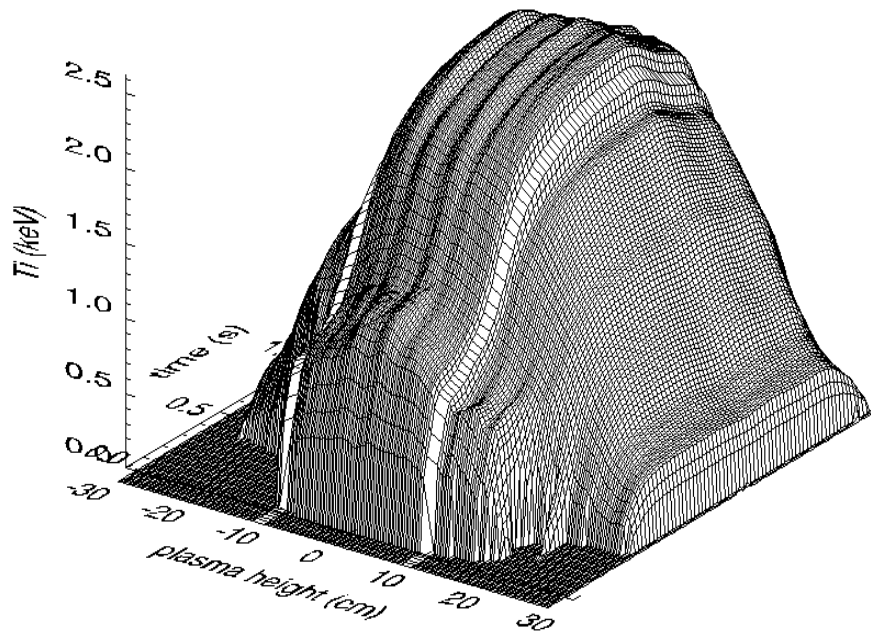
- Single-chord count rates up to $4 \times 10^7 \text{ s}^{-1}$ in center imply very good time resolution ($\sim 1 - 10 \text{ ms}$)



- 10^4 counts \Rightarrow 1% statistical error
- 10^7 counts/s \rightarrow 1% error in 1 ms

T_i and v_{tor} are inferred from these spectra with excellent spatial definition

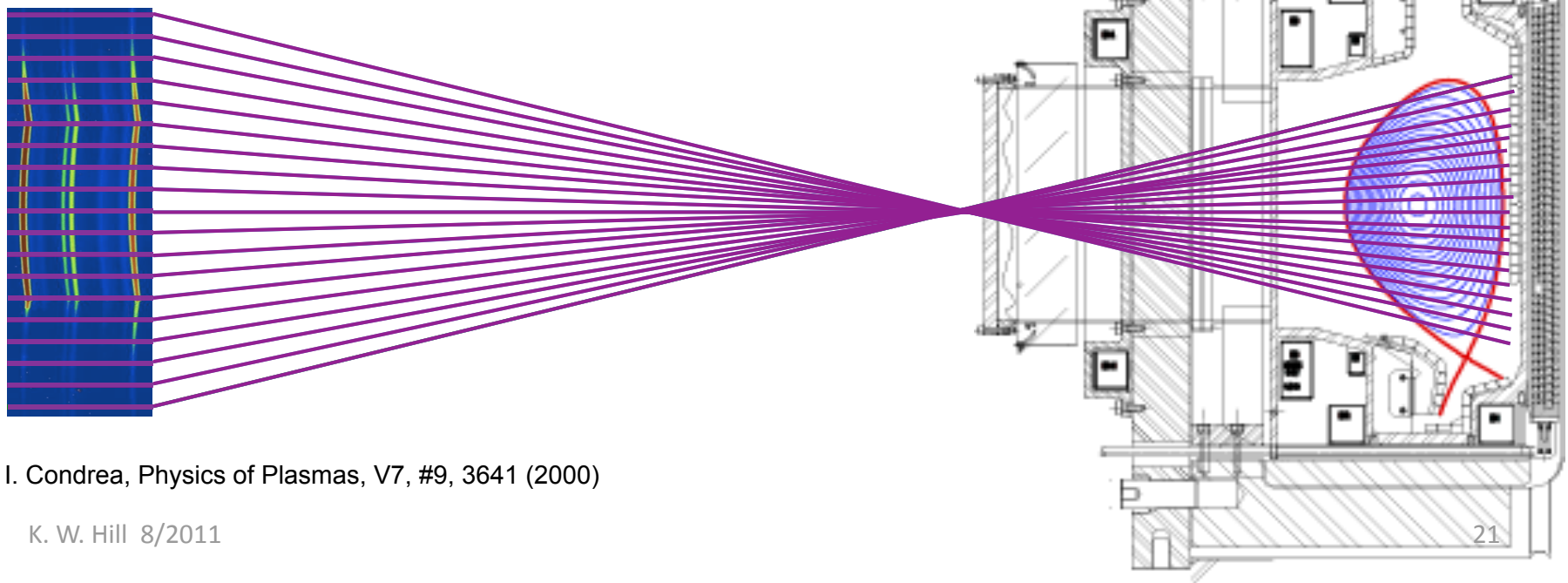
- **Uninverted ion-temperature profile** from Alcator C-Mod
- T_i increases to 2.5 keV with 3 MW of ICRF heating power
- **Toroidal rotation velocity profile**
- Zero velocity inferred from locked-mode (non-rotating) shot
- v increases to 60 km/s with ICRF and reduces with added LHCD



~ 1400 lines of sight. “Sliding” sum of ~25 pixel rows for good statistics

Many lines-of-sight enable inference of local values of v_{tor} and T_i by spectral tomography

- Multiple line integrated spectra require tomography to obtain flux surface averaged measurements
 - Flux surface provided by magnetic measurements – EFIT
 - Assume emissivity, toroidal rotation frequency and impurity temperatures are constant on a flux surfaces
 - Assume impurity distribution function is Maxwellian
 - Not simply tomography on each wavelength

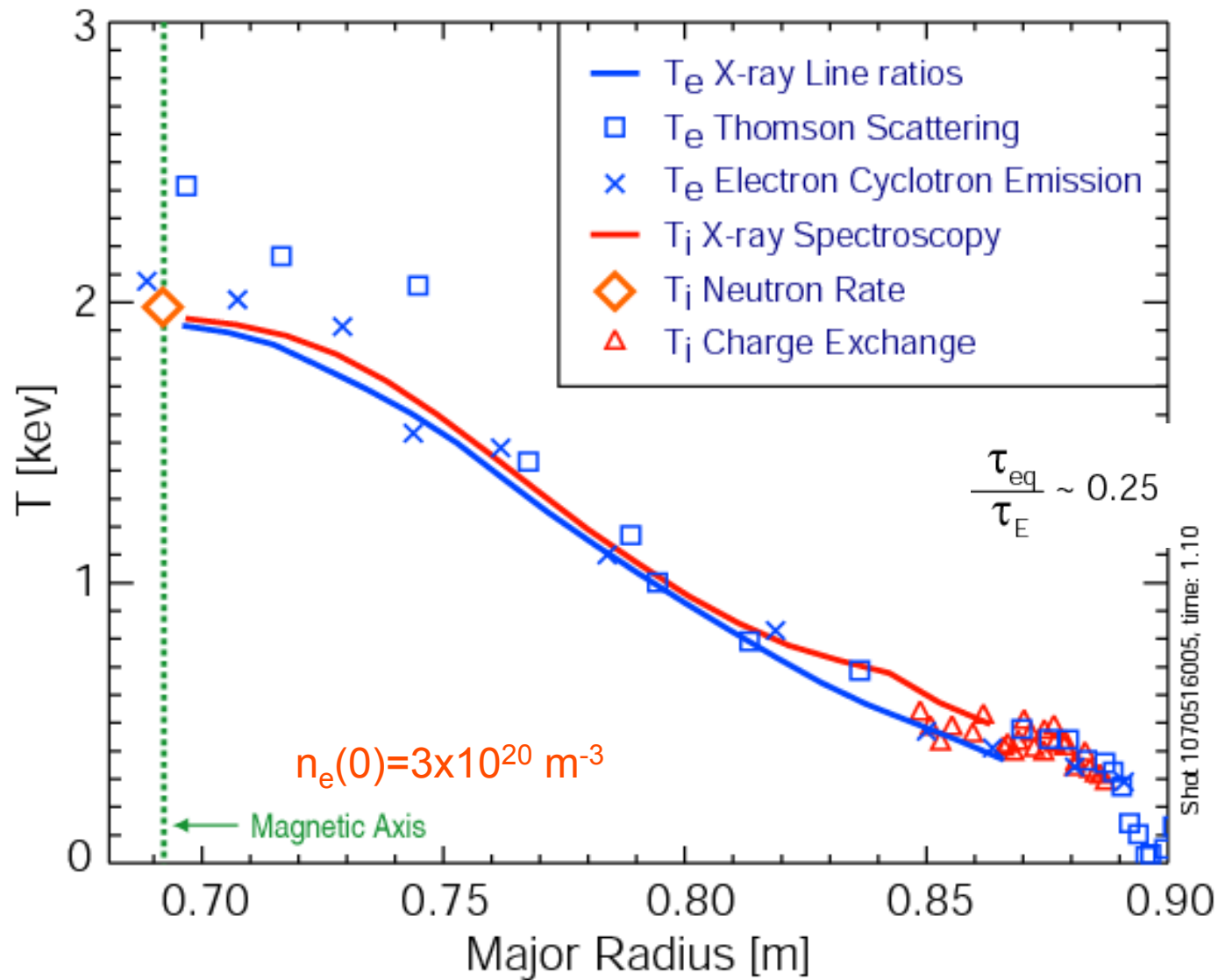


I. Condea, Physics of Plasmas, V7, #9, 3641 (2000)

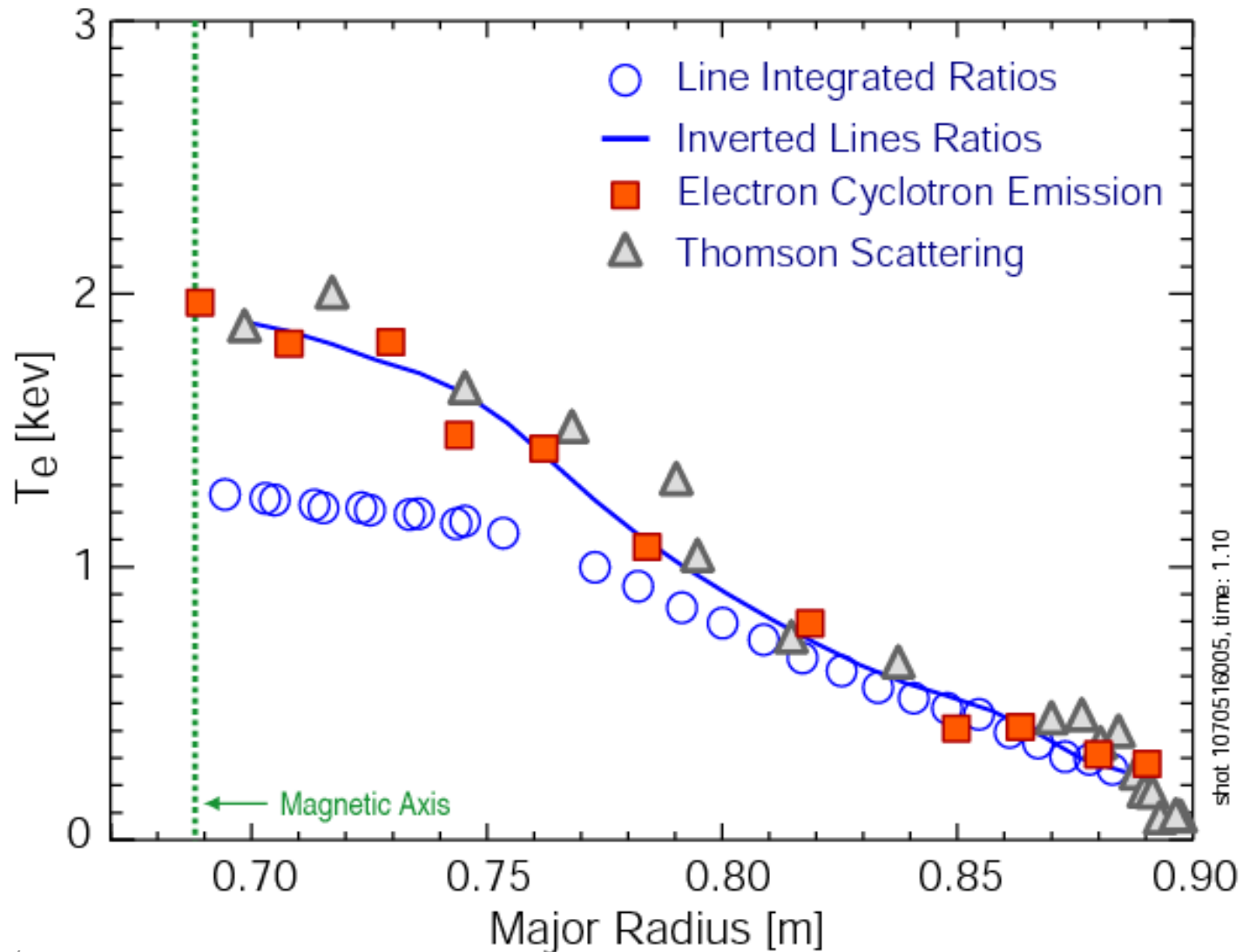
K. W. Hill 8/2011

Comparison of imaging XCS measurements with other diagnostics

Ion and electron temperatures are equal at very high density, as expected



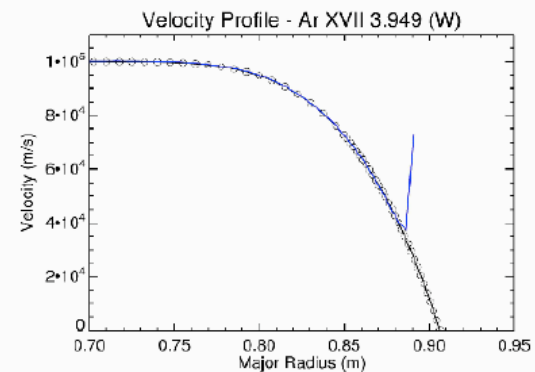
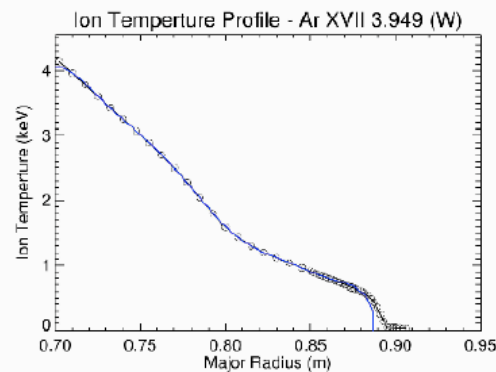
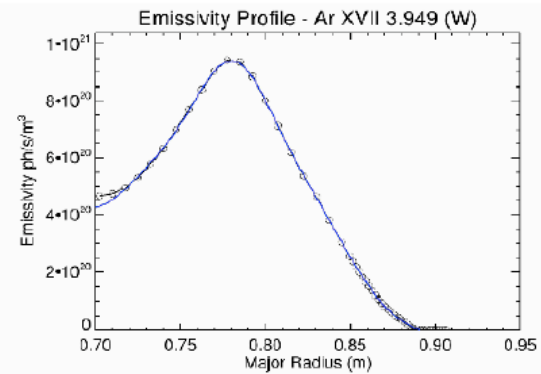
Electron temperature from inverted line ratios agrees with other T_e measurements



Reconstructed emissivity, T_i , and v_{tor} values are good even at high T_e such that the Ar 16^+ profile is hollow

Inversion Simulation: He-like 'w' line

- Black w/ circles indicate inputs
- Blue line is reconstruction
- All three profiles can be accurately reconstructed



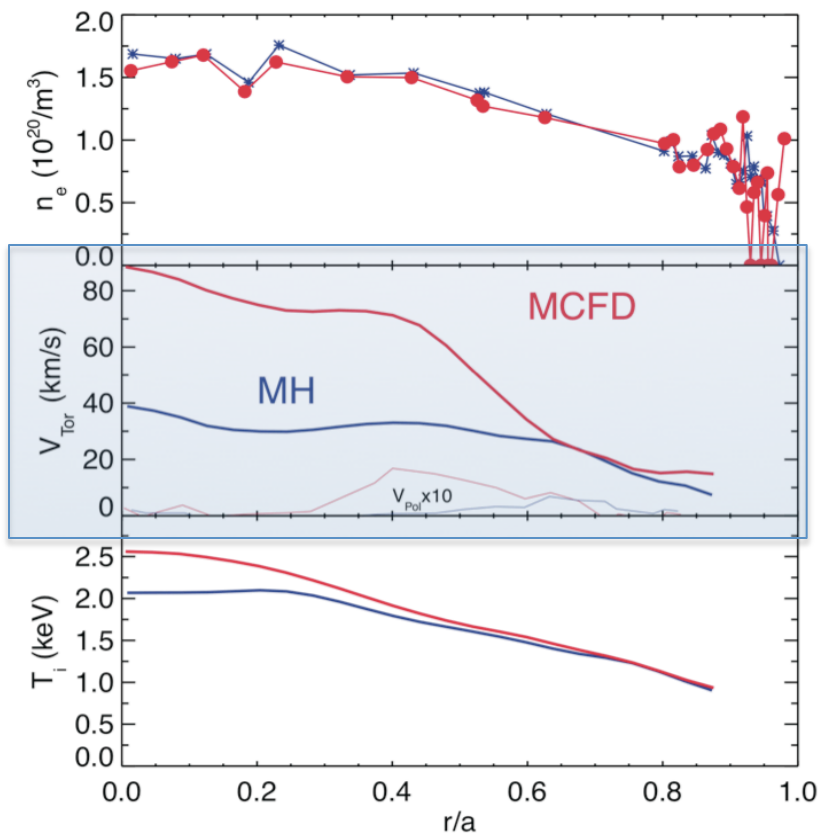
1050426022 t=1.4 H-mode

niex jr. Jr. 24

M. L. Reinke

New physics understanding of RF wave-induced flow drive is evolving: C-Mod

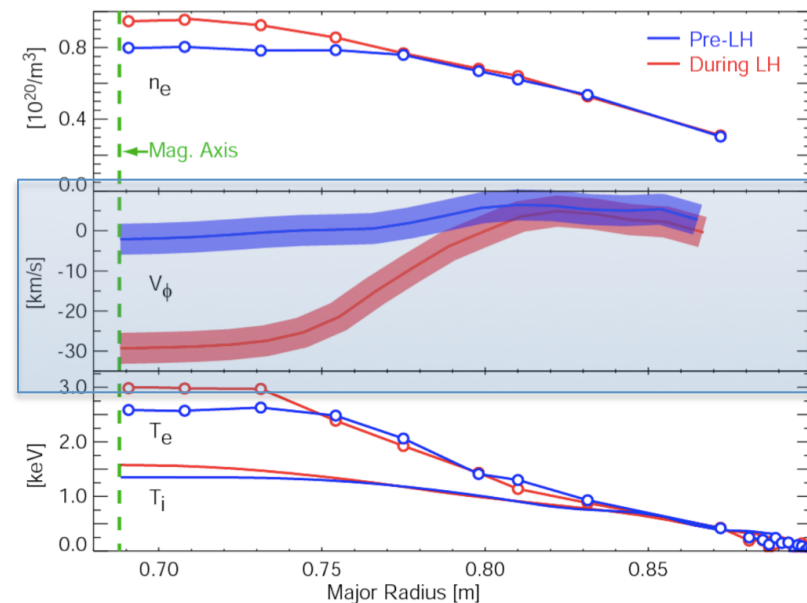
Mode-conversion ICRF produces 2x greater flow drive than does minority heating



Rice

K. W. Hill 8/2011

Lower hybrid waves produce negative toroidal rotation



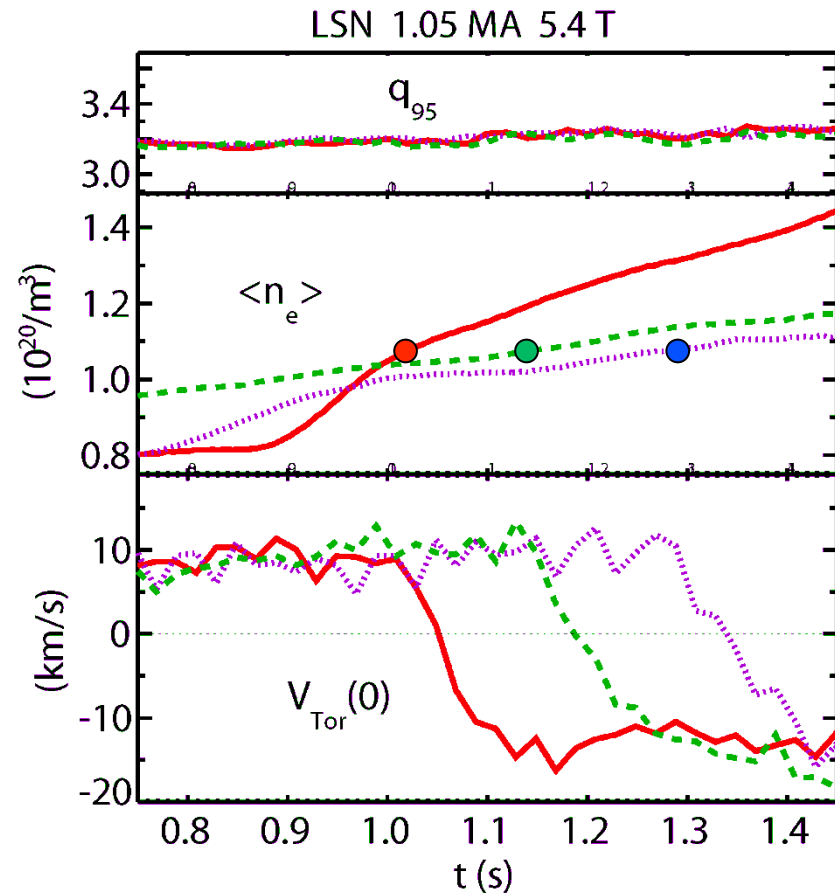
Ince-Cushman

RF injection provides some ability to control the toroidal rotation profile

26

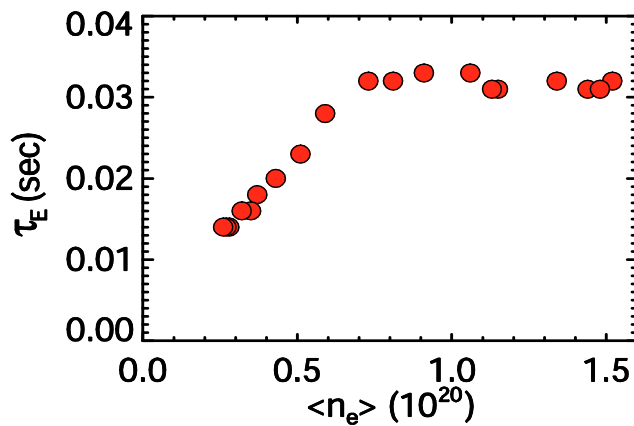
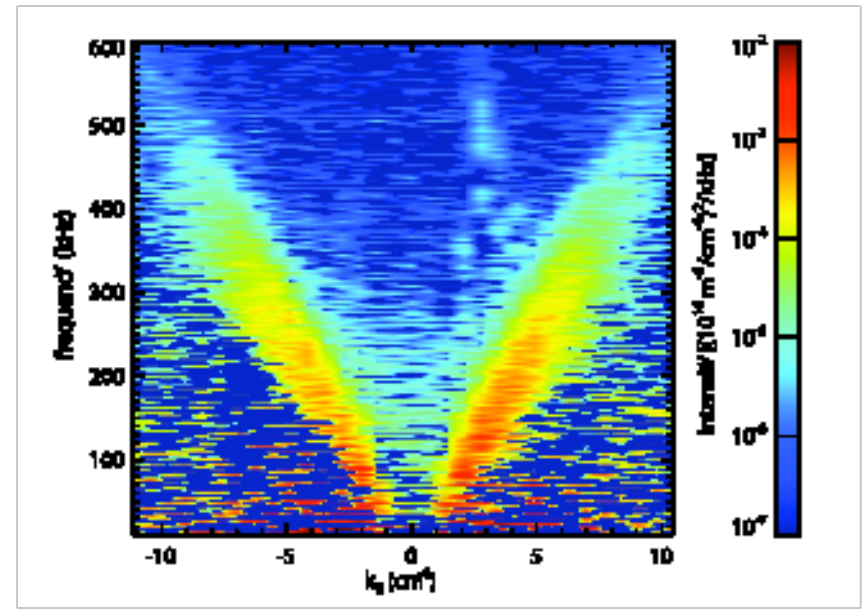
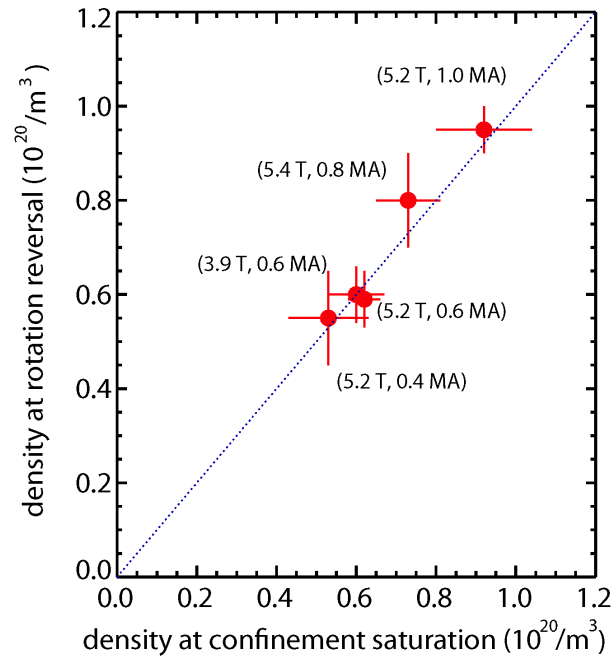
Self-Generated Flows and Momentum Transport

- Strong, co-current self generated toroidal rotation in H-modes and higher density L-modes (M up to 0.2-0.3)
- Ongoing experimental, theory and computational collaborations to understand intrinsic rotation, residual stress, momentum transport.
- Complicated behavior in L-mode including flow reversal at critical density.
 - Rotation reverses from co to counter as density is increased
 - Dependent on q_{95}
 - Reversal is inside $q = 3/2$ surface
 - Correlated with change in fluctuations and confinement regime



In L-mode, self-generated flow reverses sharply at some q dependent critical density (Rice, et al.,).

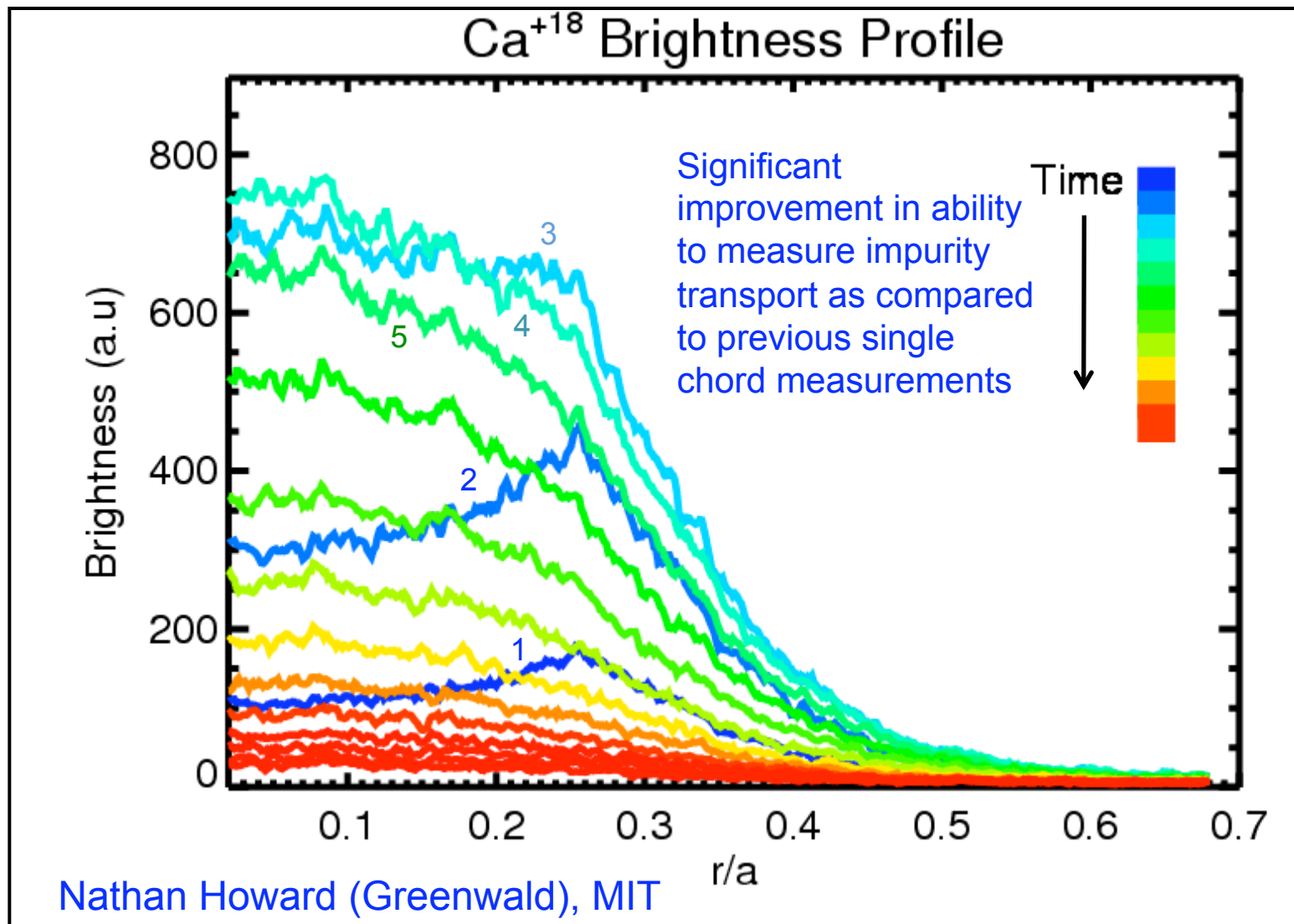
Flow reversal occurs at same density as transition between LOC and SOC



- Self-generated rotation & momentum transport
- Linear Ohmic Confinement vs Saturated Ohmic Confinement (electron dominated vs ion dominated)
- Change is accompanied by loss of fluctuation feature seen with PCI.

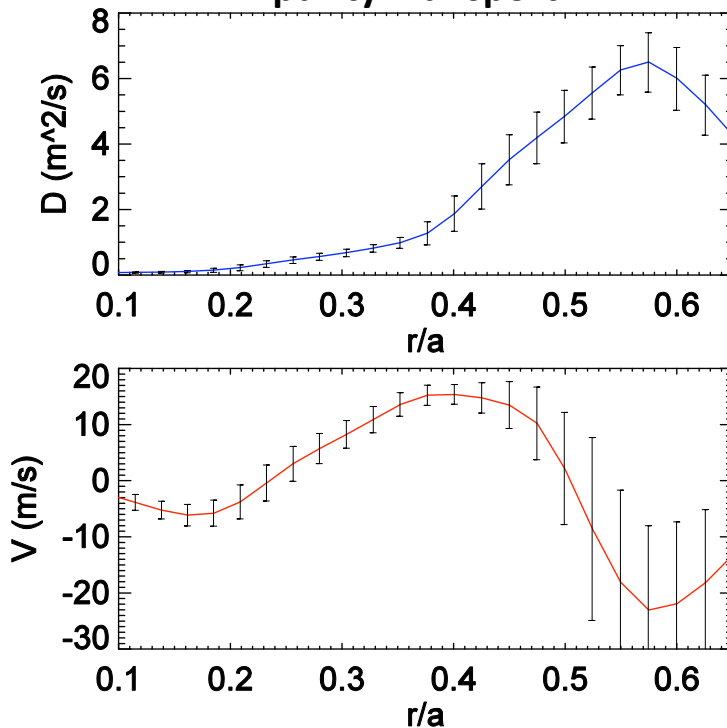
M. Greenwald

Impurity transport: Full profiles of injected He-like calcium ion are measured with good time resolution

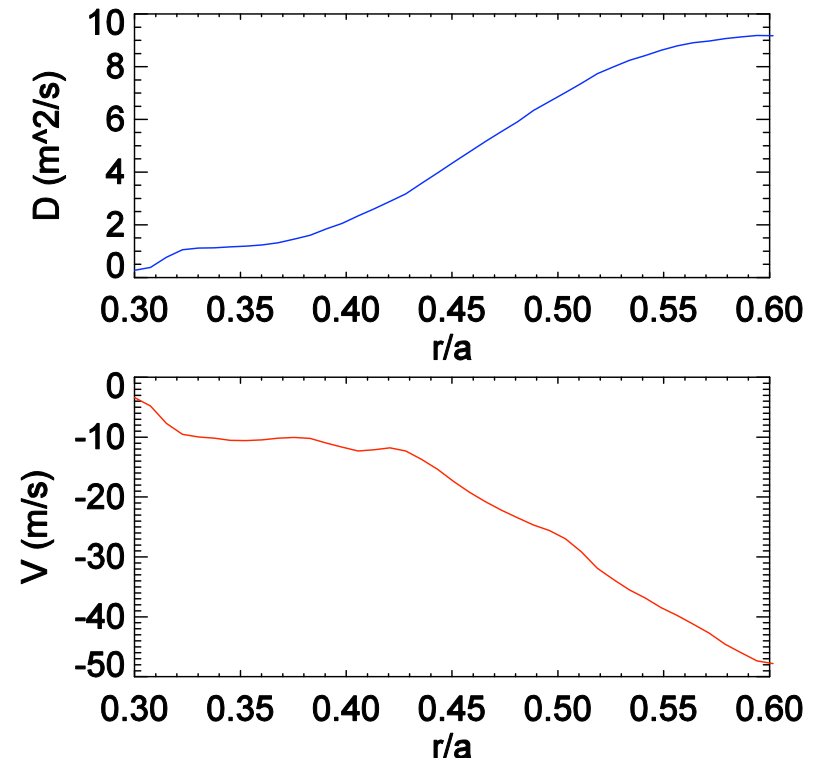


Ongoing particle transport analysis compares measurements with linear and nonlinear gyrokinetics

STRAHL/Experimentally Determined Impurity Transport



GYRO Computed Impurity Transport



- *Initial global, nonlinear simulations have been performed using GYRO for comparison with experiment.*
- *Comparisons demonstrate decent agreement but full-physics simulations using all profile diagnostics are in progress as part of an ongoing impurity transport validation effort.*

R&D for ITER XICS is being done at C-Mod

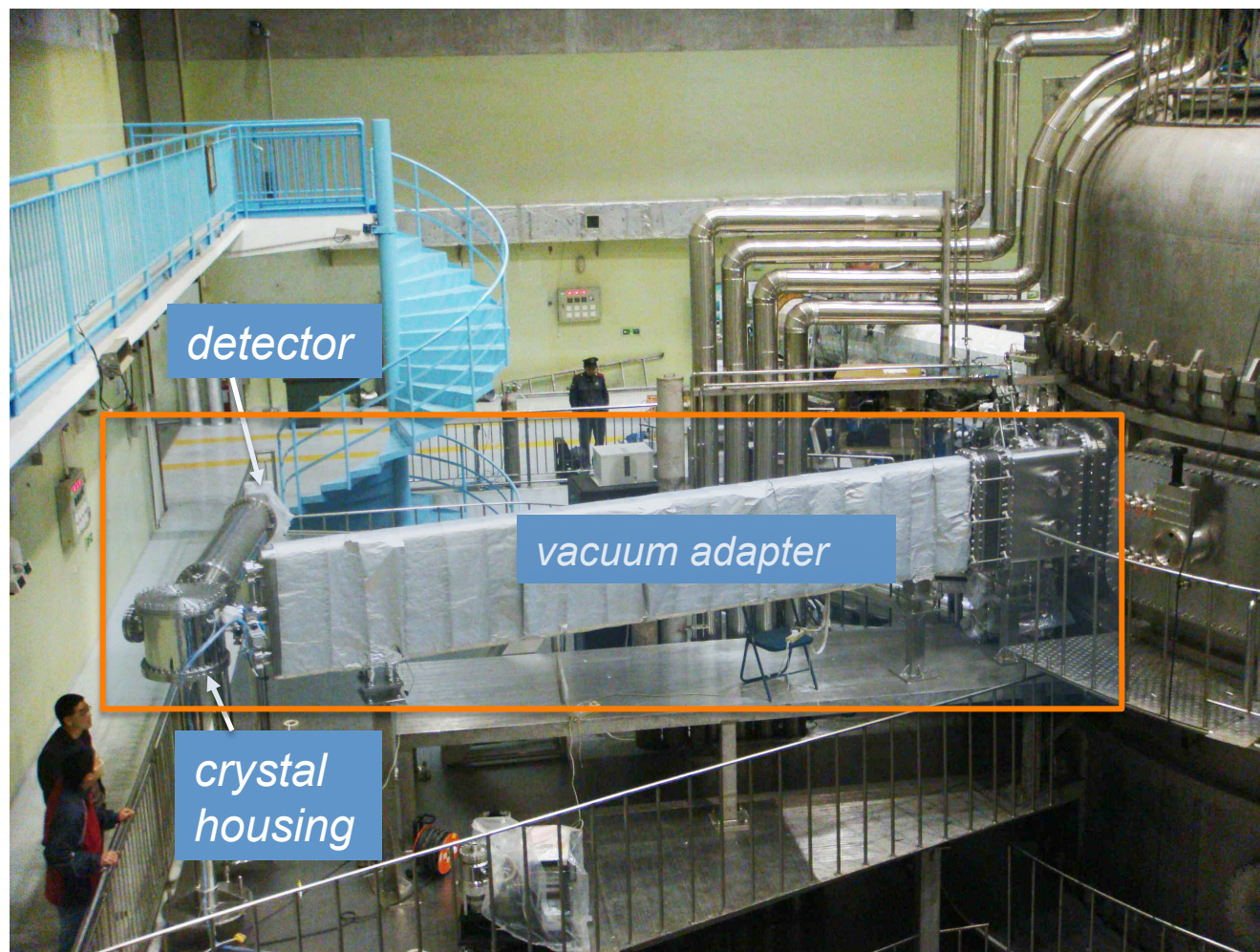
- X-ray line sources for absolute wavelength calibration
- Temperature stabilization of crystal
- Crystals to measure tungsten L lines
 - Requires $T_e > 8$ keV
 - $T_e > 8$ keV achieved briefly and in small volume
 - JET would be much better for this R&D
- Crystals to measure krypton $K\alpha$ lines

Imaging x-ray crystal spectrometers on
the **EAST** and **KSTAR** advanced
superconducting tokamaks in **China** and
Korea



Two imaging spectrometers have been installed on **EAST** in China, and two on **KSTAR** in Korea

EAST



- Large adapter enables view of most of plasma

- Using Multiwire Proportional Counters (maximum count rate 2 MHz over entire detector)

- Planning to buy Pilatus pixel detector arrays (1 MHz per pixel)

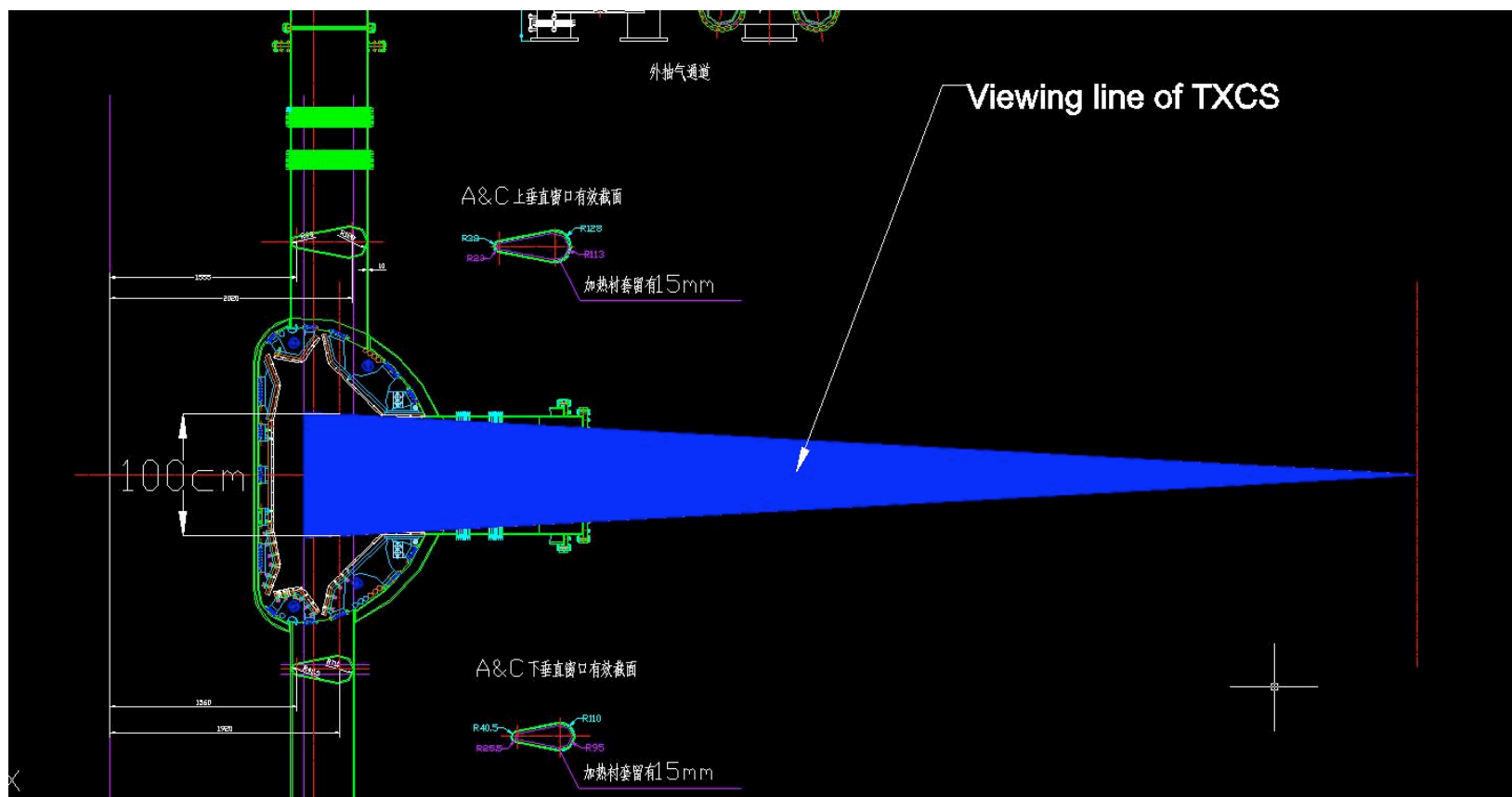
Tangential imaging XCS on the EAST tokamak

Y. Shi
B. Wan



The EAST TXCS views 100 cm of plasma height

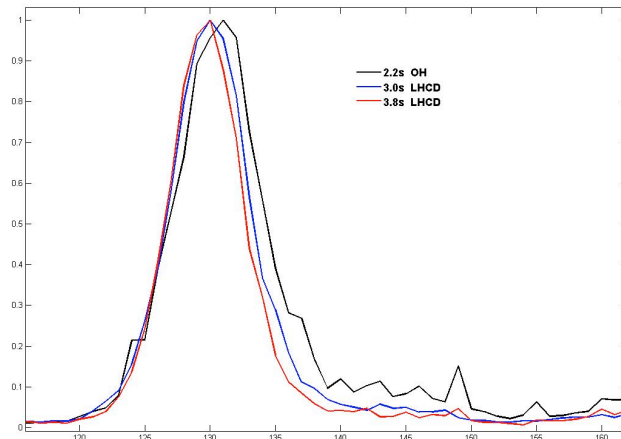
EAST



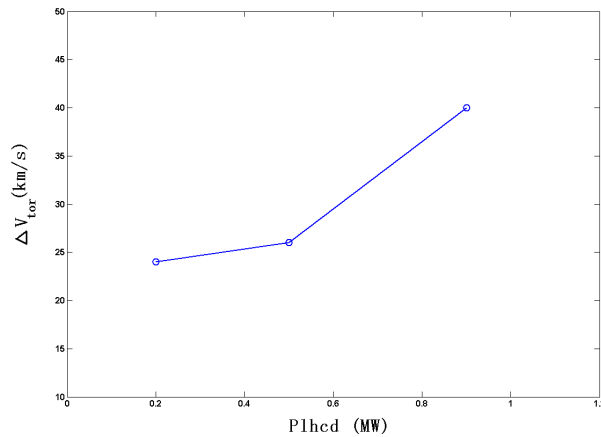


Toroidal rotation velocity profiles are being measured on EAST

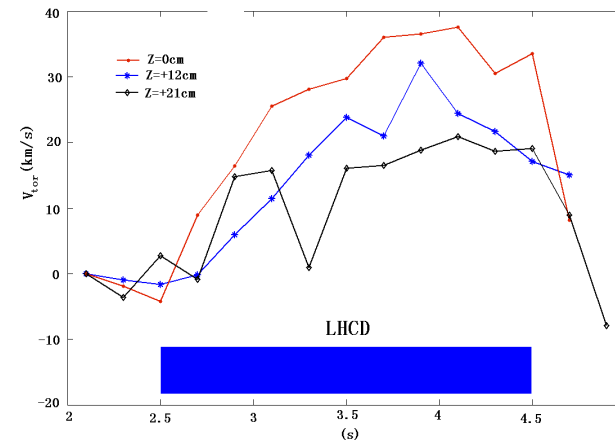
EAST



The Argon spectrum in one DN LHCD plasma. Such obvious Doppler shift cannot be found in limiter LHCD plasma.

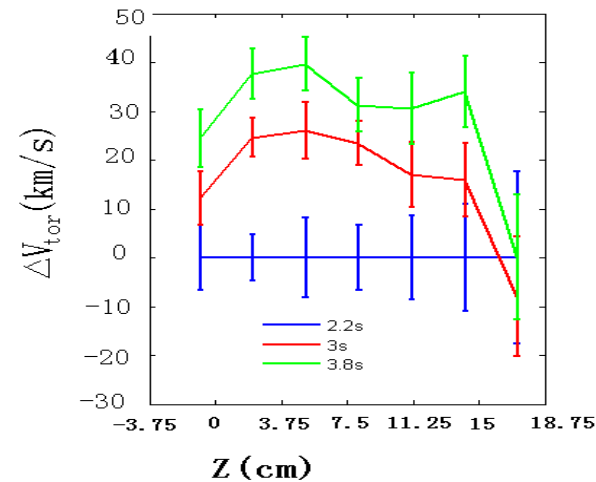


The relation between the LHCD power and the relative central toroidal rotation velocity.



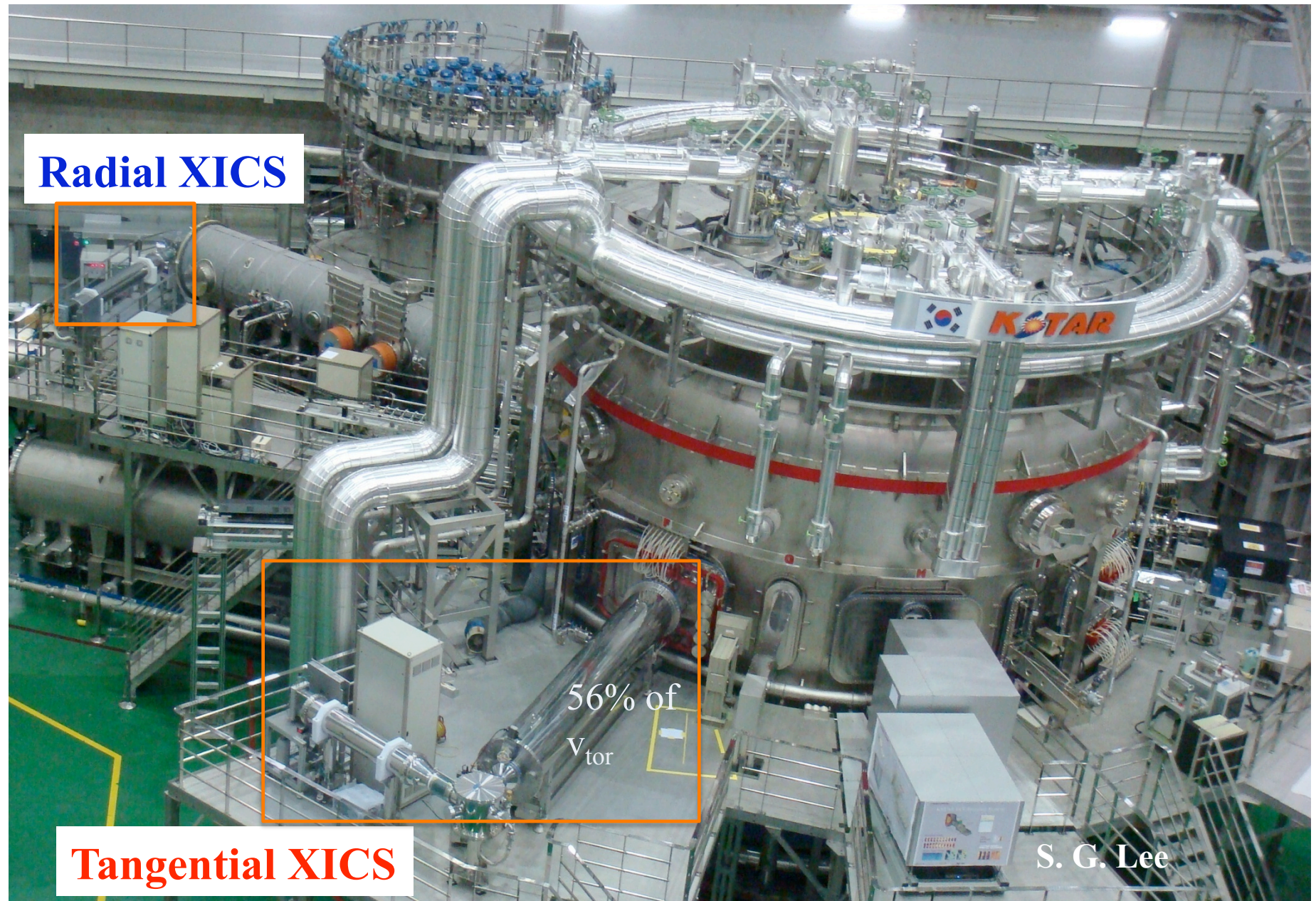
Y. Shi
B. Wan

The time evolution of toroidal rotation.

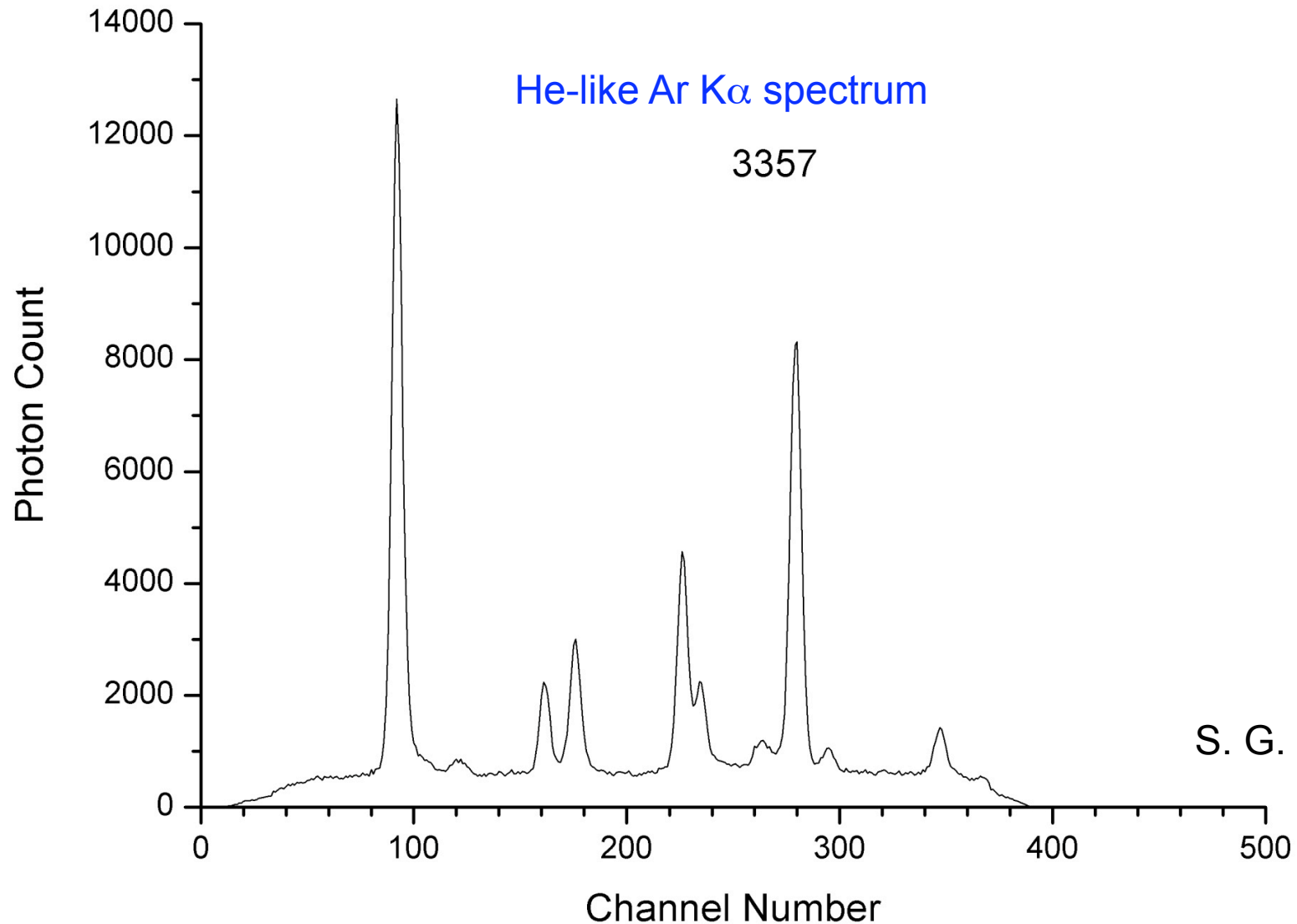


The relative toroidal rotation velocity profile in a 0.9MW DN LHCD plasma

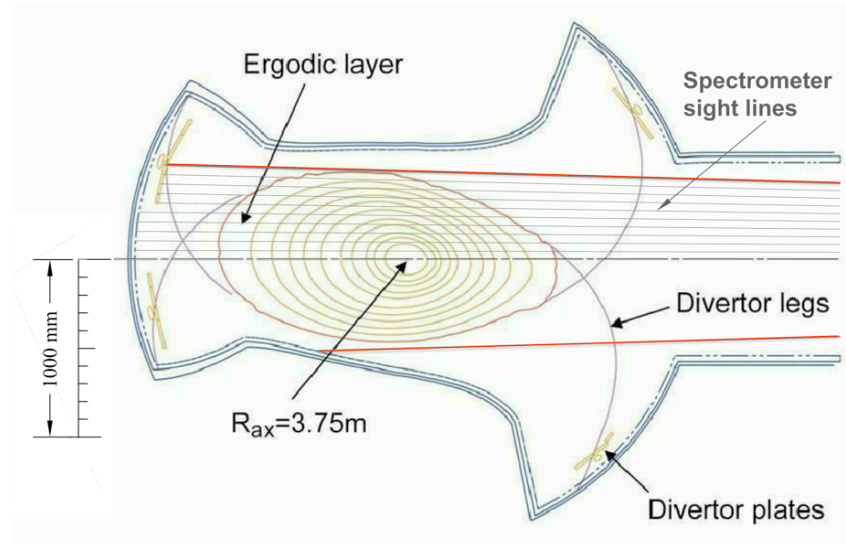
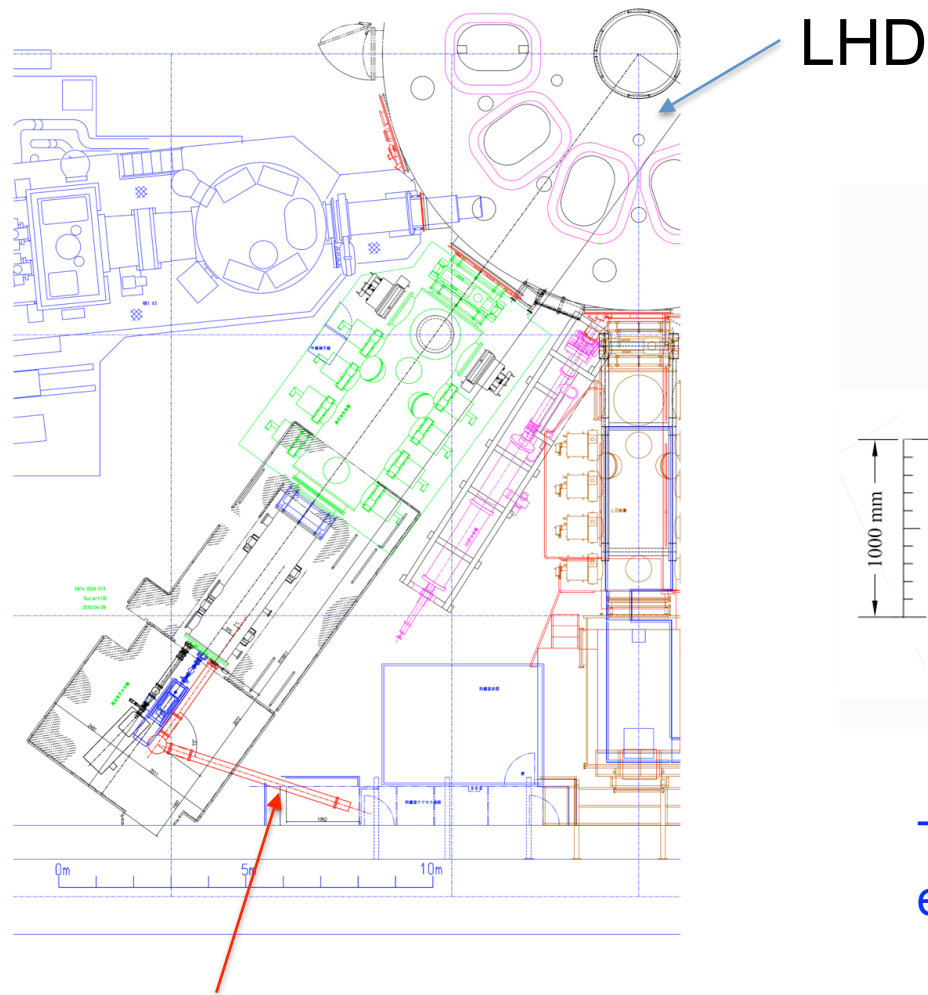
Two KSTAR XICS were available for the 2010 Experimental Campaign



T_i and v_{tor} measurements are also being made on KSTAR with two imaging XCS systems



PPPL has built and installed an imaging XCS on the LHD stellarator at NIFS; currently operating

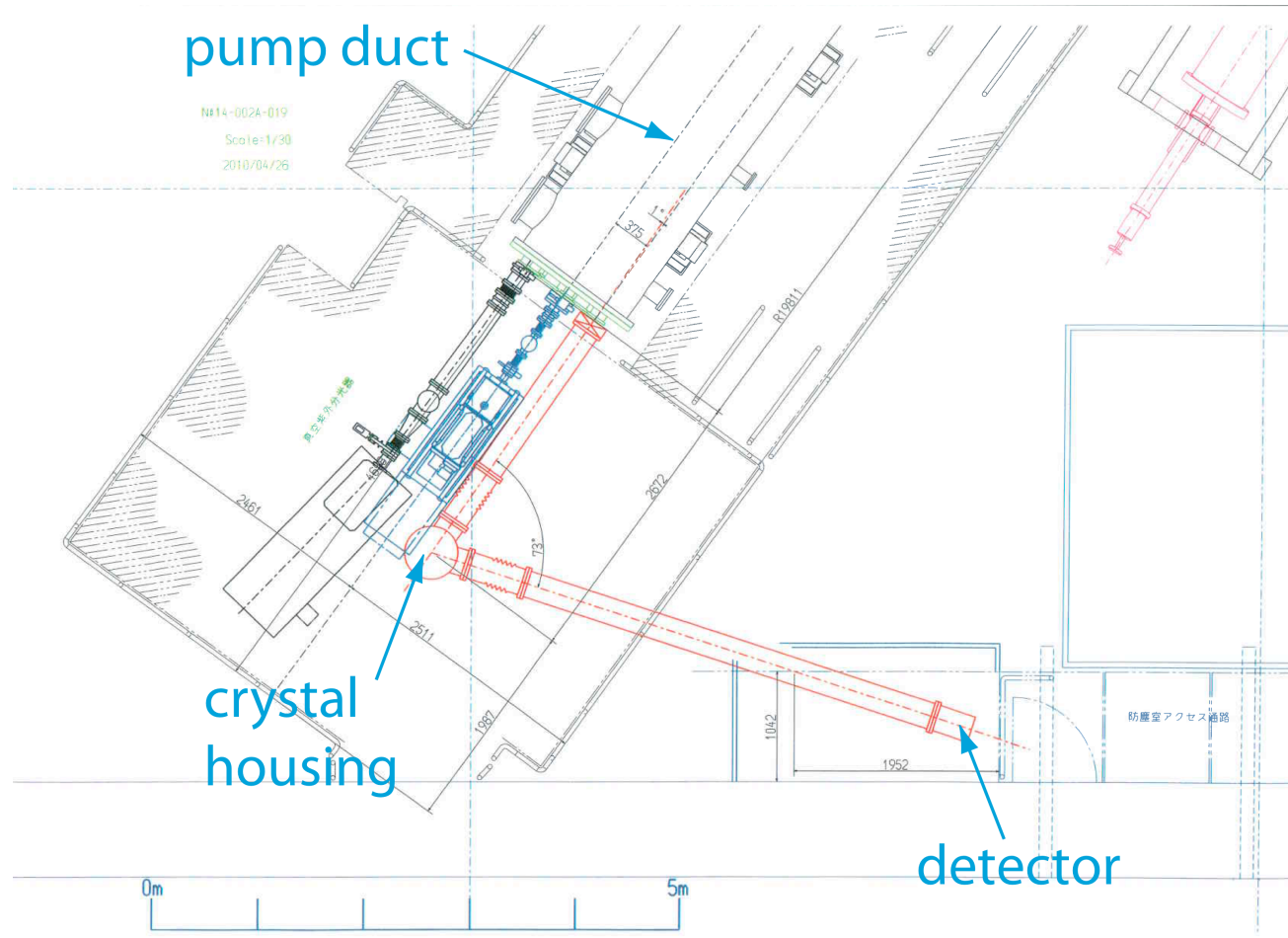


The imaging XCS can view the entire LHD minor cross section.

Imaging XCS

Crystal is ~18m from plasma

The LHD imaging XCS will view the plasma from the end of a pumping duct

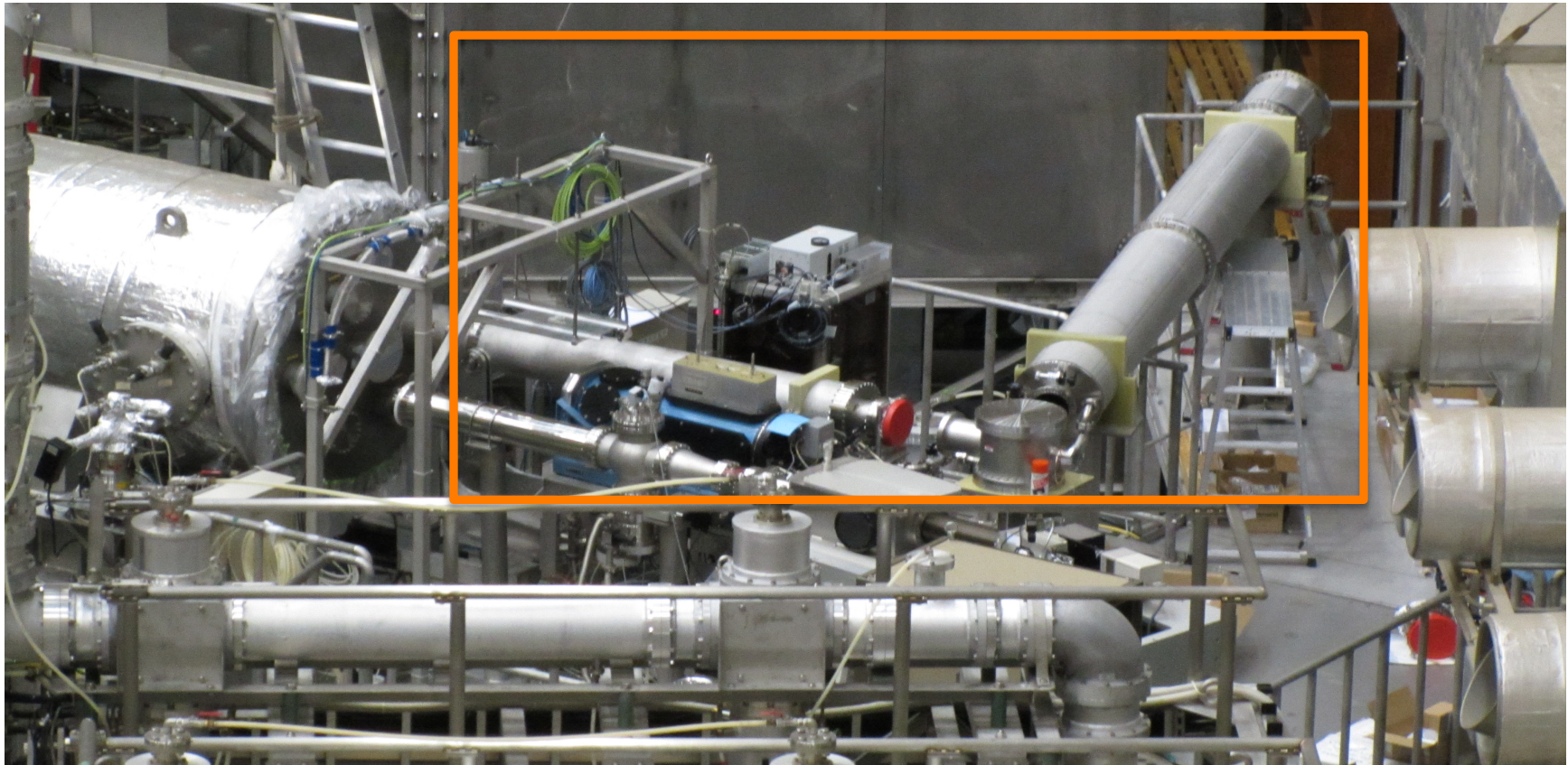


LHD personnel constructed a new platform for the imaging XCS spectrometer



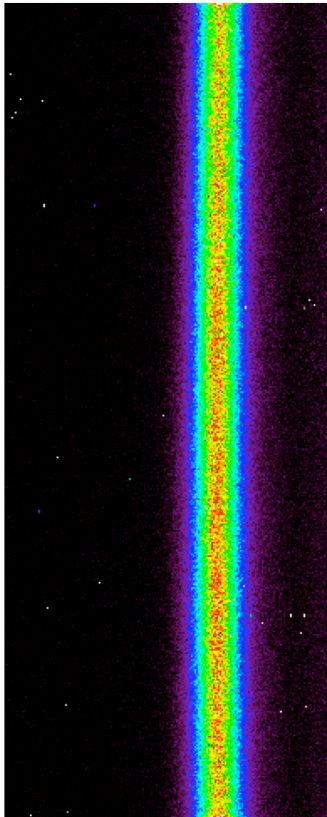
Spectrometer was installed in May, 2011

Installation of XICS in LHD machine hall is complete, and spectrometer is operating

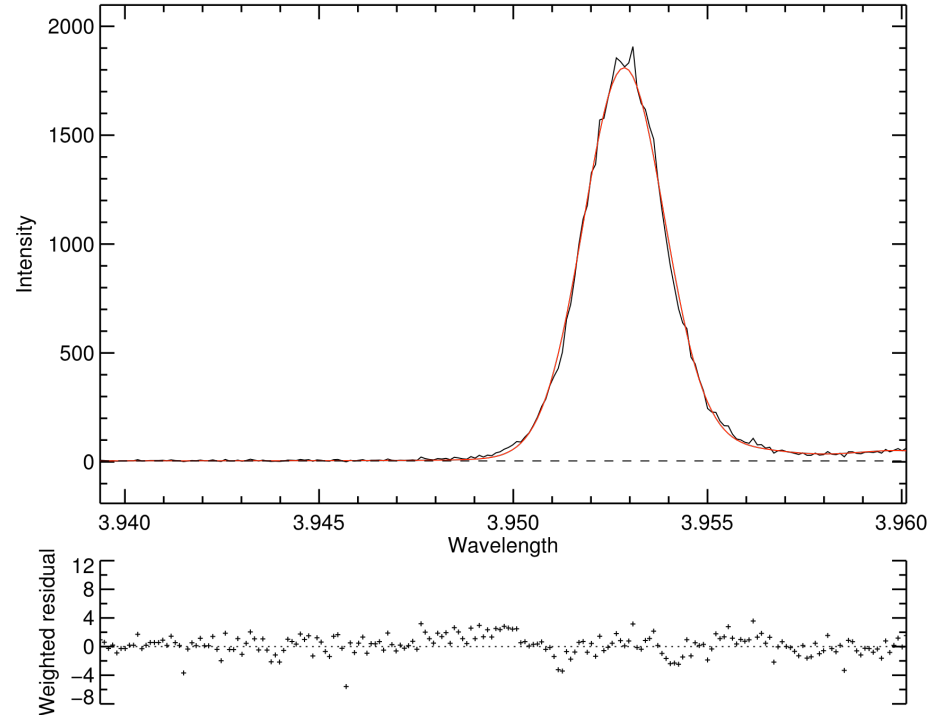


The LHD XICS measured spectra on the first shot, 104836, July 27 2011

Ar¹⁶⁺ line w within 5 mm of intended location on detector



Ti=2.51 keV, Te=2.49 keV at 3.6 s with 20 ms integration, ~1.5 cm spatial resolution



Preliminary

Novimir Pablant

One Pilatus module measures ~ 30 cm of the 100-cm high LHD plasma cross section

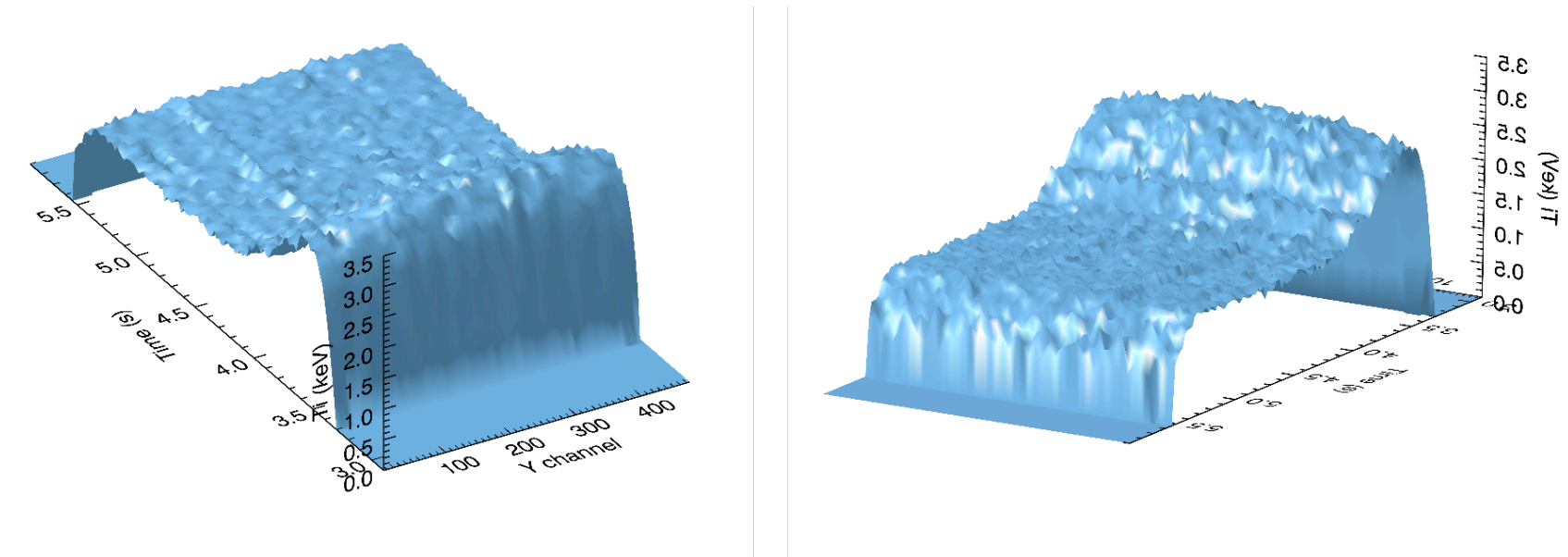


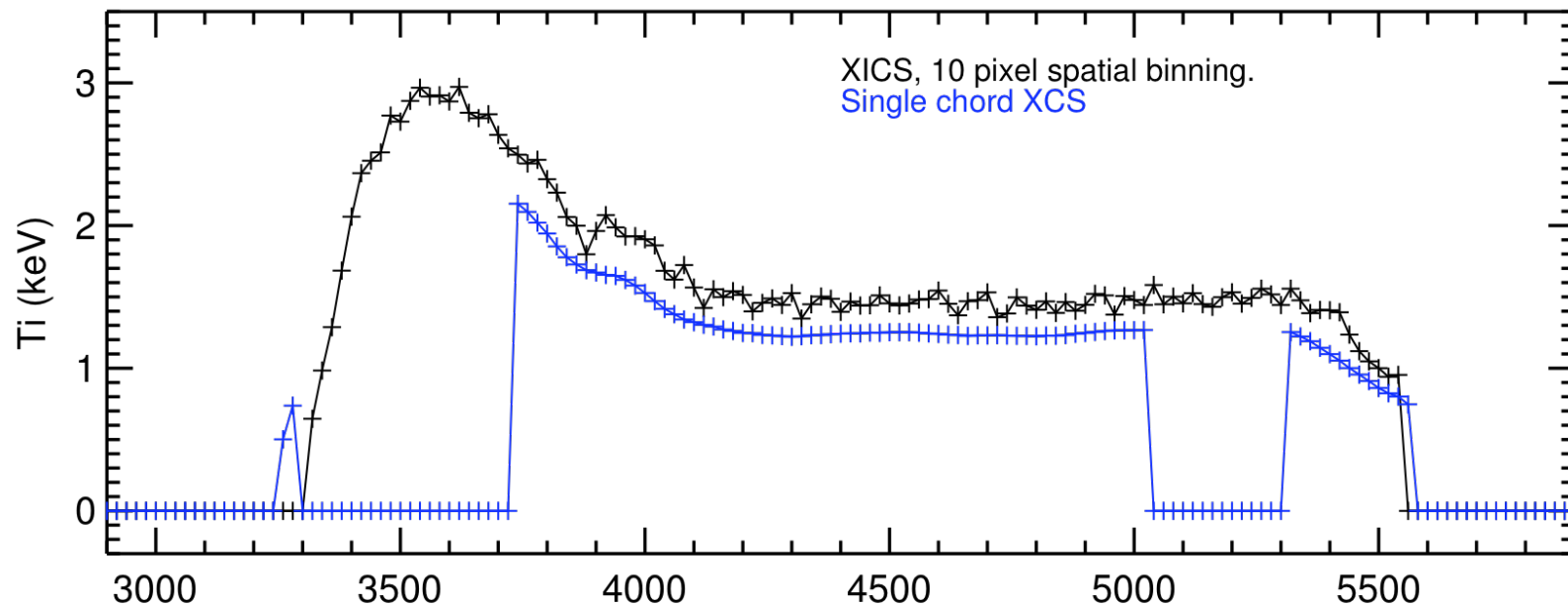
Figure 1: Ion temperature from the LHD XICS system. Shot: 104838, Integration: 20ms.

Preliminary

Novimir Pablant

New LHD XICS has similar time history as that of the existing single chord spectrometer

LHD XICS | SHOT:104838



Preliminary

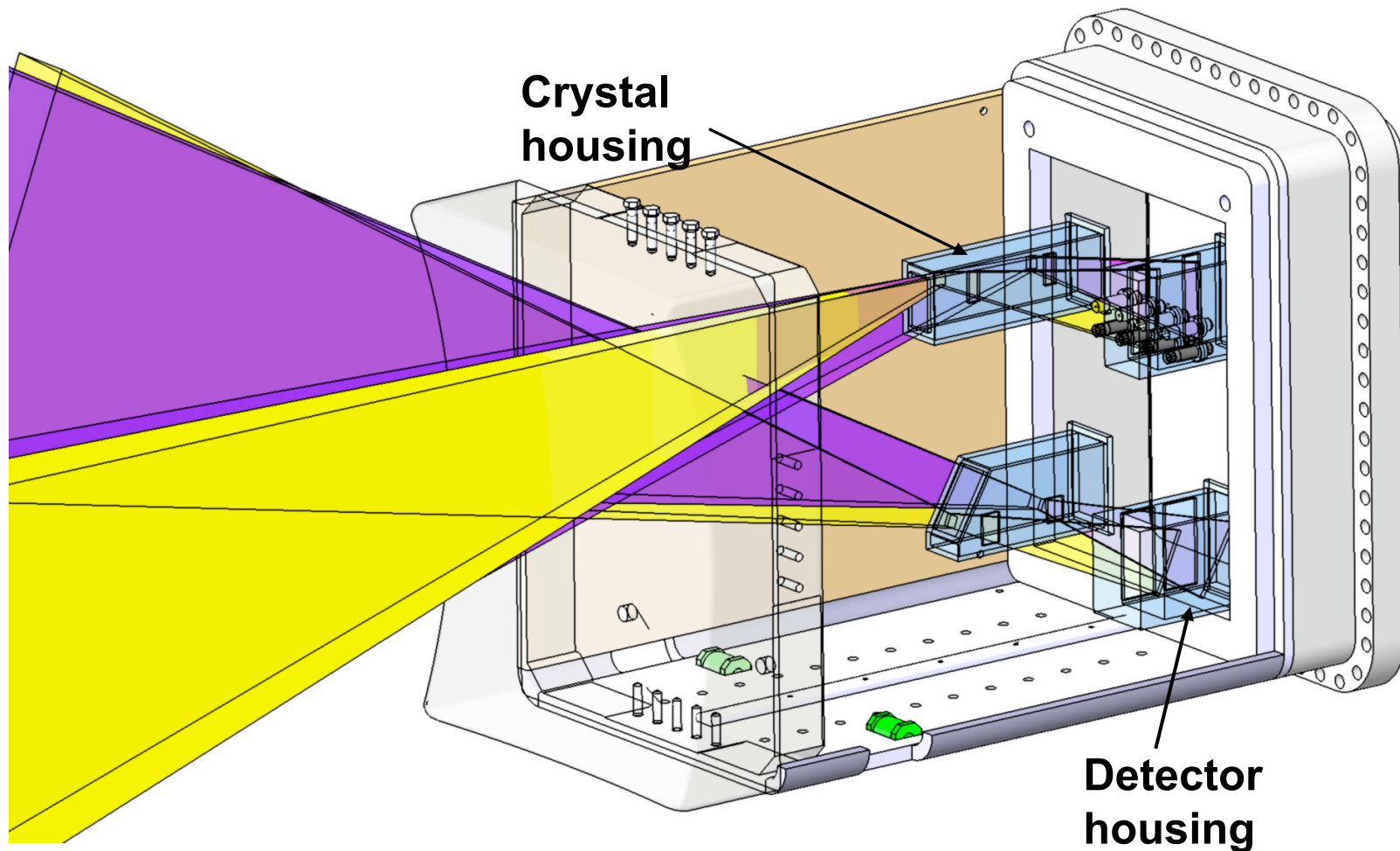
Novimir Pablant

A US-ITER Team is Designing The ITER Core Imaging X-Ray Spectrometer (CIXS)

- The CIXS is a primary diagnostic for ion-temperature (T_i) and flow-velocity (v) measurement on ITER

ITER CIXS Design

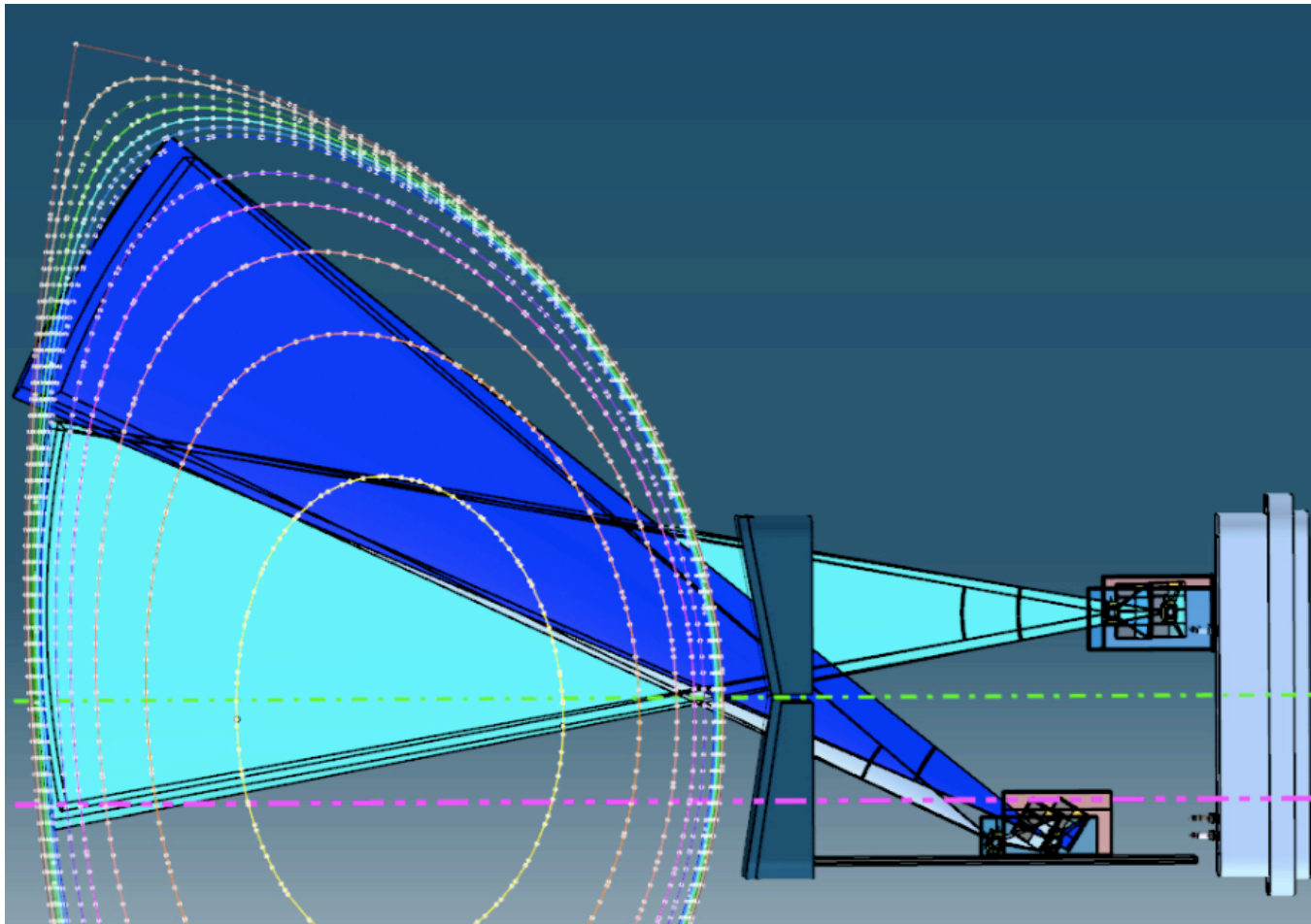
ITER core XICS dimensions similar to those of C-Mod spectrometer



CIXS sightlines will partially overlap views of edge imaging XCS, to be built by Indian team, for full plasma view.

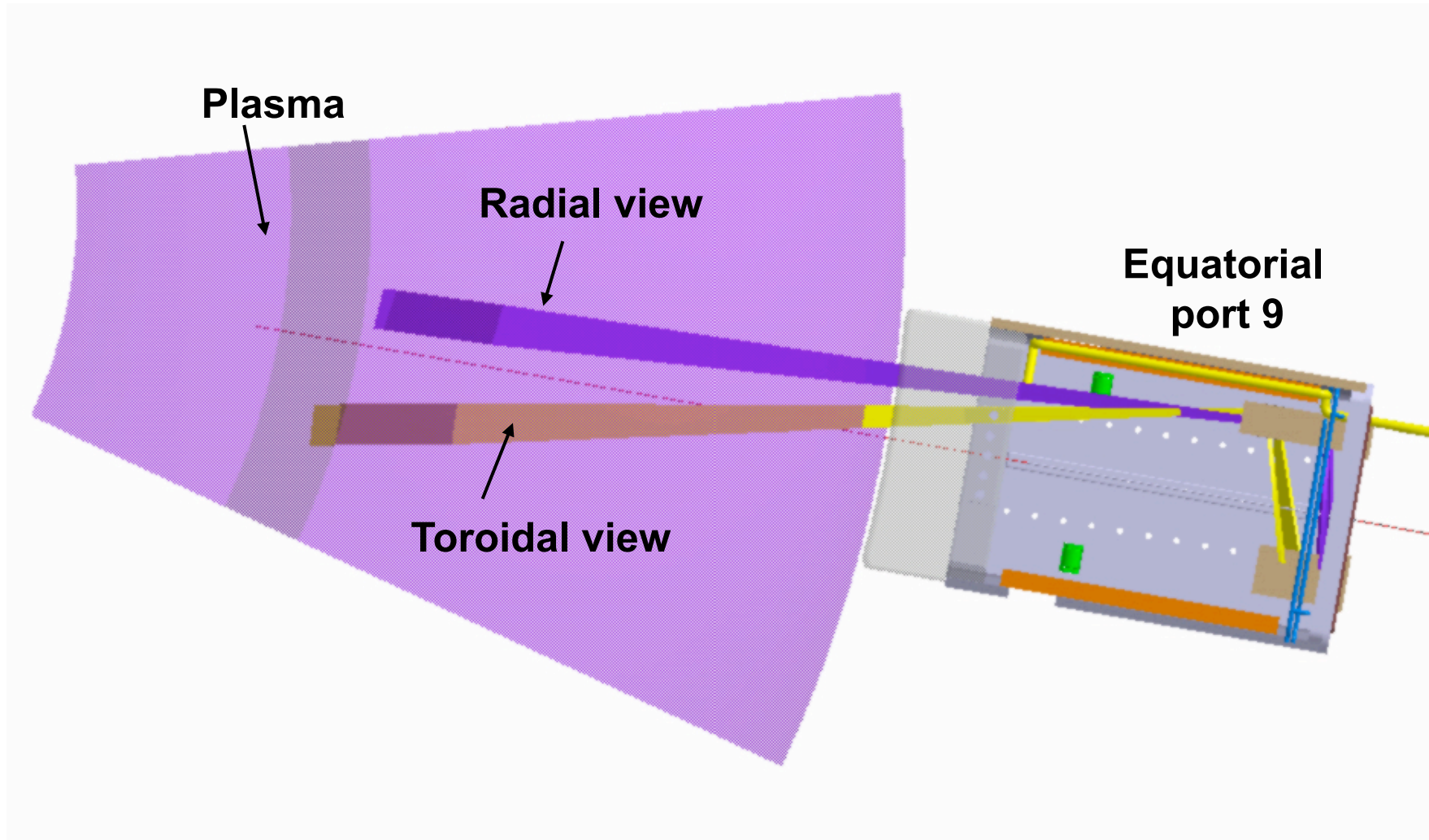
Two spectrometers cover most of plasma core

5:1 demagnification



Edge spectrometer by Indian team overlaps core spectrometer view.

Radial view for poloidal rotation and T_i , and tilted view for toroidal rotation and T_i



Performance analysis of ITER Core Imaging X-Ray Spectrometer

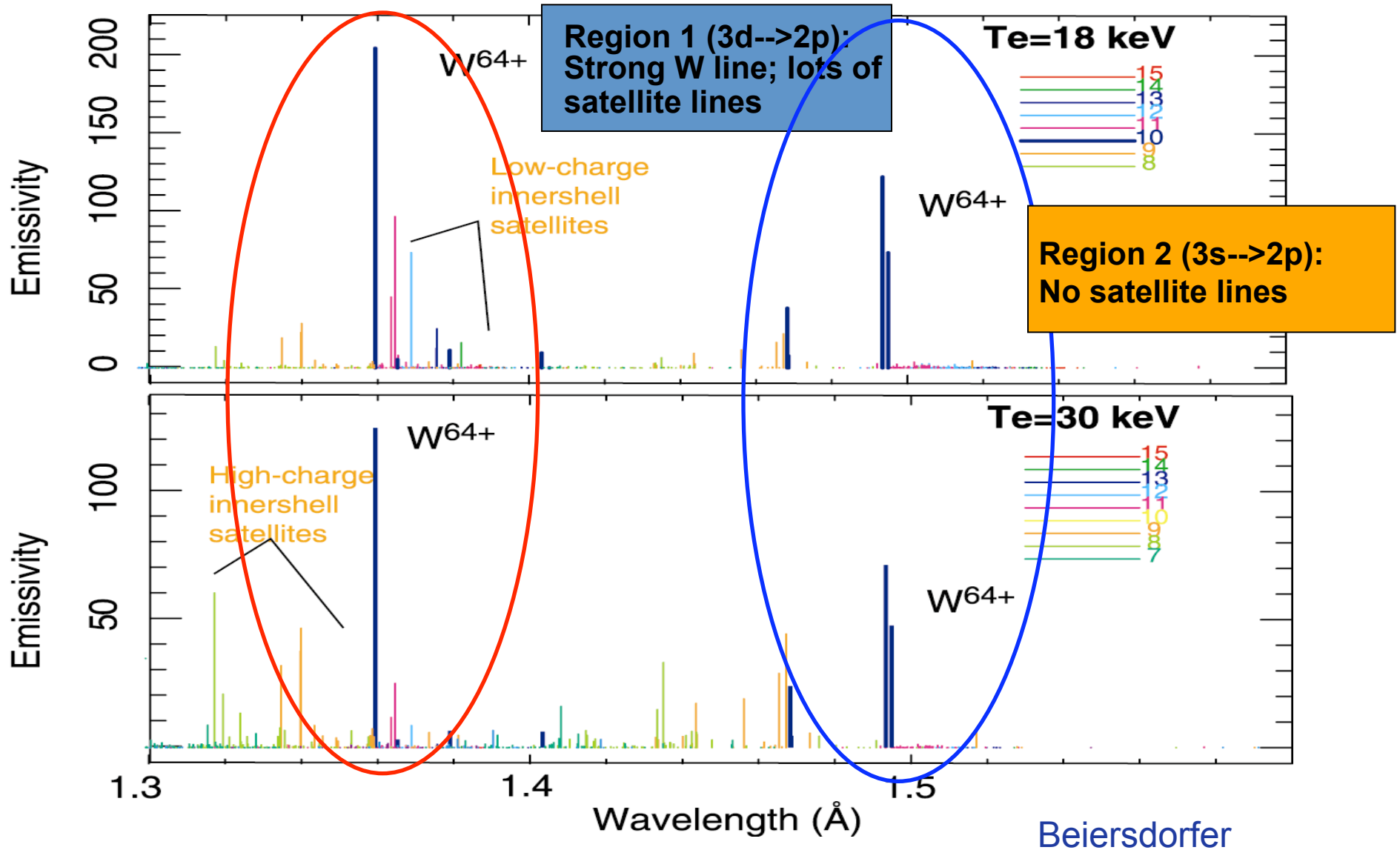
CIXS must satisfy ITER physics requirements

Parameter	Spatial coverage	Range	Time resolution	Spatial resolution	Relative accuracy
T_i	$r/a < 0.9$	0.5 – 40 keV	100 ms	$a/30$	0.1
v_{tor}	$r/a < 0.9$	1-200 km/s	10 ms	$a/30$	0.3
v_{pol}	$r/a < 0.9$	1-200 km/s	10 ms	$a/30$	0.3

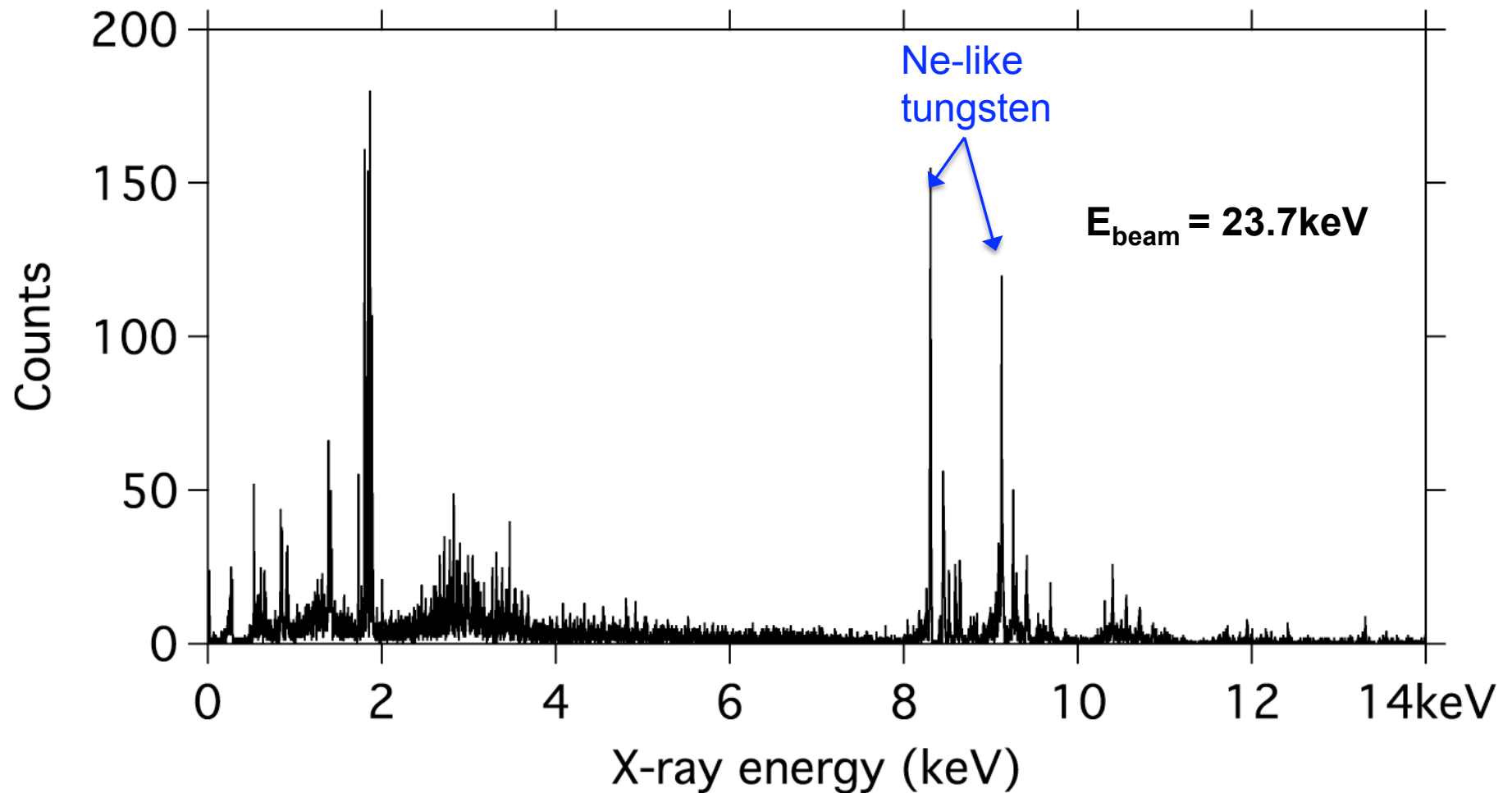
Spectrometer performance depends on several factors

- **Spectral lines measured: Fe, Kr $K\alpha$, tungsten L lines**
- **Statistics: line excitation rate (T_e), concentration,...**
 - Count rate
 - Temporal binning
- Instrumental resolution
- **Degradation due to background**
- Line overlap at high ion temperature
- **Propagation of inversion uncertainties**
 - Incomplete spatial profile coverage
 - Propagation of statistical uncertainties
 - **Errors in flux-surface calculations**

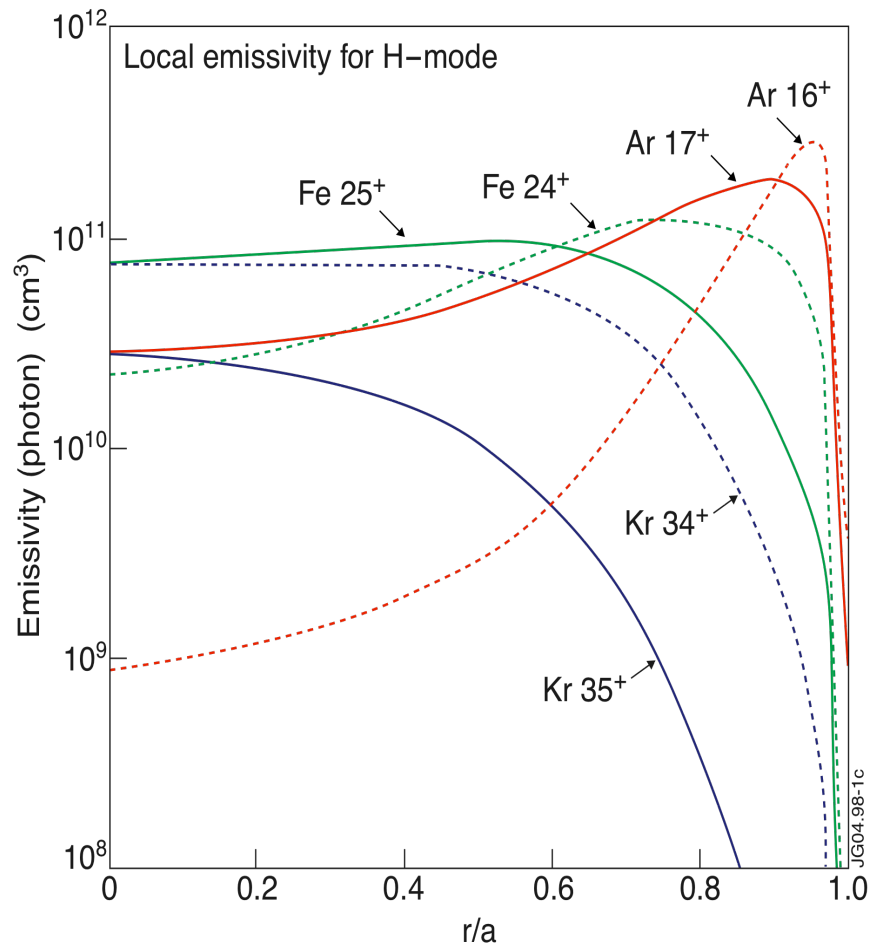
Predicted neon-like tungsten spectra reveal two regions for measurement



Full tungsten spectrum measured from EBIT with a cryogenic x-ray microbolometer



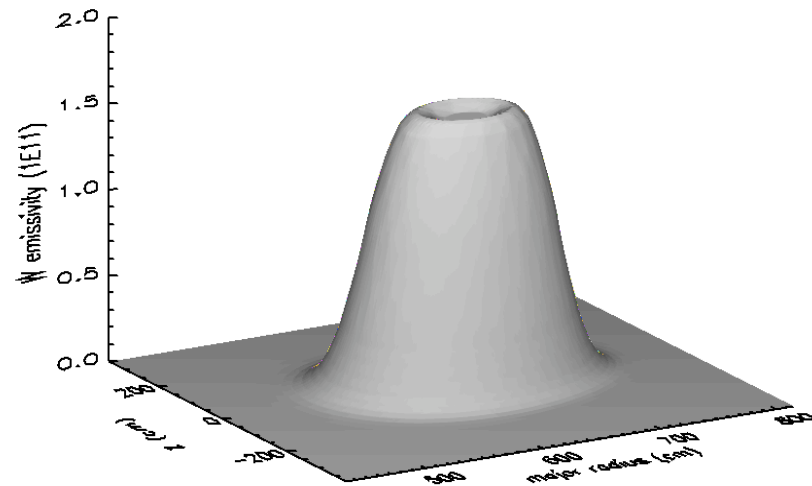
Fe & Kr $K\alpha$ and W L lines suitable for diagnosing core of ITER H-mode scenario plasmas



Barnsley

W L lines have advantages over Kr $K\alpha$

- Intrinsic
- 3-5x higher reflectivity crystals
- 8x higher emissivity
- Ne-like W abundant at $T_e=10-30$ keV

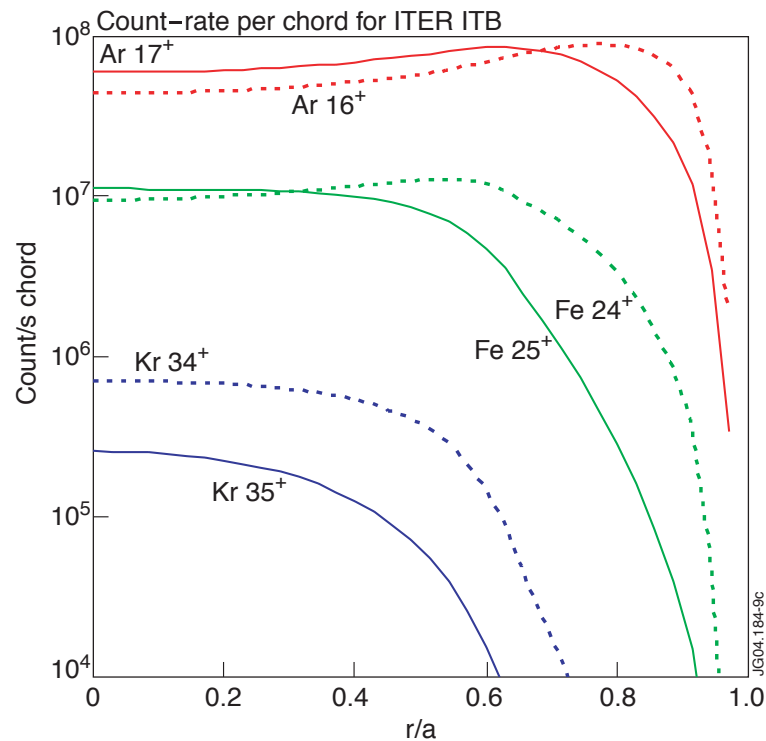


M. O'Mullane

Use lower Z elements during earlier phases with cooler plasmas

Chordal integrations of emissivity give MHz count rates per spatial-resolution element in center

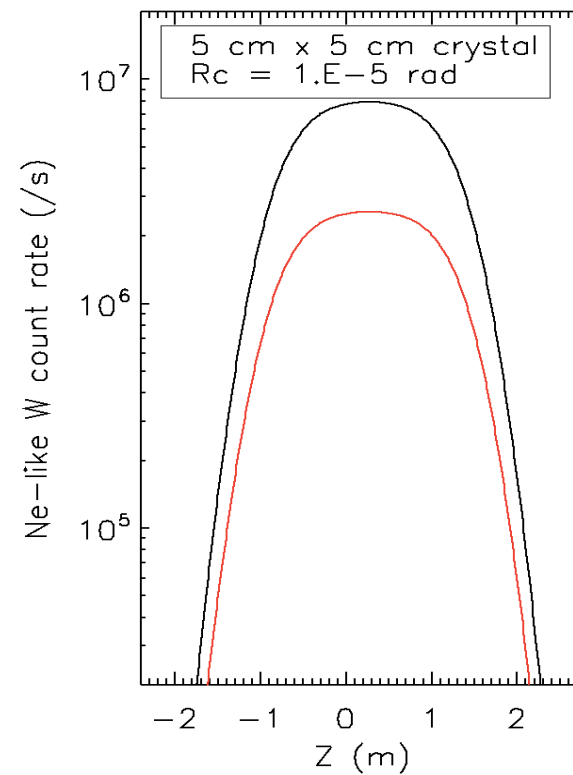
Fe K lines; 0.5 MW power
Barnsley



Statistical error 1% for 10000 counts in line

K. W. Hill 8/2011

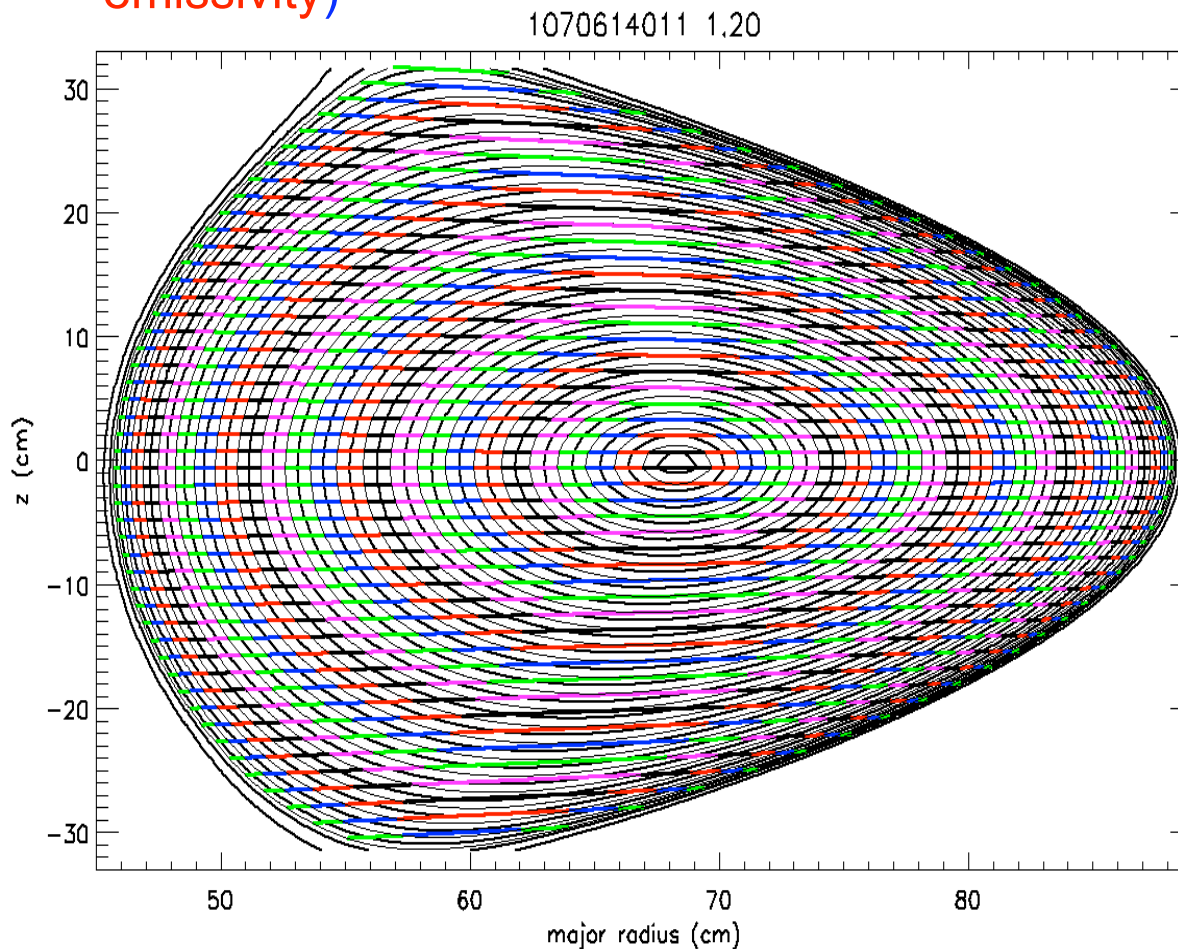
Ne-like W L lines, H-mode
 $r/a < 0.65$, $n_W/n_e = 10^{-5}$



Emissivity from Martin O'Mullane

Local emissivity is inferred from surface brightness using inverse path-length matrix

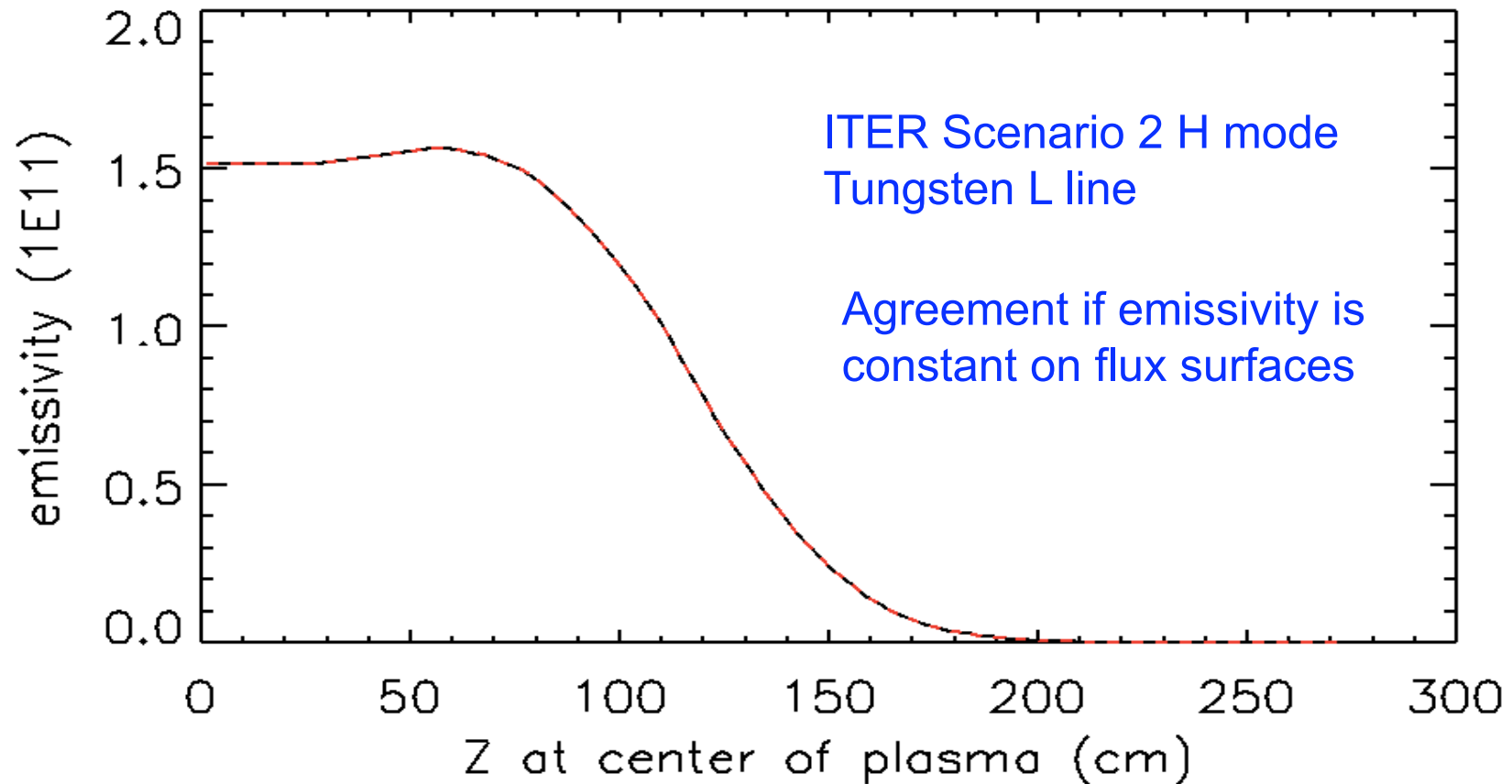
Chordal path lengths through zones of constant poloidal flux (constant emissivity)



- $B_i = \sum_j L_{ij} E_j$
- $E_i = \sum_j L_{ji}^{-1} B_j$
- $v_j = \frac{\sum_i M_{ji}^{-1} B_i u_i}{\sum_i L_{ji}^{-1} B_i}$
- $M_{ij} = L_{ij} \cos \theta_{ij}$
- Additional matrices for ion temperature

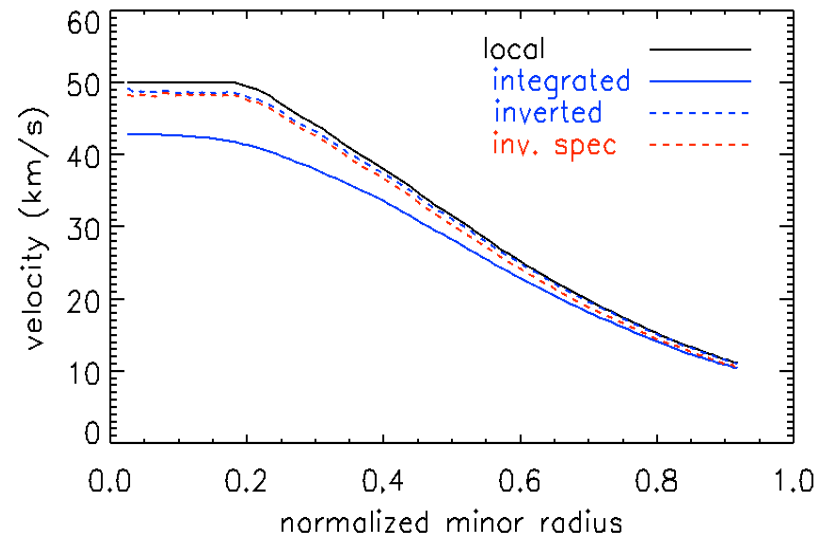
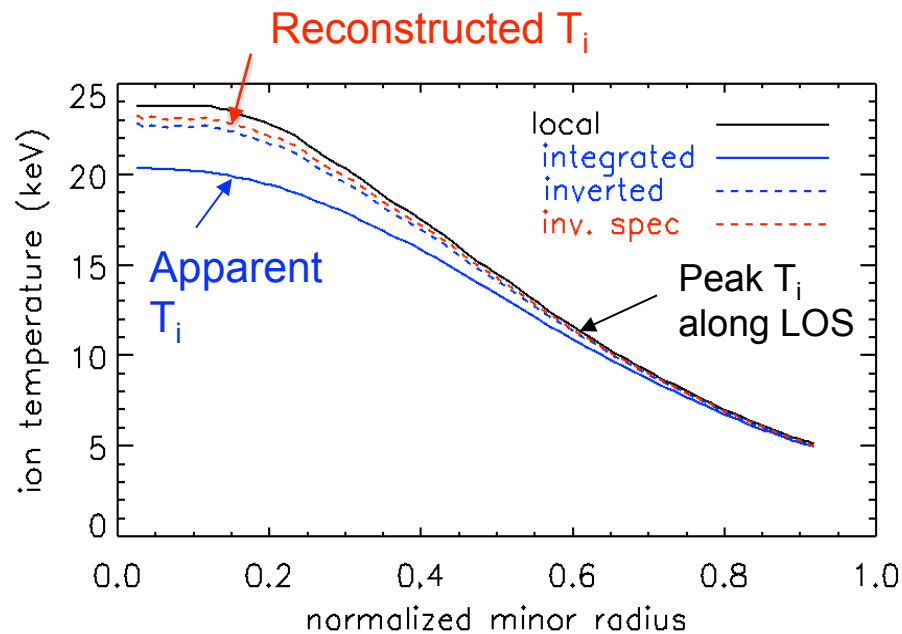
I. Condrea, Phys. Plasmas 7, 3641 (2000)

The emissivity reconstructed from our simulated brightness agrees with the local emissivity



Tomographic reconstructions of T_i and v_{tor} are reasonably good

- Reconstructed T_i and v_{tor} slightly lower than peak values along spectrometer lines of sight (LOS).
- Chordally integrated Ne-like W L spectra



- Moment calculation of local T_i breaks down when $v_{\text{tor}} \sim$ ion thermal velocity
- Inversion of spectra before T_i determination is robust to high values of v_{tor}

Several factors affect measurement uncertainties

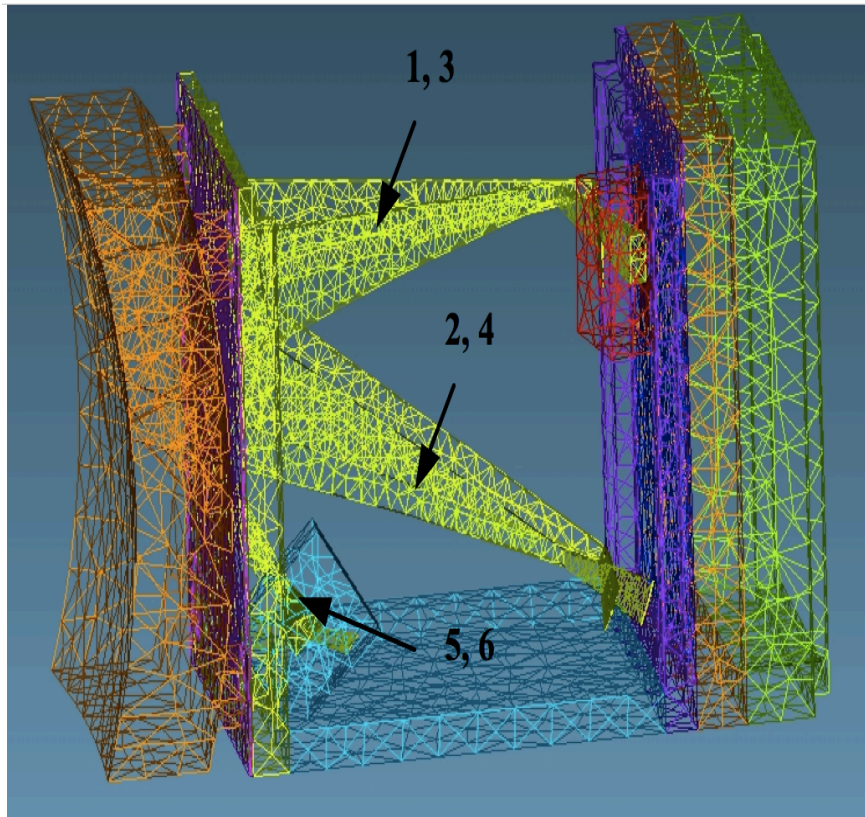
- Statistics
 - Count rate
 - Temporal binning
- Instrumental resolution
- **Degradation due to background**
- Line overlap at high ion temperature
- Propagation of uncertainties through inversion
 - **Incomplete spatial profile coverage**
 - Propagation of statistical uncertainties
 - Errors in flux-surface calculations

Neutron/gamma-ray background low on present tokamaks, but will be high for ITER

- Pilatus x-ray count rates per pixel $\sim 1000 - 10000 \text{ s}^{-1}$ in peak of line for MIT tokamak, Alcator C-Mod
- n/ γ background 20 s^{-1} for C-Mod producing 10^{13} n/s, unshielded
- Background 250 s^{-1} in PPPL's NSTX producing 10^{14} n/s, unshielded
- ITER will produce $10^{20} - 10^{21}$ n/s, 10^6 x higher than NSTX
- ITER will have extensive shielding, and the imaging XCS will be shielded heavily, but it will be only ~ 5 m from the plasma
- A careful, realistic neutronics analysis is required.

Preliminary (optimistic) neutronics analysis suggests n/γ background levels tolerable for Medipix and Pilatus detectors **except** near front of port plug

- Radiation background noise levels acceptable (<100 counts/pix/s)



Detector location	Total neutron+ γ flux > 1 keV (n/cm ² .s)	Total neutron+γ count-rate For QDE= 0.01 (count/cm ² .s)	Total neutron+γ count-rate For QDE= 0.01 (count/pixel.s)
1	6.4 .10 ⁶	6.4 .10 ⁴	19
2	3.29 .10 ⁵	3.22.10 ³	1
3	1.5 . 10 ⁷	1.5 . 10 ⁵	45
4	5.7 . 10 ⁴	8.8 . 10 ⁴	16
5	1.53 . 10 ¹²	5.3 . 10 ⁹	4.5 . 10 ⁶
6	4.26 . 10 ¹⁰	4.26 . 10 ⁸	1.26 . 10 ⁵

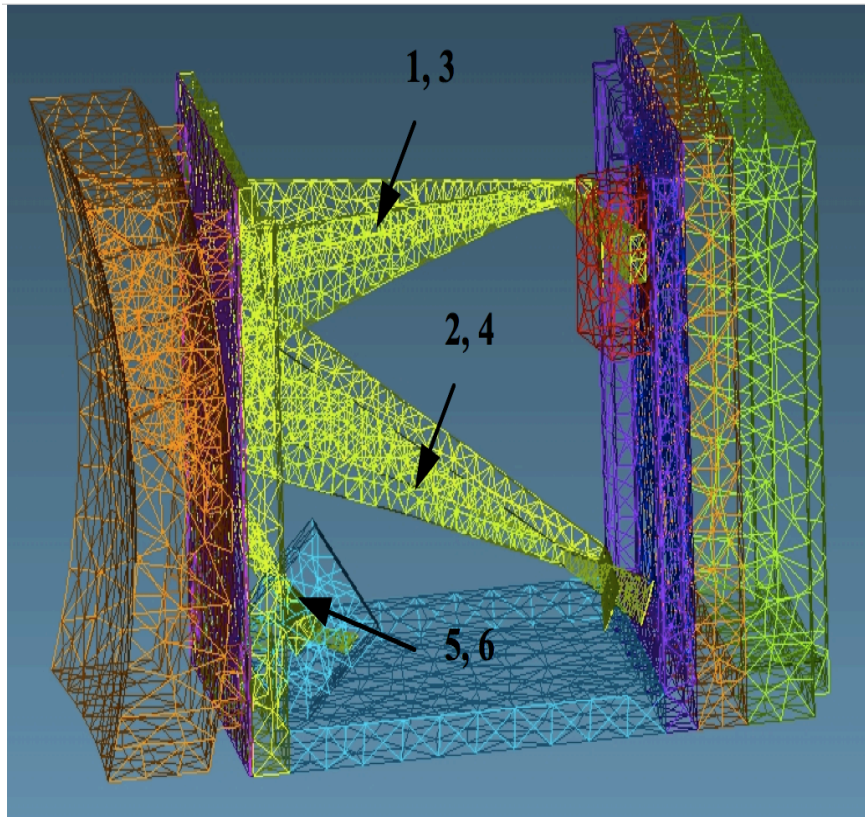
Davis, Barnsley & Pampin,
Contract EFDA 05-1350 D5.1

Peak x-ray count rates/pixel 10³ – 10⁴ s⁻¹ for C-Mod

Realistic neutronics analysis for present diagnostic configuration is being done.

Preliminary (optimistic) neutronics analysis suggests Medipix and Pilatus detectors can survive **except** near front of ITER port plug

- Radiation background noise levels acceptable (<100 counts/pix/s)



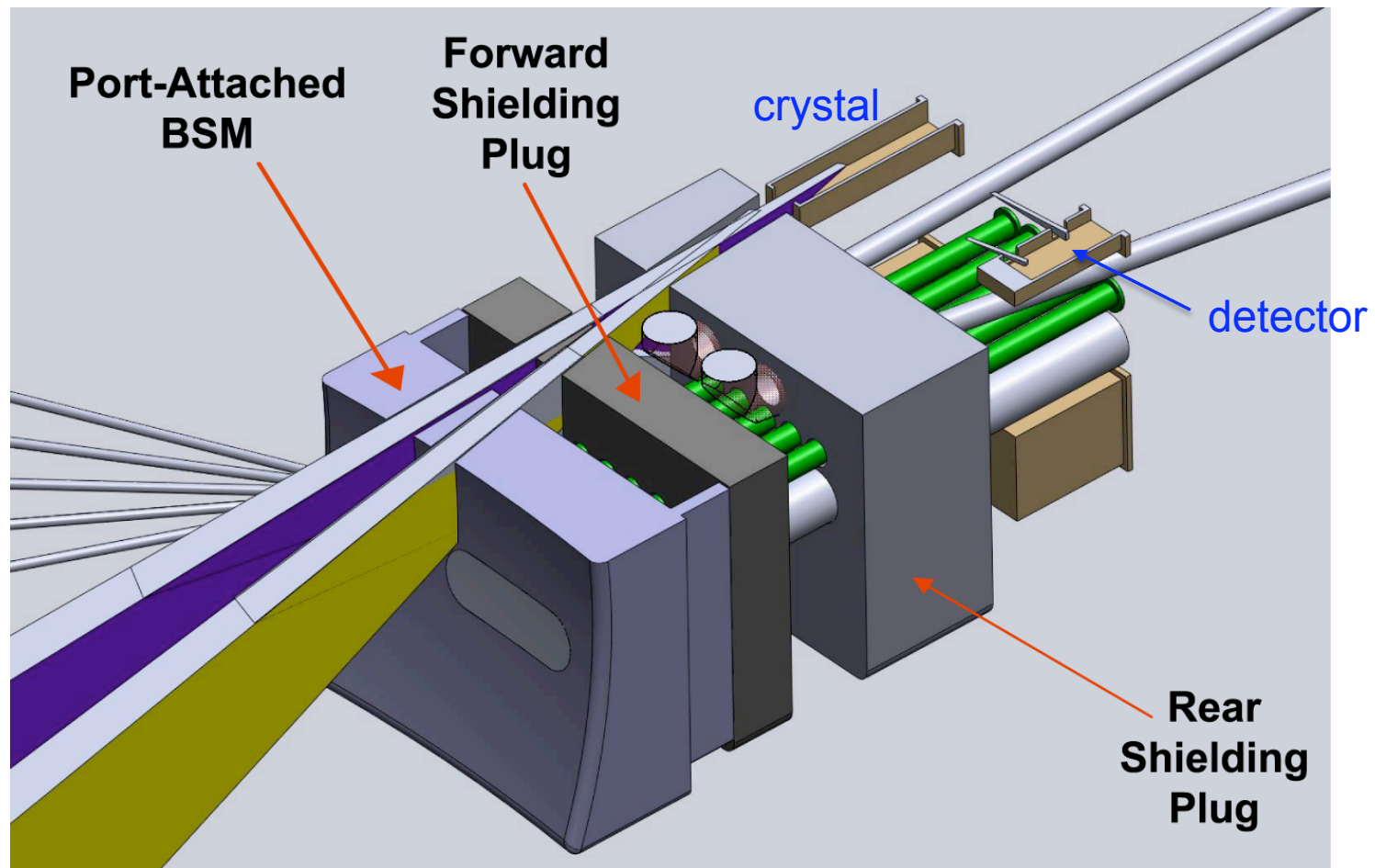
Davis, Barnsley & Pampin,
Contract EFDA 05-1350 D5.1

Table 7: Estimates of detector lifetimes due to neutron damage.
 10^7 s: ITER lifetime. 10^6 s: maintainable

Detector location	Flux >100 keV (n/cm ² .s)	Time for fluence of 10^{14} /cm ² (s)	Time for fluence of 10^{16} /cm ² (s)
1	$3.3 \cdot 10^6$	$3 \cdot 10^7$	$3 \cdot 10^9$
2	$2.9 \cdot 10^3$	$3.4 \cdot 10^{10}$	$3.4 \cdot 10^{12}$
3	$5.8 \cdot 10^6$	$1.7 \cdot 10^7$	$1.7 \cdot 10^9$
4	$2.0 \cdot 10^4$	$5 \cdot 10^9$	$5 \cdot 10^{11}$
5	$2.0 \cdot 10^{11}$	500	$5 \cdot 10^4$
6	$4.9 \cdot 10^9$	$2 \cdot 10^4$	$2 \cdot 10^6$

Realistic neutronics analysis for present diagnostic configuration is being done.

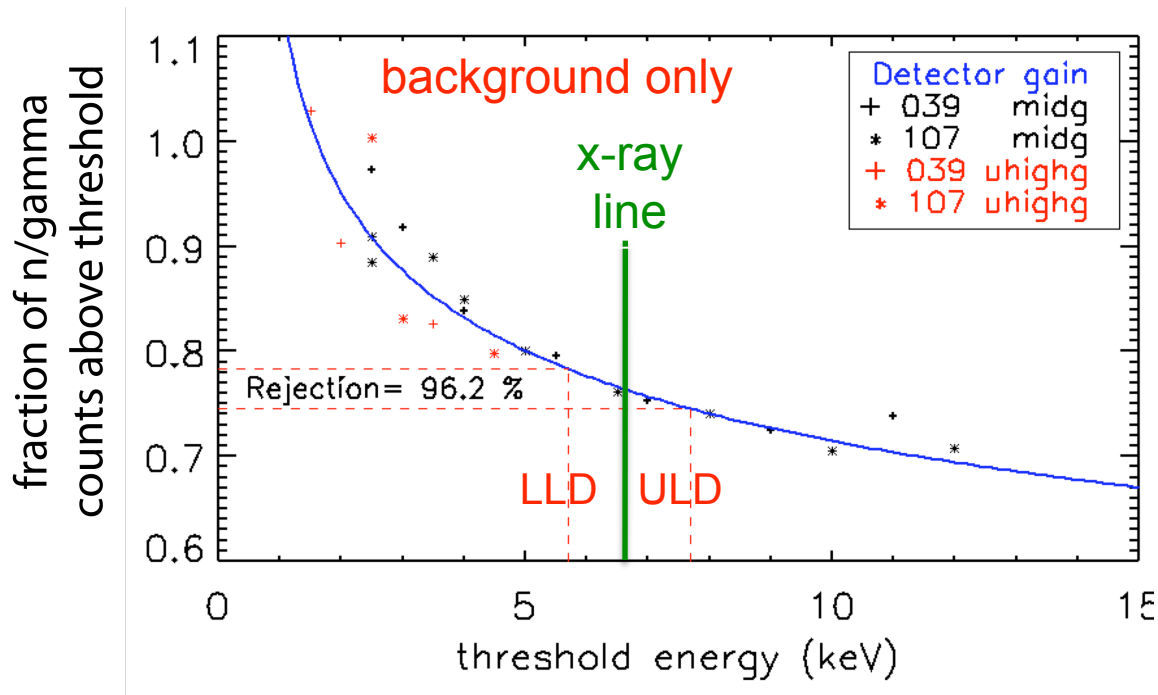
Penetrations through neutron shielding for other diagnostic sightlines will increase neutron/gamma fluxes at CIXS detectors



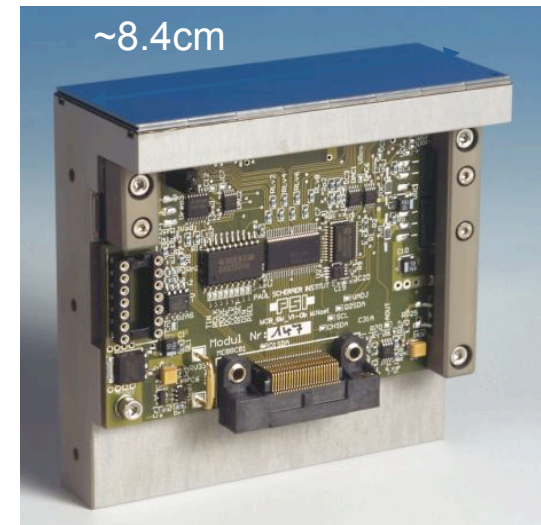
- CIXS shares port with ECE diagnostic and toroidal interferometer polarimeter
- A realistic neutronics analysis of the port plug is in progress

Higher background levels could be tolerated with electronic pulse-height discrimination

- Upper level discriminator (ULD) could eliminate 90 – 95% of neutron/gamma background
- Pilatus has only lower discriminator (LLD); eliminates 20% of background



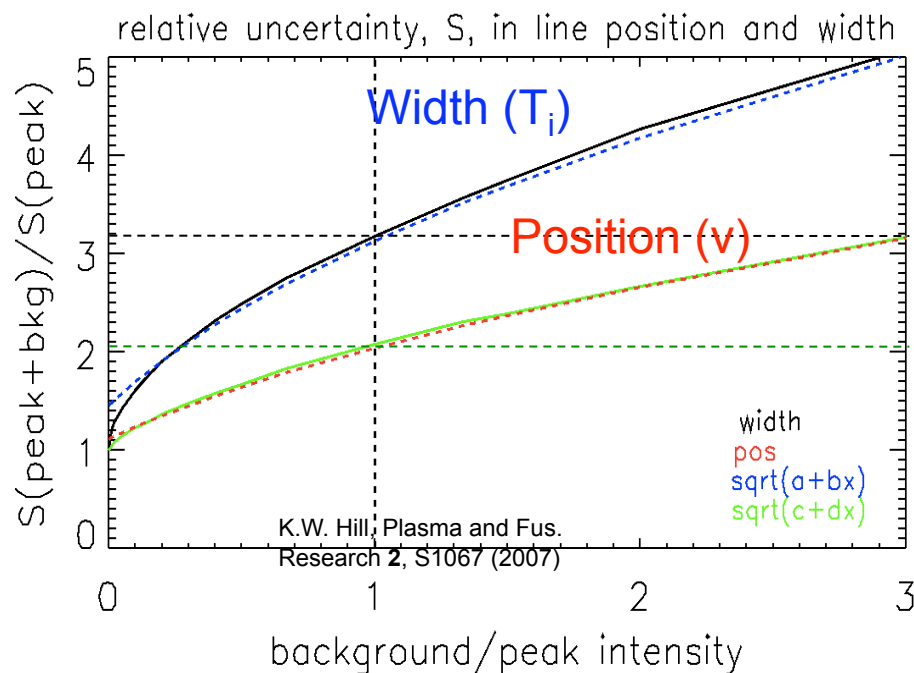
Pilatus detector



- MEDIPIX2 sensors have both lower- and upper-level discriminators.
- CERN will make available a Medipix2 detector for testing of background discrimination at PPPL or MIT in 2011.

We know how to correct for the increased measurement uncertainty due to background counts

- To compensate for higher statistical uncertainty we have to count longer => poorer time resolution
- Two components of background: x-ray continuum and nuclear



$$\sigma_{\mu} = \frac{\sigma_I}{\sqrt{N_I}} \sqrt{1 + \frac{\sigma_B^2 N_B}{\sigma_I^2 N_I}} \quad \text{Position (v)}$$

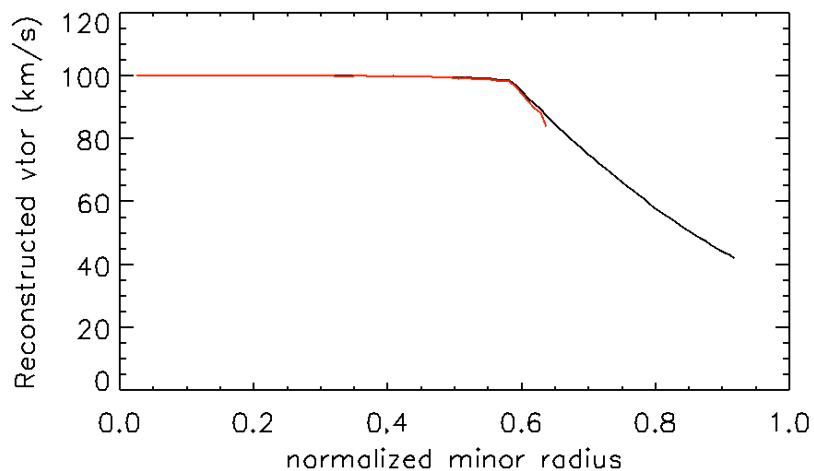
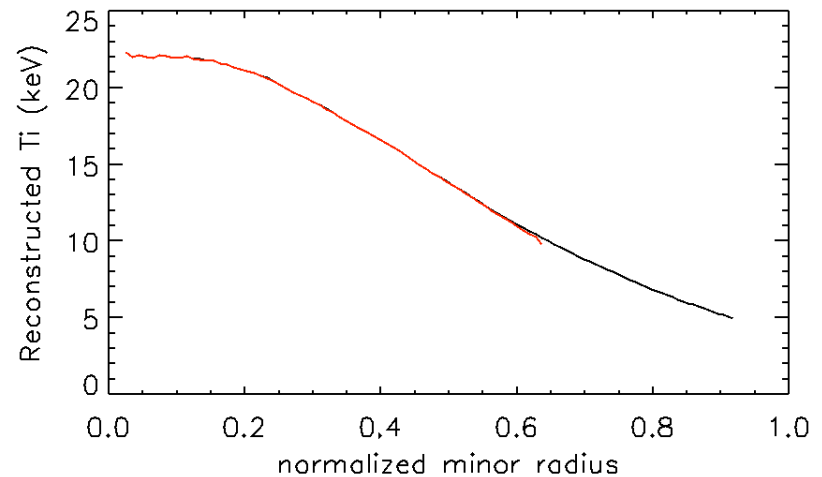
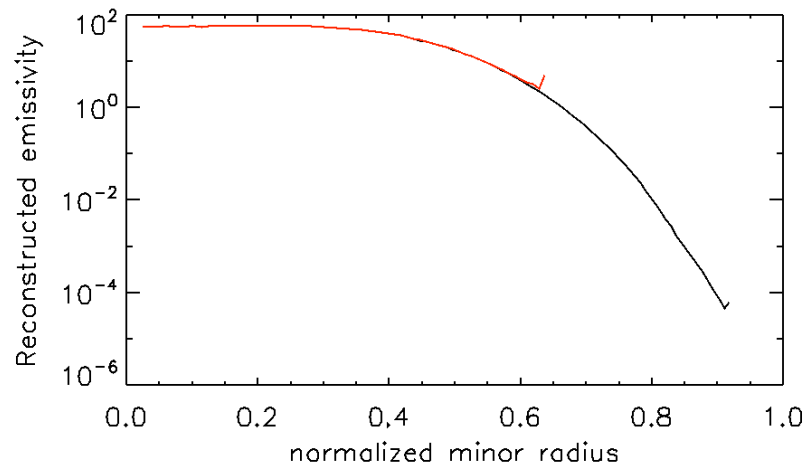
$$\sigma_S = \frac{\sigma_I}{\sqrt{2N_I}} \sqrt{1 + \frac{\sigma_B^4 N_B}{\sigma_I^4 N_I}} \quad \text{Width (T}_i\text{)}$$

Ian Hutchinson, unpublished

For peak/background=1

- Position uncertainty 2x higher (v)
- Width uncertainty 3x higher (T_i 6x)

Inversion works for partial profiles in peaked intensity profile case



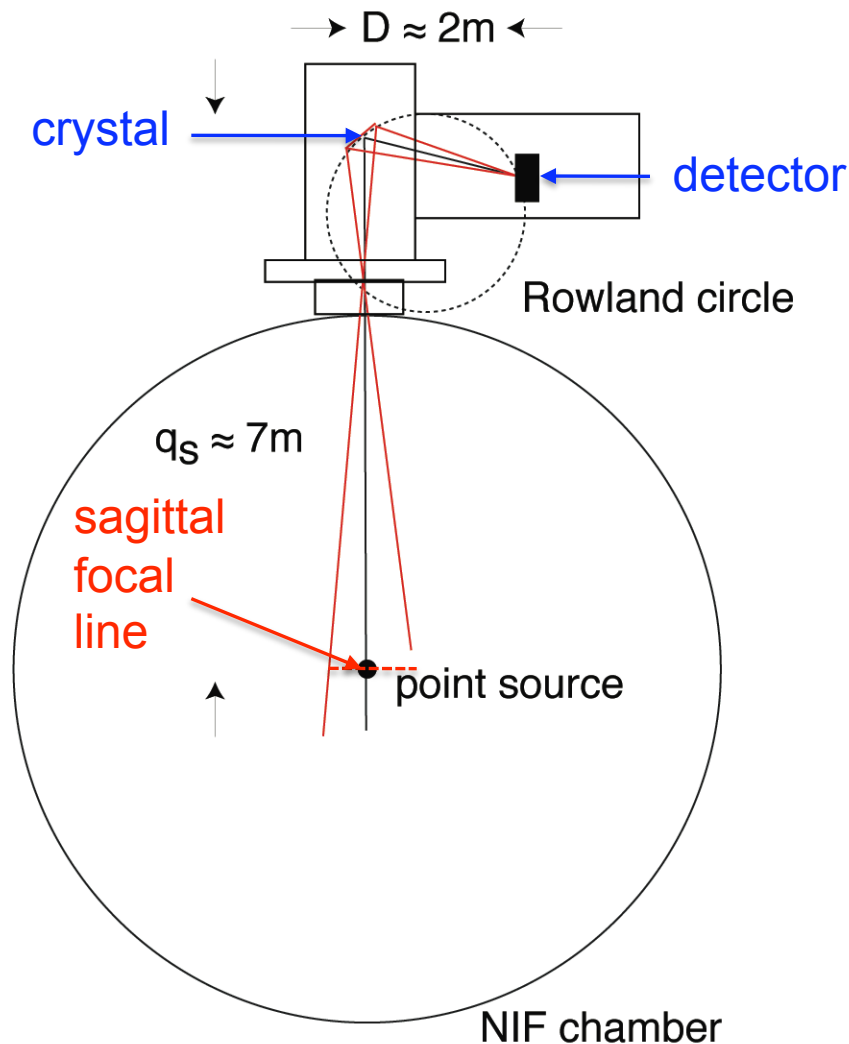
- Preliminary results
- Emissivity profile highly peaked – outer zones insignificant
- Study flat and hollow profile cases
- Study propagation of statistical errors

R&D is required to address several issues

- X-ray tube or edge filters for v_{tor} calibration
- 0.2° C stability required for $dv_{\text{tor}}=1$ km/s for Ge crystal
- Long-pulse operation possible: up to 65k frames for Pilatus
- Realistic neutronics analysis required for background determination
- Calculation of continuum background for W L lines
- Measurement of W L lines and Kr $K\alpha$ lines

Application of XICS for ICF targets

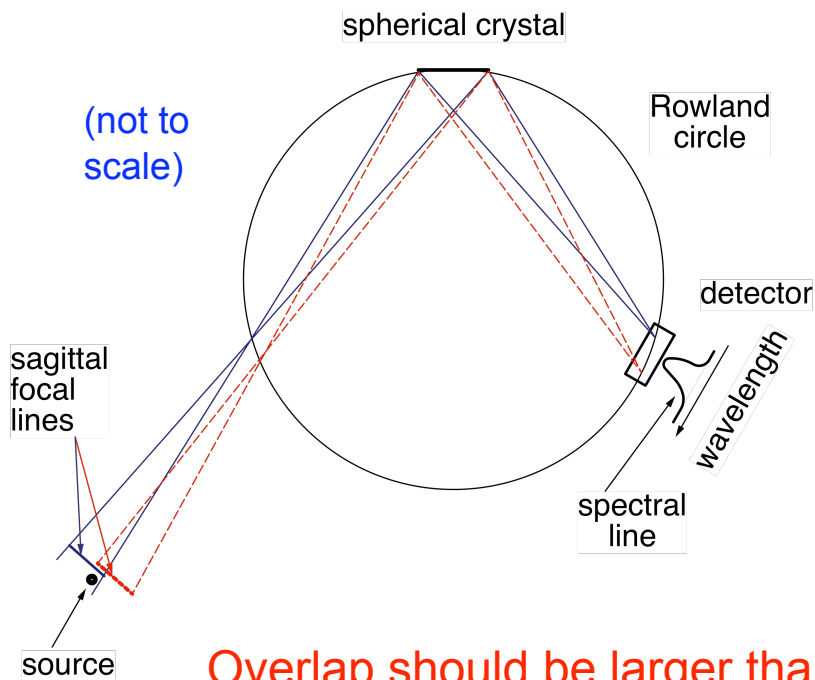
Implementation of XICS on NIF is straightforward



- Locate point source on sagittal focal line
- Crystal and detector safely outside target chamber
- Adequate space to shield detector from neutrons and gamma rays
- Spectrometer can have a 1-atm helium fill, if necessary, to reduce x-ray attenuation

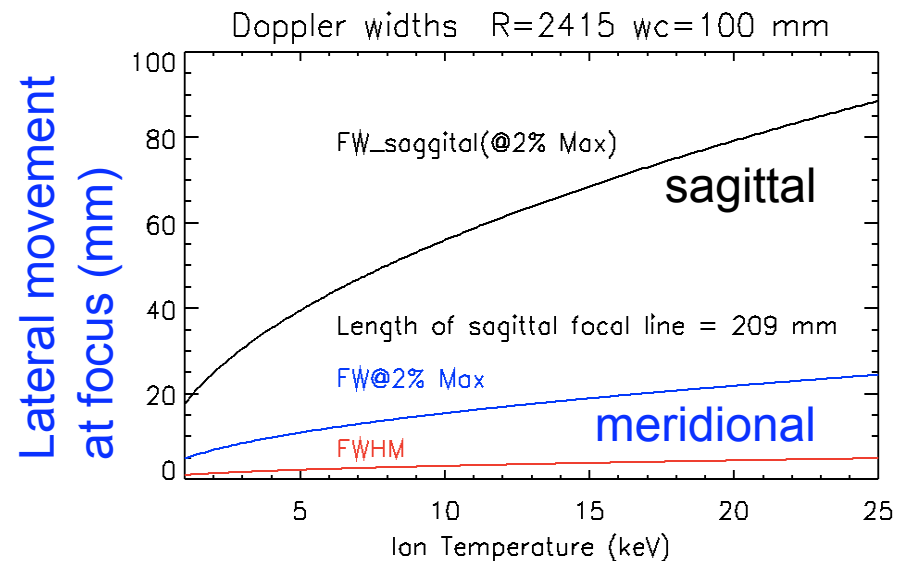
Sagittal focal (SF) line must intersect source for all wavelengths of Doppler broadened x-ray line

SF line moves laterally with λ



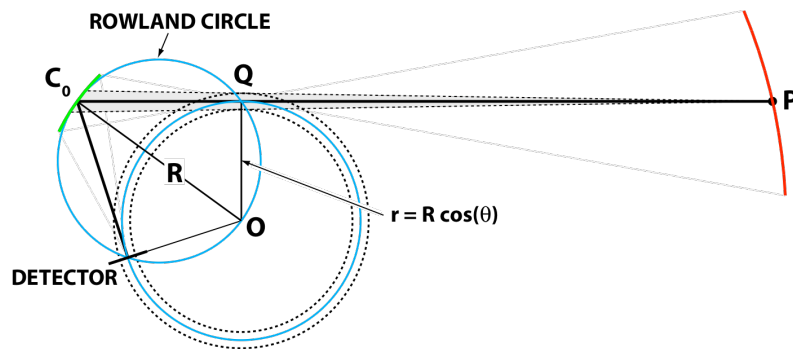
For Cu ions at $T_i=25$ keV,
 Doppler spread at SF (90 mm)
 < SF line length (210 mm)

$$R = 242 \text{ cm}, w_c = 10 \text{ cm}, \theta_B = 53^\circ$$



High throughput of spherical crystal may enable time resolved measurement of NIF target spectra

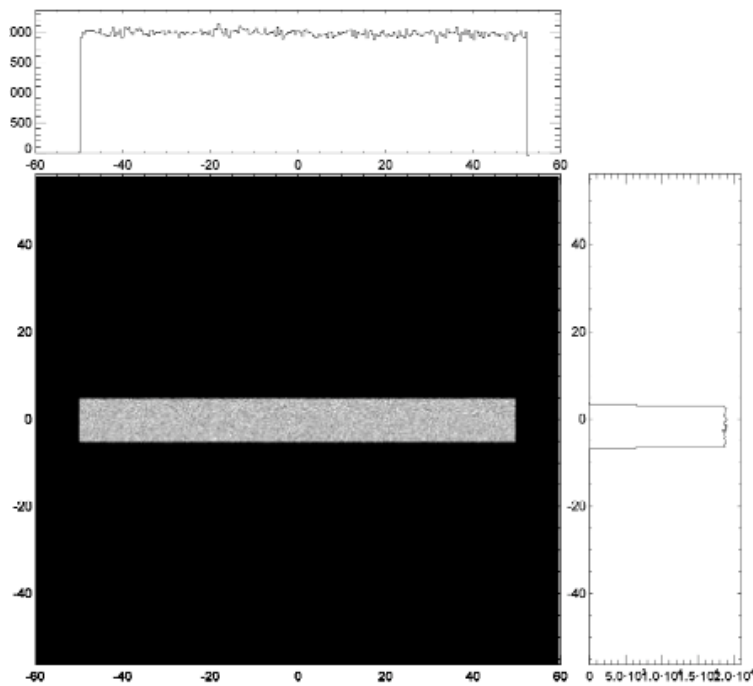
$$N' = \frac{N}{4\pi} \cdot \frac{\cos(2\theta_0)}{\cos(\theta_0) \cdot \tan(2\theta_0)} \cdot \frac{H}{R} \cdot I_{ref}$$



- $R = 240 \text{ cm}$, $H = 10 \text{ cm}$, $\theta_0 = 53^\circ$
- $I_{ref} = 1.9 \times 10^{-5} \text{ rad}$ for Ge[260] at 8.7 keV
- $\rightarrow N'/N = 7 \times 10^{-9}$
- For $100 \mu\text{m}$ target with $n_e = 10^{22} \text{ cm}^{-3}$, $n_l/n_e = 0.001$ we estimate $n_{ph} = (0.3 - 2) \times 10^{12}$ in 100 ps
- $\rightarrow 1,500 - 10,000$ photons detected in 100 ps

Preliminary ray tracing suggests 1D imaging on the micron scale might be possible

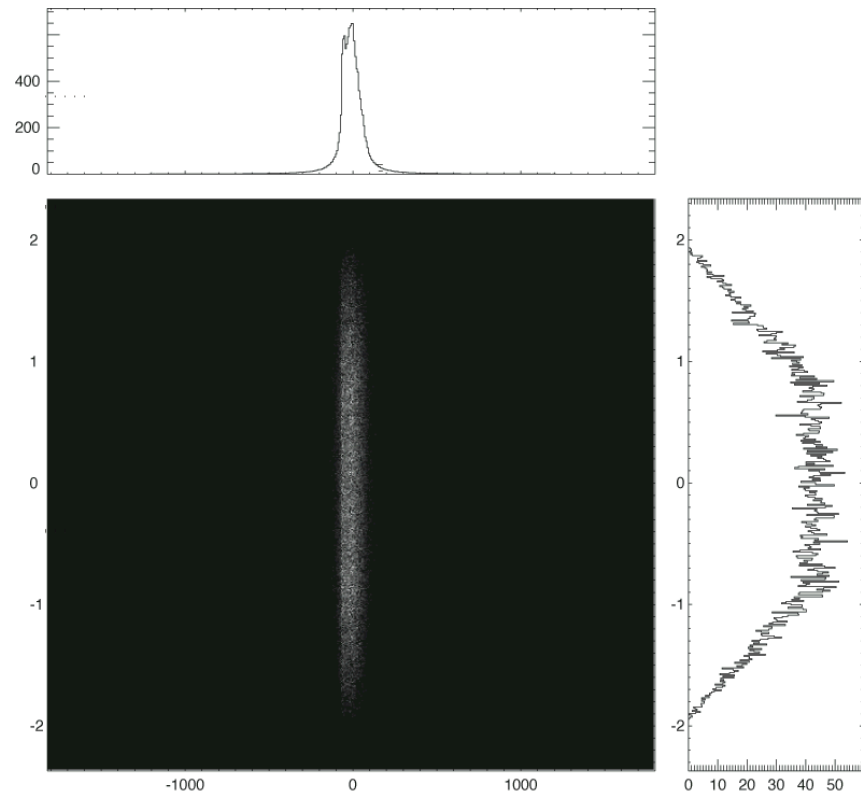
A $100 \times 10 \mu\text{m}^2$ source images to:



Manuel Sanchez del Rio, SHADOW code

K. W. Hill 8/2011

A $4 \times 2.6 \mu\text{m}^2$ image at one λ . Expected height is $10 \times 2\text{m}/7\text{m} = 2.8 \mu\text{m}$



• More detailed calculations planned for this summer

The XICS is a primary diagnostic for measurement of profiles of T_i and v on ITER

- The ITER core XICS has been assigned to the US
- A US-ITER team is doing the conceptual design toward a CDR in October, 2011
- XICS instruments have been very successful on present day machines (MIT, China, Korea, Japan)
- A preliminary performance analysis for the ITER core XICS looks mostly favorable
- JET would be an ideal venue for more ITER-like R&D for XICS, particularly for studying tungsten L lines
- Our x-ray optical schemes may have applications in other areas of physics

Future: Improvements in time and spatial resolution, background rejection, and radiation hardness of detectors

- Improved detector spatial resolution needed for ITER spectrometers-smaller size, lower dispersion, smaller Doppler width for W
 - Eiger (75 μm pixel size, no dead time)
 - Medipix (55 μm)
- Faster framing rate for T_i and v fluctuation measurements (Medipix3, Eiger [24 kHz])
- Nuclear noise rejection (90 - 95% with energy window – Medipix2)
- Higher neutron damage threshold detectors
 - 10^{15} n/cm² for ATLAS sensors
 - 6×10^{15} n/cm² possible with new processing of silicon (SLHC)

We would like to identify alternate applications of our x-ray optical diagnostics schemes

- X-ray imaging crystal spectrometer (XICS) using a single spherically bent crystal and a 2D imaging detector enable spatially resolved Doppler measurements of ion temperature and flow velocity in tokamaks with good spatial and temporal resolution
- The technique is also applicable to inertial confinement fusion (ICF) “point” sources
- New schemes with matched pairs of spherically bent crystals should enable 2D imaging of small x-ray sources with favorable geometry and micron resolution
- **We are looking for other applications or collaborations** – x-ray lithography, x-ray imaging for biological research on light sources, x-ray beam manipulation, x-ray imaging spectroscopy on other light-source experiments

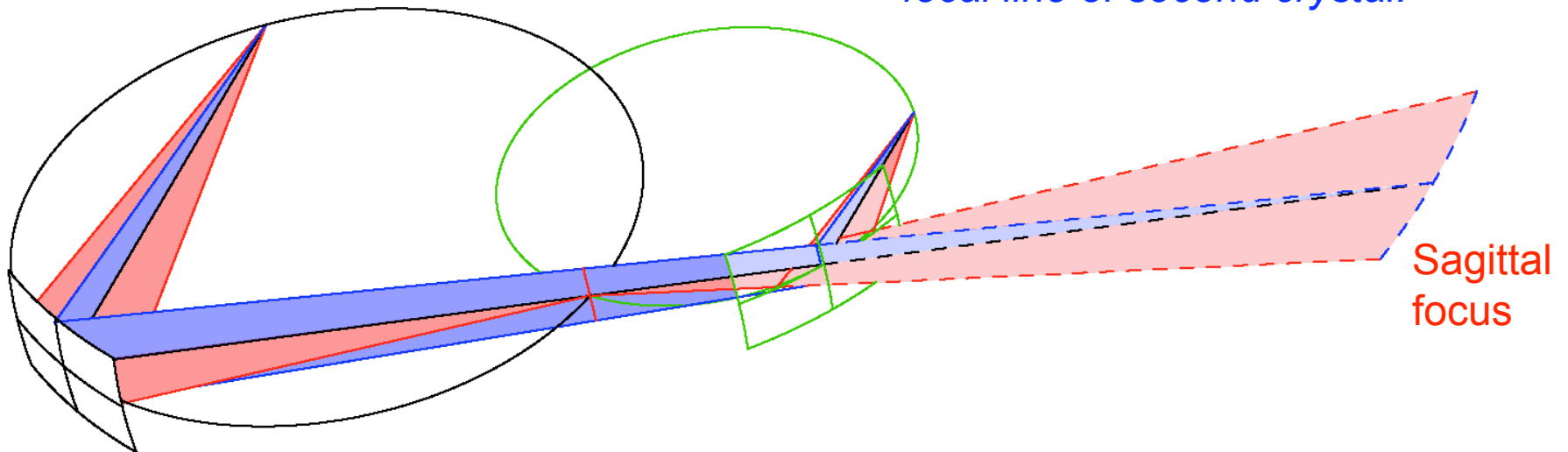
Two-dimensional x-ray spectral imaging
at almost arbitrary Bragg angles without
astigmatism using matched pairs of
spherically bent crystals

Astigmatism can be eliminated by use of matched, spherically bent crystal pair

Preferable Arrangement with Source on Rowland circle because of overlap of Johann aberration

2d spectral imaging

Real sagittal focal line of first crystal overlaps virtual sagittal focal line of second crystal.

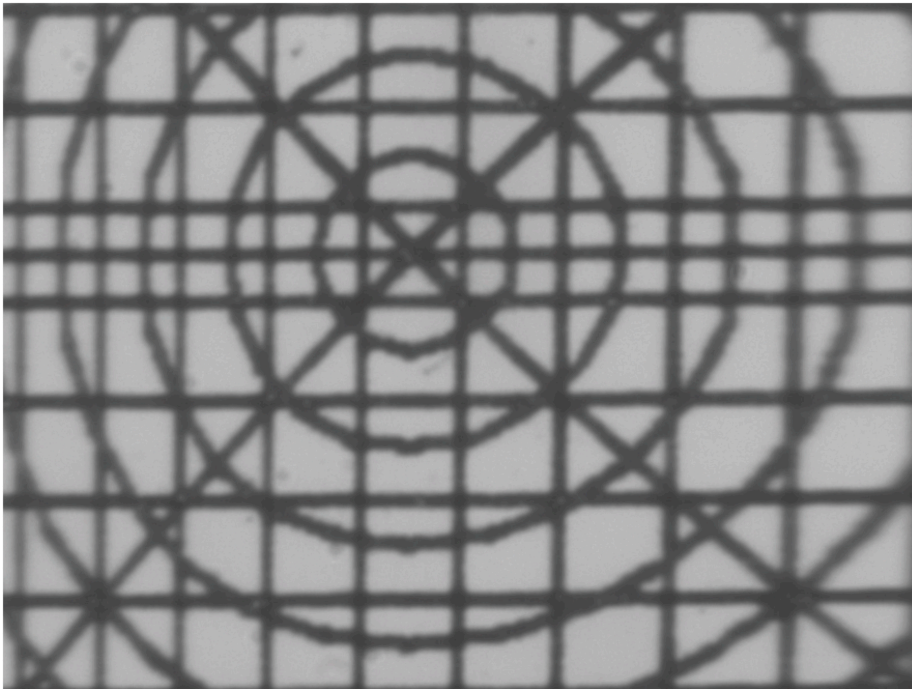


Possible applications: x-ray imaging of ICF plasmas, biological x-ray imaging, x-ray lithography

Future: Improvements in time resolution, background rejection, and radiation hardness of detectors are coming

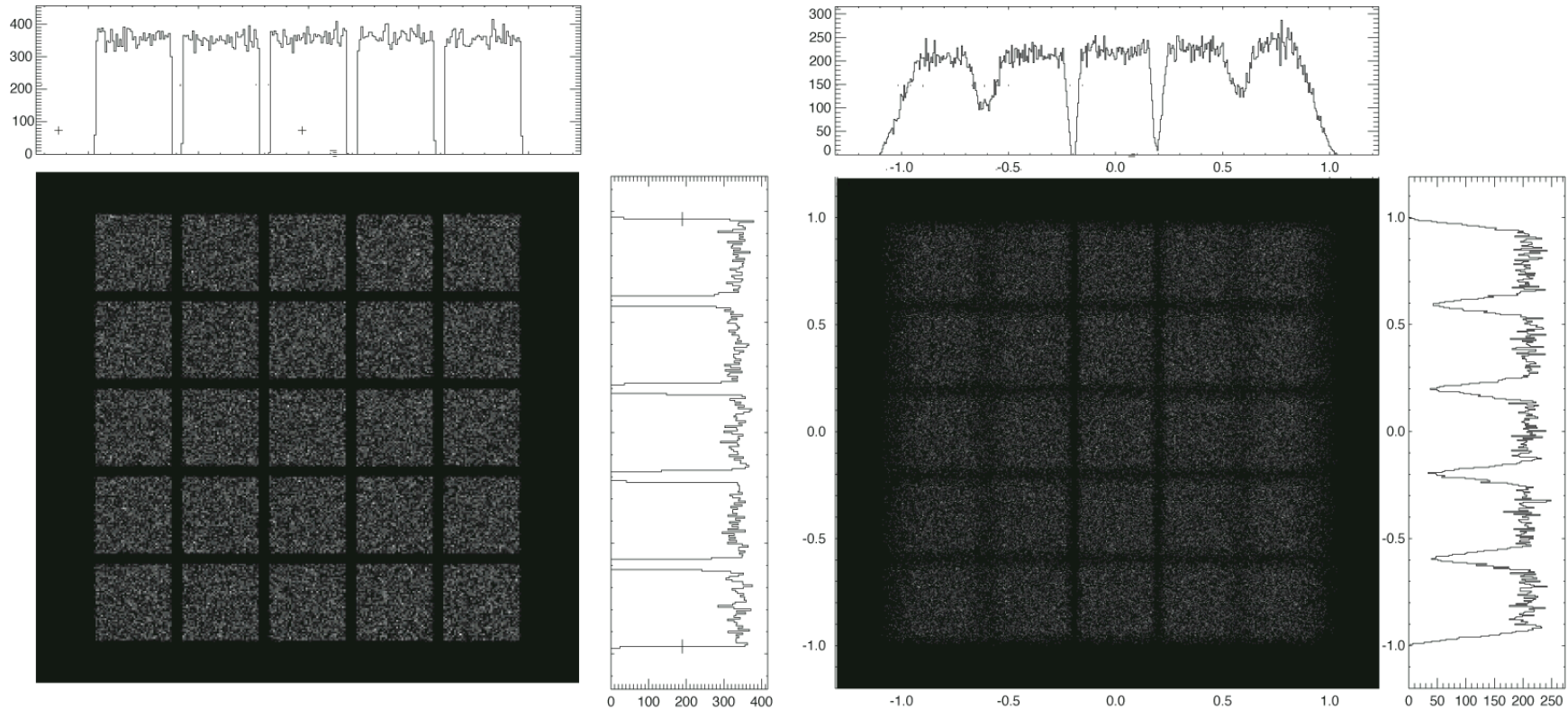
- Improved detector spatial resolution needed for ITER spectrometers-smaller size, lower dispersion, smaller Doppler width for W
 - Eiger (75 μm pixel size, no dead time)
 - Medipix (55 μm)
- Faster framing rate for T_i and v fluctuation measurements (Medipix3, Eiger [24 kHz])
- Nuclear noise rejection (90 - 95% with energy window – Medipix2)
- Higher neutron damage threshold detectors
 - 10^{15} n/cm² for ATLAS sensors
 - 6×10^{15} n/cm² possible with new processing of silicon (SLHC)

Matched pair of spherical mirrors exhibit stigmatic 2d imaging with visible light



- 50 micron line size
- Will be tested with finer grid
- Tests with x rays are planned

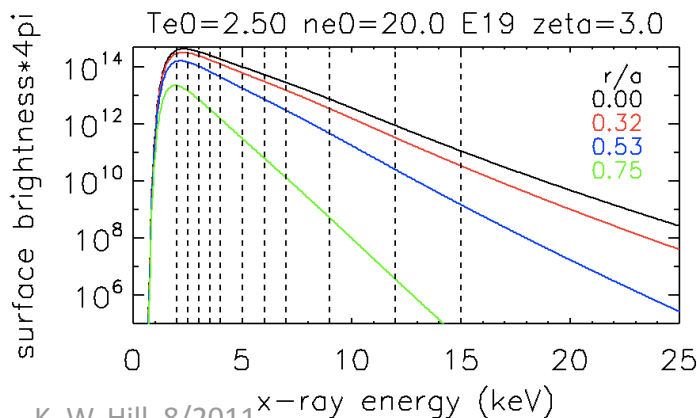
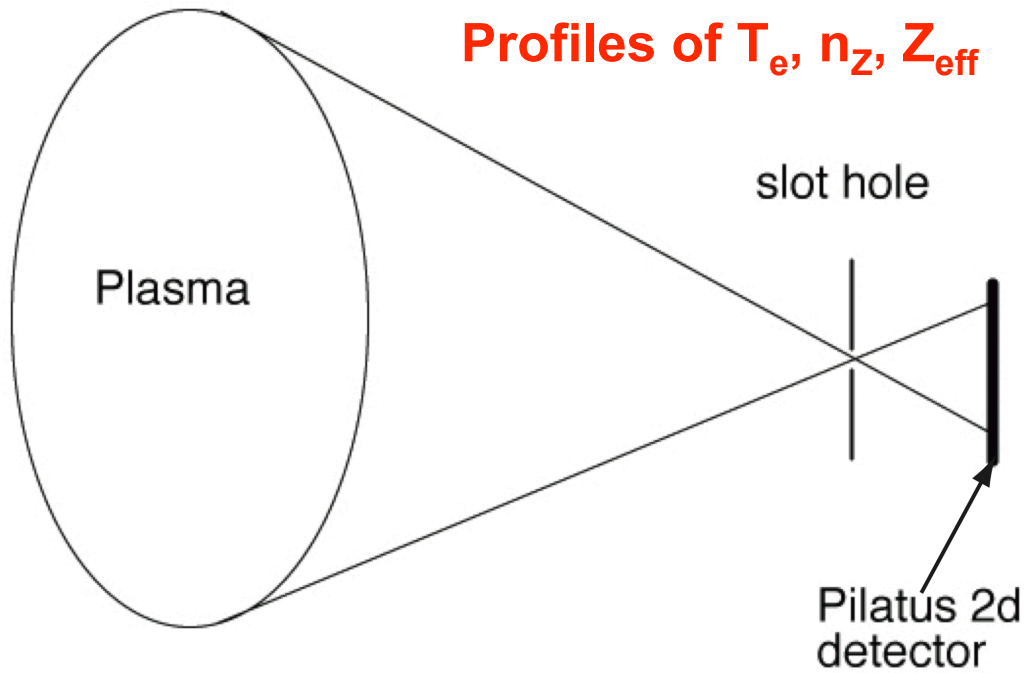
Preliminary ray tracing for 2D x-ray imaging with 2 matched spherical crystals looks promising



Manuel Sanchez del Rio, SHADOW code. More detailed calculations soon.

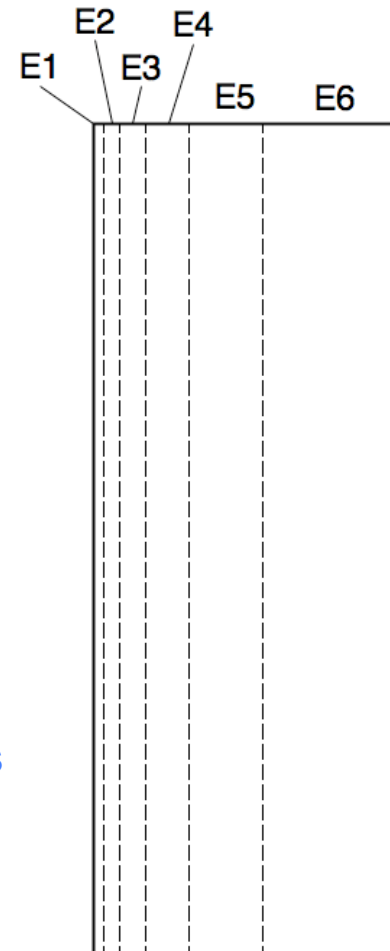
New pinhole camera images broad-band x-ray spectrum vertically and provides energy discrimination horizontally

Profiles of T_e , n_Z , Z_{eff}



50 – 600 pixels
Per spatial/E bin
counting at rates
up to 1 MHz per
pixel => good
statistics in ms

Increasing threshold energy
For different groups of columns



195 columns

- 6 bits (64 values) of threshold adjustment per pixel

Pilatus hybrid pixel detector
95000 pixels

487 rows of pixels

- E window important; neutron shielding difficult (Medipix2)

Main Points

- A new 1d imaging x-ray crystal spectrometer (XCS) has been developed to measure **full profiles** of ion temperature (T_i) and flow velocity. **NBI is not required.**
- Should play a prominent role in future fusion research
- Imaging XCS systems are successfully operating on NSTX, Alcator C-Mod, EAST, KSTAR and (soon) LHD
- **The concept has been adopted as a primary diagnostic for measurement of T_i and v in ITER**
- A U. S. team is designing the ITER spectrometers; CDR in 2011
- Performance and preliminary neutronics simulations look favorable
- Continuing improvements in detector technology from the HEP and synchrotron radiation communities will improve our capabilities.
- 2d x-ray imaging schemes with matched pairs of spherically bent crystals look favorable in visible light

We would like to identify alternate applications of our x-ray optical diagnostics schemes

- X-ray imaging crystal spectrometer (XICS) using a single spherically bent crystal and a 2D imaging detector enable spatially resolved Doppler measurements of ion temperature and flow velocity in tokamaks with good spatial and temporal resolution
- The technique is also applicable to inertial confinement fusion (ICF) “point” sources
- New schemes with matched pairs of spherically bent crystals should enable 2D imaging of small x-ray sources with favorable geometry and micron resolution
- **Other applications are sought** – x-ray lithography, x-ray imaging for biological research on light sources, x-ray beam manipulation, x-ray imaging spectroscopy on other light-source experiments

- 
- Extra slides

X-Ray Line-Shape Diagnostics and Novel Stigmatic Imaging Schemes for the National Ignition Facility

Kenneth W. Hill , M. L. Bitter, L. Delgado-Aparicio, N. Pablant
Princeton Plasma Physics Laboratory, Princeton, NJ

P. Beiersdorfer, J. Dunn
Lawrence Livermore National Laboratory, Livermore, CA, USA

M. Sanchez del Rio
ESRF, 38043 Grenoble, Cedex, France

Presented at the:

Intense field, Short Wavelength Atomic and Molecular Processes Workshop

(I-SWAMP 2011)

July 21 to July 23, 2011

Dublin City University

Glasnevin, Dublin, Ireland

Main Points

- A new 1d imaging x-ray crystal spectrometer (XCS) has been developed to measure **full profiles** of ion temperature (T_i) and flow velocity. **NBI is not required.**
- Should play a prominent role in future fusion research
- Imaging XCS systems are successfully operating on NSTX, Alcator C-Mod, EAST, KSTAR, and LHD
- The concept has been adopted as a **primary diagnostic** for measurement of T_i and v in **ITER**
- A U. S. team is designing the ITER spectrometers; CDR in Oct or Nov 2011
- Performance and preliminary neutronics simulations look favorable
- We continue to benefit from improvements in detector technology from the HEP and synchrotron radiation research communities.
- 2d x-ray imaging schemes with matched pairs of spherically bent crystals look favorable in visible light

Main points

- 1D imaging x-ray spectrometer provides fast spatial profiles of ion temperature and flow velocity in tokamaks via Doppler spectroscopy
- The 1D scheme can also be used for x-ray line-shape measurements of ICF targets
- Schemes using matched pairs of spherically bent crystals should enable high throughput 2D stigmatic imaging of ICF targets

Motivation

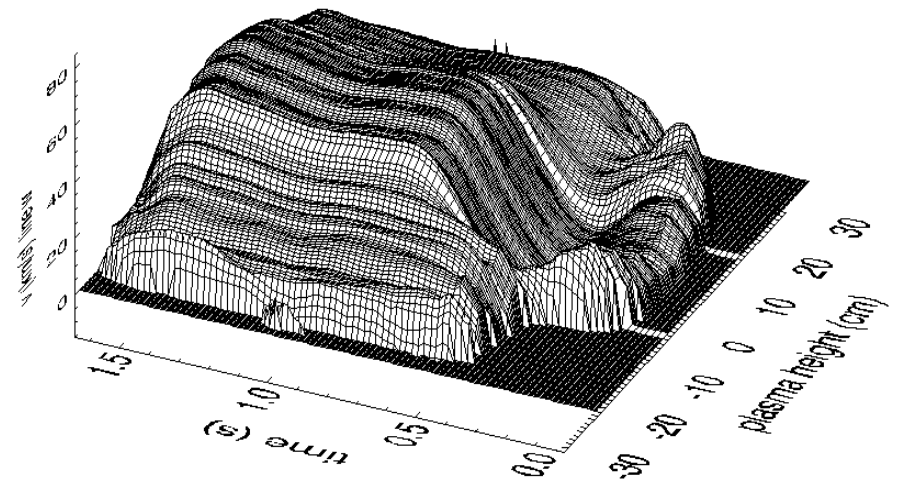
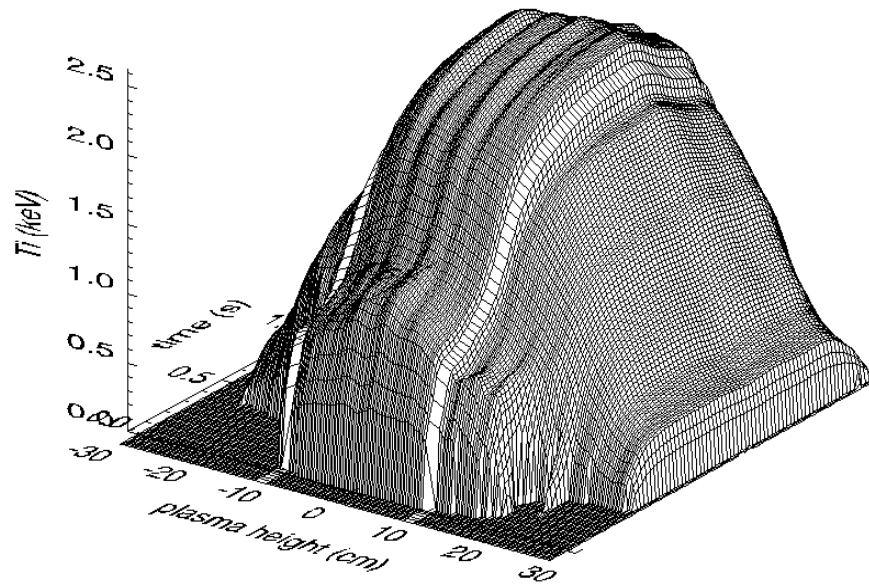
- 1D x-ray imaging with spherical crystals can provide higher resolution ($\lambda/d\lambda > 5000$) and higher throughput than other schemes currently used for ICF spectroscopy ($\lambda/d\lambda \sim 800 - 2000$), yielding improved definition of x-ray line shape
- 2D stigmatic imaging with 2 spherical crystals offers significant improvements in geometry and throughput relative to imaging with single crystal or pinhole imaging, respectively
- Other possible applications of the 2D imaging schemes include x-ray lithography with fewer reflections, x-ray microscopy for biological research, synchrotron x-ray beam-transport optics (?), etc.

Motivation

- Understanding and learning to control the intrinsic toroidal rotation profile is important for optimizing confinement and reducing MHD instabilities in future tokamaks
- Measurement of full ion-temperature profiles and flow-velocity profiles is important for understanding transport

T_i and v_{tor} are inferred from these spectra with excellent spatial definition

- Uninverted ion-temperature profile from Alcator C-Mod
- Toroidal rotation velocity profile
- Zero velocity inferred from locked-mode (non-rotating) shot



~ 1400 lines of sight. "Sliding" sum of ~25 pixel rows for good statistics

Local parameters are inferred from line integrated information by tomographic inversion

- Inversion equations from I. Condrea, Phys. Plasmas 7, 3641 (2000)
- Local emissivity inferred from measured brightness array using inverse of zonal path-length matrix

$$E_j = \sum_i L_{ji}^{-1} B_i \qquad B_i = \sum_j L_{ij} E_j$$

- Local velocity requires path lengths weighted by $\cos\theta$, where θ is angle between line-of-sight and velocity.

$$v_j = \frac{\sum_i M_{ji}^{-1} B_i u_i}{\sum_i L_{ji}^{-1} B_i} \qquad M_{ij} = L_{ij} \cos\theta_{ij}$$

- Reconstruction equation for T_i is more complicated.

CIXS instrumental reliability considerations

- Wavelength calibration vs. thermal, mechanical movement
 - Lateral movement of detector ($0.7 \mu\text{m} \leftrightarrow 1 \text{ km/s}$)
 - Rotation of crystal ($0.16 \text{ arcsec} \leftrightarrow 1 \text{ km/s}$)
 - Temperature stabilization of crystal vs. 2d changes
 - X-ray source or absorption edges for absolute cal.
- Neutron damage of crystal or detector
- Thermal protection during bakeout, operation

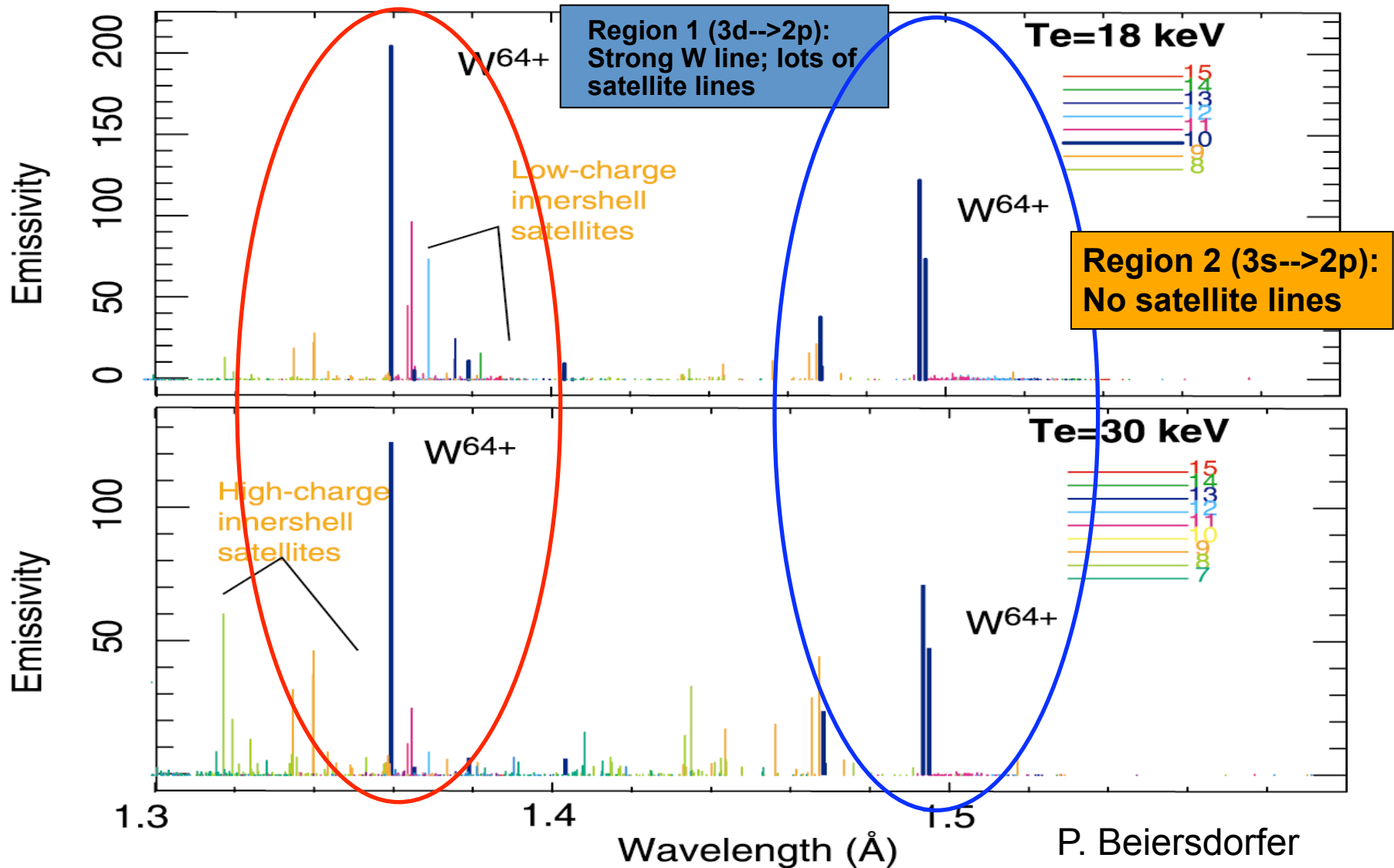
Mitigation, other issues

- Use pulse-height window to reduce nuclear background
- Injection of Fe penta-carboneel if $T_e(0)$ too low or not enough tungsten in plasma
- Fast readout and analysis to provide T_i feedback for machine operation

Mitigation of uncertainties

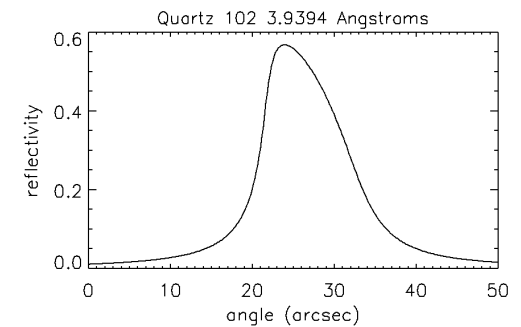
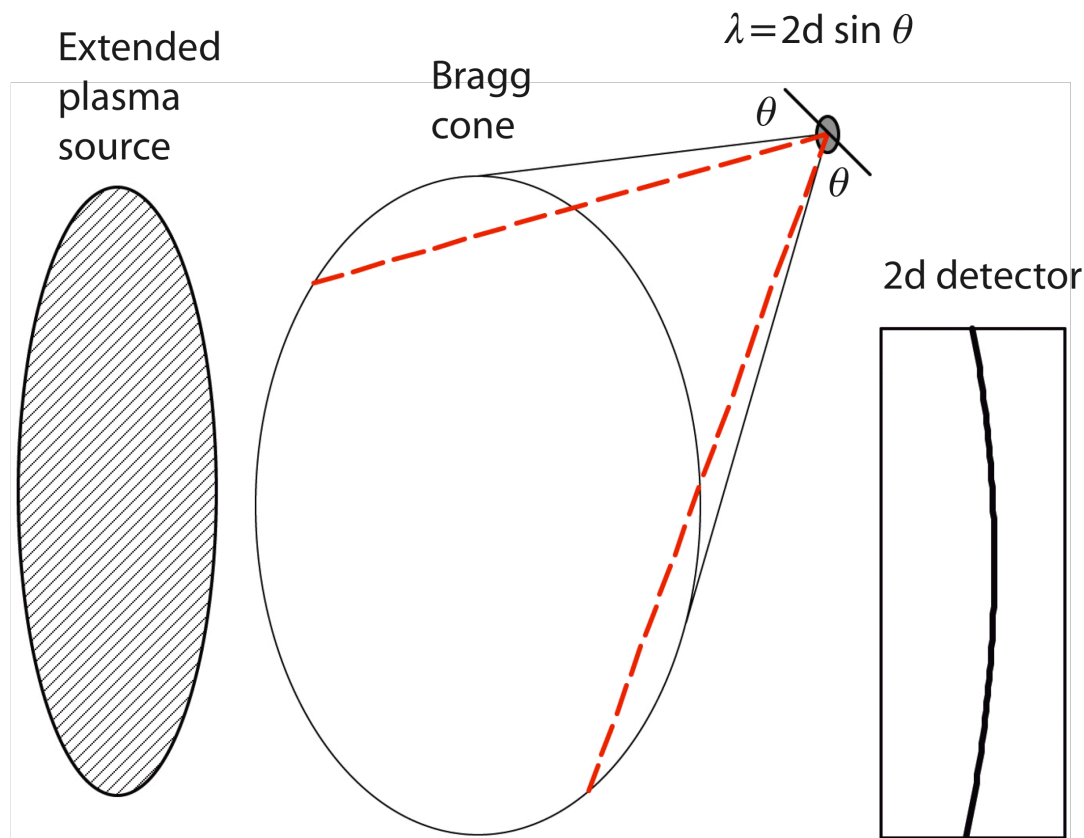
- Line overlap at high T_i
 - Multiple overlapping Gaussian fitting
 - Detailed knowledge of atomic physics
- Incomplete spatial coverage
 - Overlap with Edge IXS
 - Extrapolate emissivity and $T_{i_apparent}$ to edge
 - Use measured T_e profile and impurity transport modeling to simulate spectra in spatial gaps

Our predicted tungsten spectra reveal two regions for measurement: 8.3 keV and 9.1 keV



A single x-ray wavelength λ from an extended plasma source diffracts on a cone defined by the Bragg equation

fixed $\lambda \Rightarrow$ fixed $\theta \rightarrow$ cone



“Rocking curve”
57% peak reflectivity
10 arcsec width
 $\lambda/d\lambda \sim 35,000$

New Stigmatic Imaging Schemes

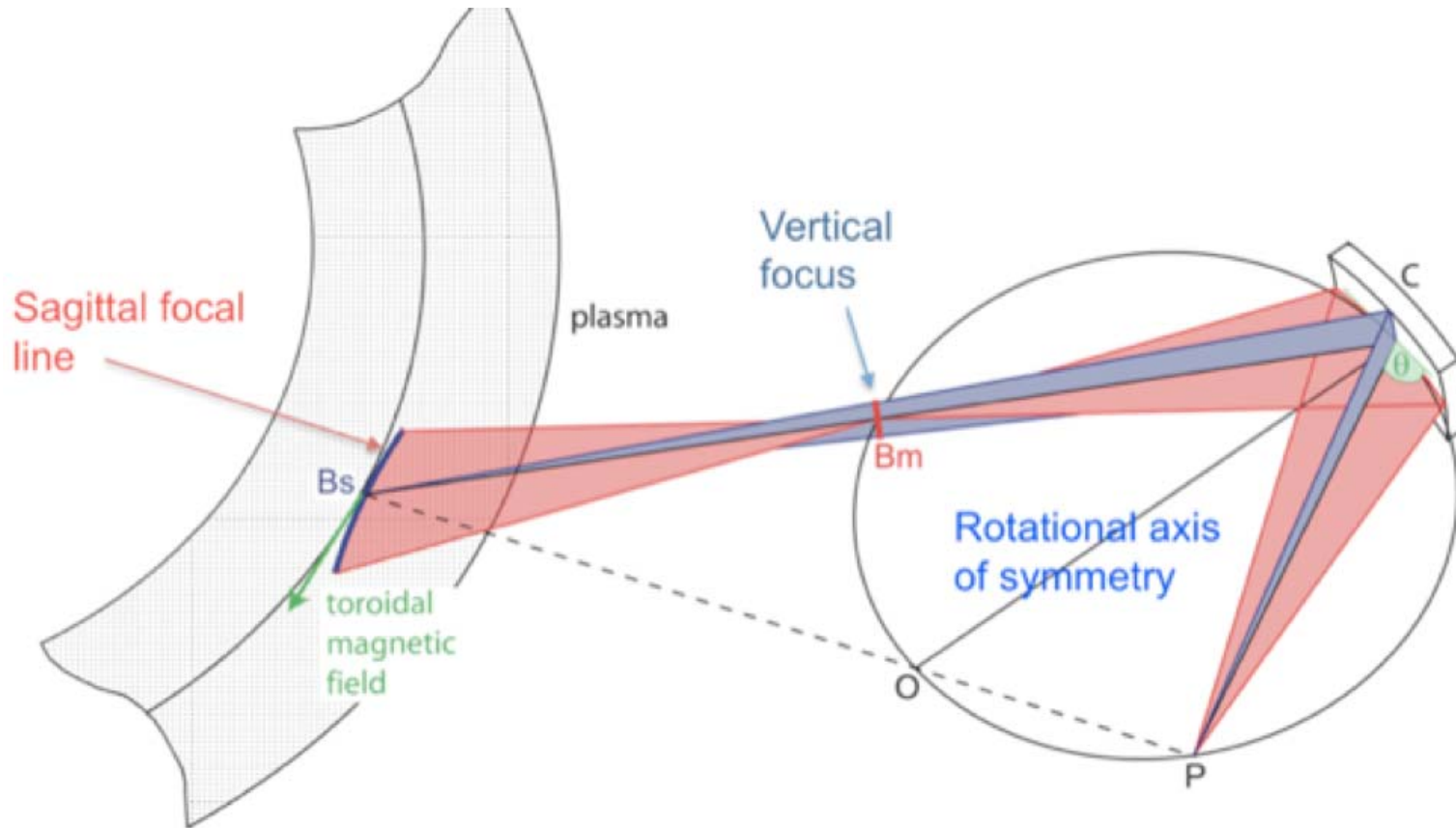
M. Bitter and K. W. Hill

- The astigmatism of spherically bent crystals can be used with advantage to design one-dimensional imaging schemes that provide spatial resolution in extended tokamak plasma.
- This is possible because of the toroidal symmetry of tokamak plasmas - or uniformity of the electron density, electron temperature, and x-ray emissivity along the toroidal magnetic field.
- However, the astigmatism is a nuisance, when such symmetries are absent and when stigmatic imaging of an object is required.

New Stigmatic Imaging Schemes

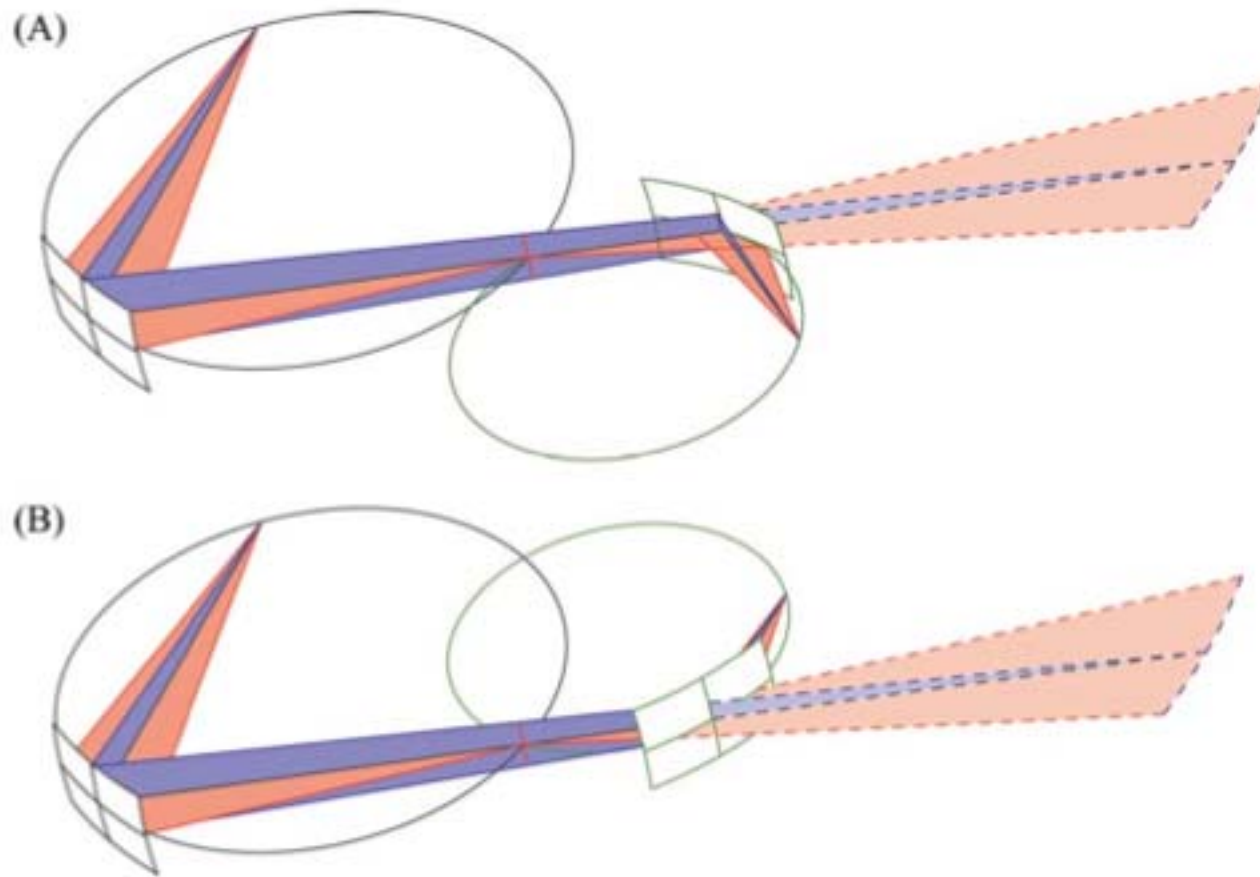
- In such cases, one usually works with near-normal incidence to minimize astigmatic imaging errors.
- This is, however, a problem for the diagnosis of laser-produced plasmas, where the detectors are then in direct view of the target and at risk of being damaged by debris.
- We are presently developing new imaging schemes, where
 - (a) the astigmatism is fully eliminated by the use of a matched pair of spherically bent crystals; and
 - (b) stigmatic imaging is obtained for almost arbitrary angles of incidence

Imaging Properties of a Spherical Crystal



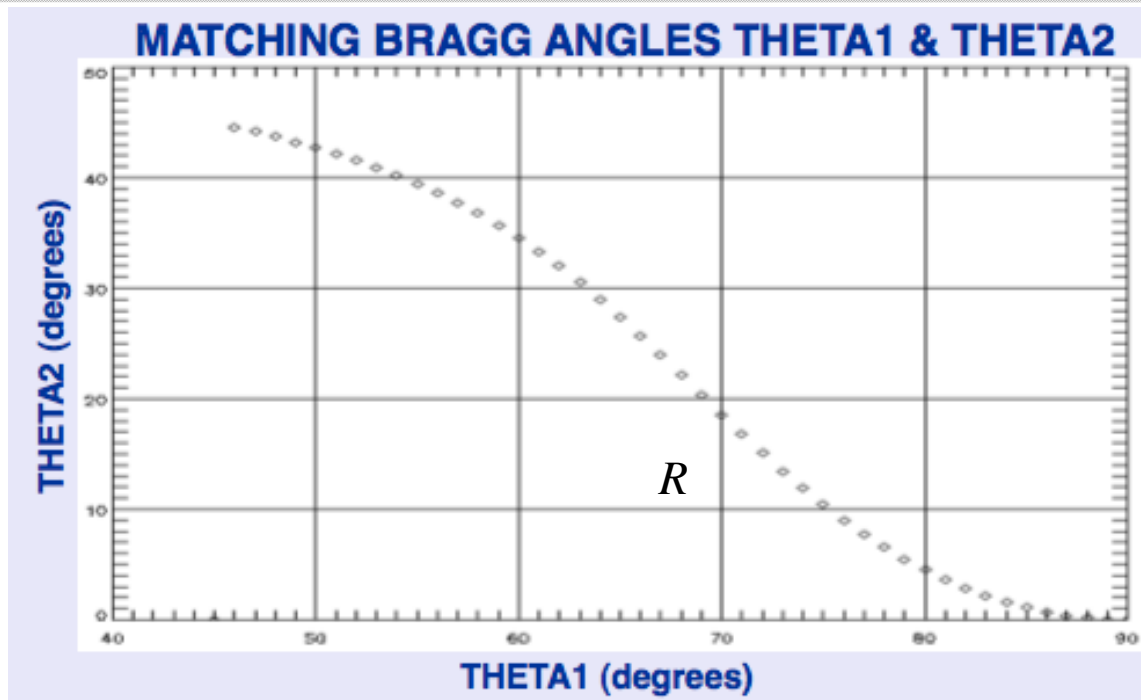
The astigmatism depends on the angle of incidence or Bragg angle

Elimination of Astigmatism by a matched pair of spherically bent crystals



Only version (B) works for x-rays, since the Bragg condition must be satisfied on both crystals and since the Johann aberrations for both crystals must be equal.

Allowed combinations of Bragg angles



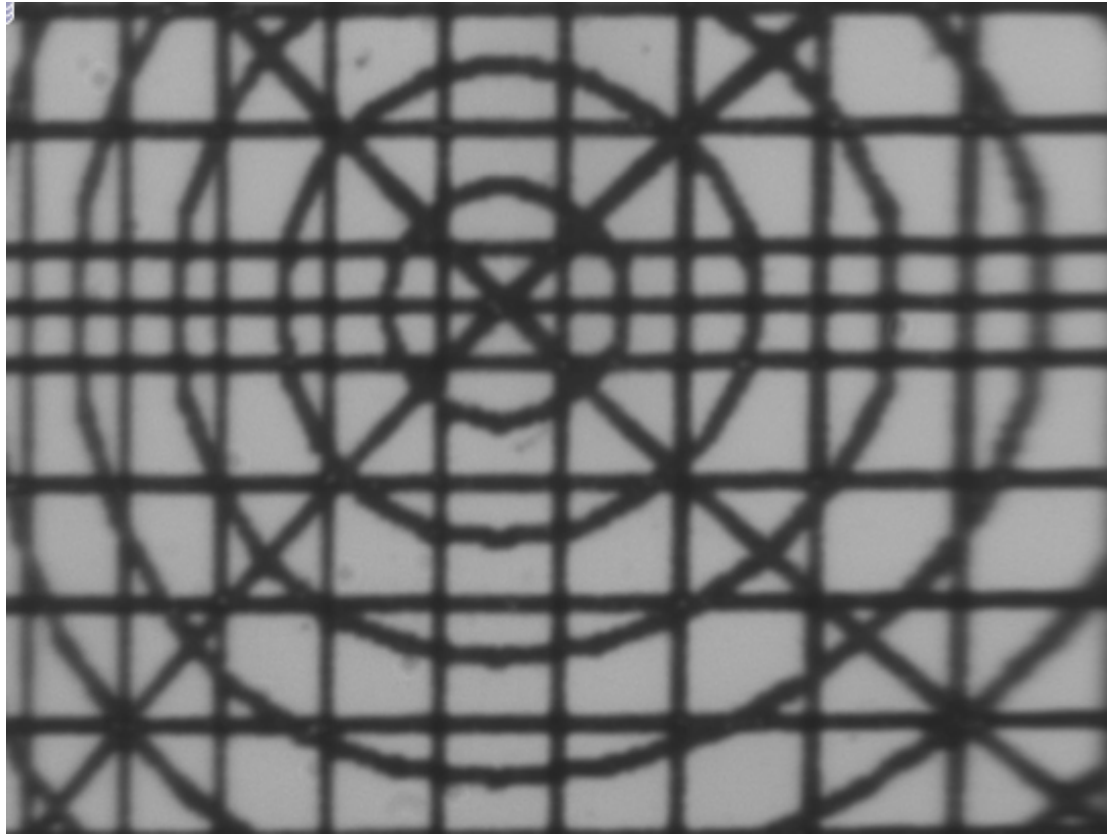
Principle Condition: *The sums of the distances of the meridional and sagittal images from the two crystals must be equal.*

$$y_{s1} + y_{s2} = y_{m1} + y_{m2}$$

$$(1) \quad -R_1 \cos(\theta_1) \cdot \tan(2\theta_1) = R_2 \cos(\theta_2) \cdot \tan(2\theta_2)$$

The Figure shows the solutions of equation (1) for $R_2/R_1=0.25$

Proof-of-Principle Test with visible light



Stigmatic image of a large (area: 5mm x 5mm) grid, using scheme (B) with Bragg angles: $\theta_1 = 68^\circ$ and $\theta_2 = 22^\circ$ and mirror radii: $R_1 = 1m$ $R_2 = 0.4m$
The line width is 50 microns. The smallest squares are 0.4mm x 0.4mm.

Additional conditions for x-rays

Additional conditions for x-rays due to the fact that the Bragg condition must be simultaneously fulfilled on both crystals:

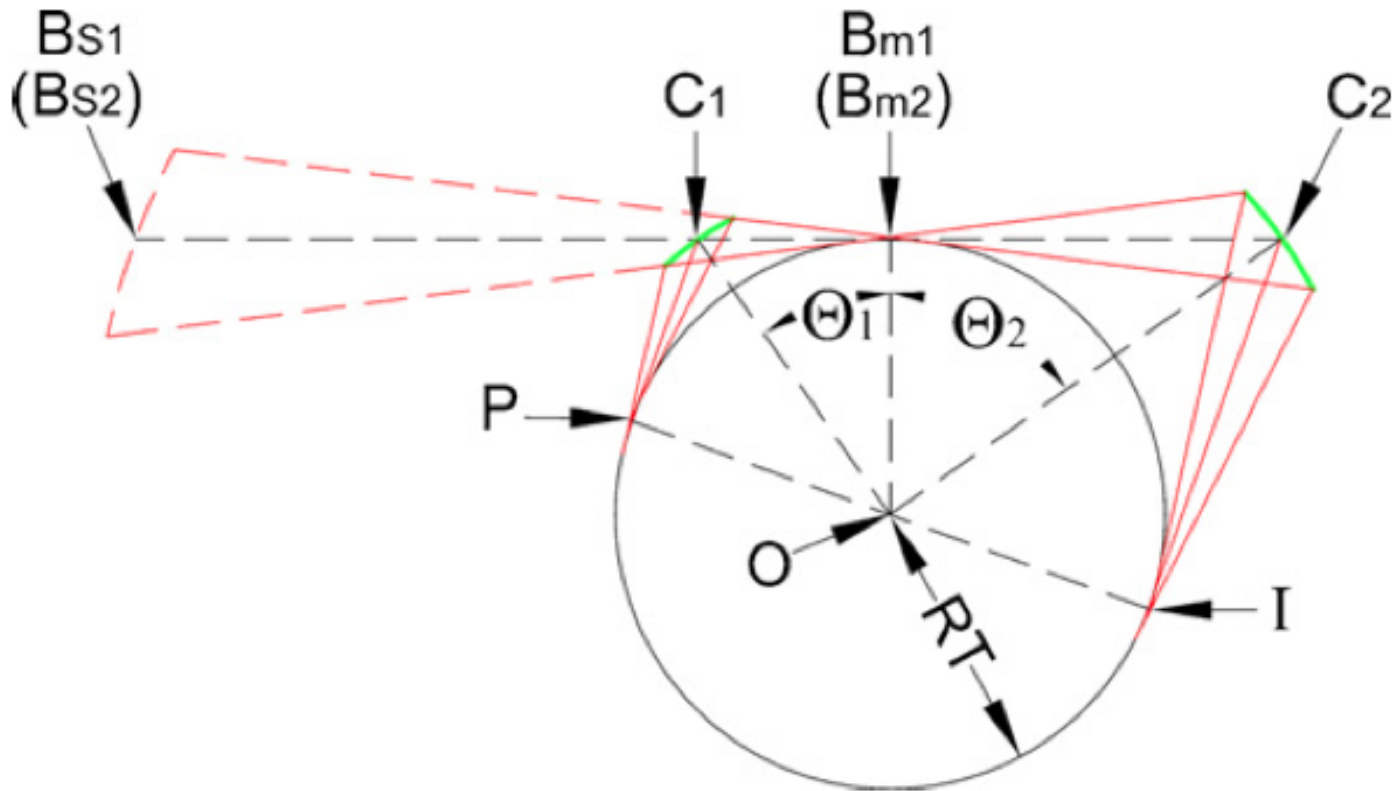
- (i) Only version (B) of the imaging scheme works for x-rays.
- (ii) The two crystal spheres must be concentric.
- (iii) The origin of the tangency circle for the rays between the two crystals is at the origin of the two crystal spheres; and the radius ρ of this circle must fulfill the condition:

$$(2) \quad \rho = R_1 \cos(\theta_1) = R_2 \cos(\theta_2)$$

With the additional condition (2), equation (1) has only one solution:

$$(3) \quad \theta_1 + \theta_2 = 90^\circ$$

Solution for x-rays



The scheme shown satisfies the necessary conditions (1), (2), and (3) for x-rays. The Bragg angles are $\theta_1 = 35^\circ$ and $\theta_2 = 55^\circ$. The ratio of the radii of curvature is $R_2/R_1 = 1.43$, and the radius of the tangency circle is: $\rho = RT = R_1 \cos(\theta_1) = R_2 \cos(\theta_2)$

Other Imaging Schemes

- Other imaging schemes to eliminate the astigmatism have been proposed in the literature:

(1) **Missalla et al.** proposed the use of a toroidally bent mirror, where the

ratio of the vertical and horizontal radii equals: $\frac{R_v}{R_h} = \sin^2(\theta)$

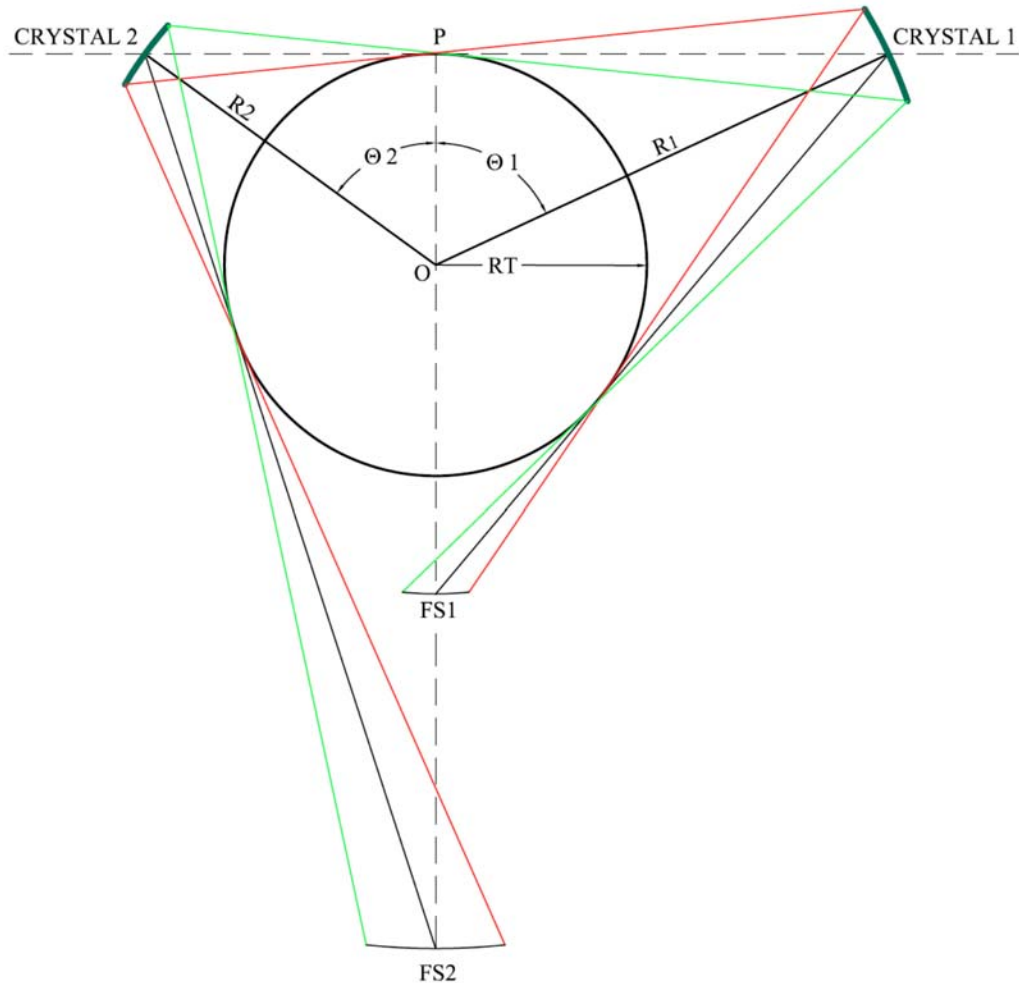
so that $f_h = \frac{R_h \sin(\theta)}{2} = \frac{R_v}{2 \sin(\theta)} = f_v$

This works only for one particular Bragg angle. However, toroidal mirrors have a lower degree of symmetry than spherical mirrors and they produce other image distortions.

(2) **Podorov et al.** proposed a combination of two toroidal mirrors, with concave and convex curvatures. However, they used a Bragg angle of 83° , which is still close to normal incidence.

- We point out that our imaging scheme works for almost arbitrary Bragg angles.

Another Imaging Scheme



This imaging scheme has two real sagittal line images and allows to vary the magnification by choice of the Bragg angles. Again the condition

$$\rho = RT = R_1 \cos(\theta_1) = R_2 \cos(\theta_2)$$

must be fulfilled.